The pharmacology of valinate and tert-leucinate Synthetic Cannabinoids

Shivani Sachdev

MACQUARIE University

A thesis submitted in fulfillment of the requirements for the degree of

Master of Research

Macquarie University

Faculty of Medicine and Health Sciences

Department of Biomedical Sciences

October 2016

This is to state that the work presented in this thesis entitled **"The pharmacology of valinate and tert-leucinate Synthetic Cannabinoids"** represents original idea in my own words and where others ideas or words have been included; I have adequately cited and referenced the original sources.

Shivani Sachdev

To Mom

For making me who I am today..love you to the moon and back..

ACKNOWLEDGEMENT

After eight months of intensive research, finally the day has come. Time flies so fast, for the first day I started, I never thought that I would come this far. I know, I could not have accomplished this much alone. I would like to express my sincere gratitude to my supervisor, Professor Mark Connor, you have been tremendous mentor for me. Your advice on both research as well as on my career has been priceless. Thank you for being such an amazing support system.

My sincere thanks also goes to Dr. Marina Santiago, for her assistance at all the levels of the research project. A very special thanks goes out to Rochelle Boyd for helping me with Immunocytochemistry, without her I couldn't get all those beautiful fluorescent images. Appreciation also goes out to Dr. Amelia Edington, for getting my hands on EndNote. In addition, special thanks to Professor Helen Rizos, for providing us with some novel inhibitors.

Thanks to all my friends for being there for me, especially my lab mate Preeti Manandhar. Thanks for listening to, and at times, tolerating me over past few months. I am very grateful for everything you guys have done, and I can't thank you enough. Love you guys! This is not the end, but only the beginning.

Thanks to Mom and dad for your unwavering support and providing me with a wonderful life. To my little bro, "keep on shining, you crazy diamond". Last, I could not have asked for a better place "It's a new dawn. It's a new day. It's a new life, And I am happy"

CONTENT

LIST OF FIGURES

ABBREVIATIONS

2-AG	2-Arachidonoyl Glycerol
AC	Adenylyl Cyclase
AEA	Anandamide
βARK	beta-Adrenergic Receptor Kinase
BSA	Bovine Serum Albumin
CAMKII	Calmodulin-dependent Protein Kinase II
cAMP	Cyclic Adenosine 3′,5′-monophosphate
CB	Cannabinoid
CB1	Cannabinoid type 1 receptor
CB2	Cannabinoid type 1 receptor
Cmpd 101	Compound 101
CNS	Central Nervous System
CRC	Concentration Response Curve
DAPI	4',6-diamidino-2-phenylindole
DMEM	Dulbecco's Modified Eagle Medium
DMSO	Dimethyl Sulfoxide
EMCDDA	European Monitoring Centre for Drugs and Drug Addiction
ERK	Extracellular Signal–Regulated Kinases
EWA	Early Warning Advisory
FBS	Fetal Bovine Serum
FLIPR	Fluorescence Imaging Plate Reader
FRT	Flp Recombinase Target
GIRK	G protein-Coupled Inwardly-Rectifying Potassium Channels
GPCR	G-protein Coupled Receptors
GRK	G-protein Coupled Receptor Kinase
GTP	Guanosine Triphosphate

HA	Hemagglutinin
HBSS	Hank's Balanced Salt Solution
HEK	Human Embryonic Kidney
JNK	c-Jun N-terminal Kinases
L-15	Leibovitz Medium
LC	Locus Coeruleus
MAPK	Mitogen-Activated Protein Kinases
MEK	Mitogen-Activated Protein Kinase Kinase
MOR	μ-Opioid Receptor
mRNA	messenger Ribonucleic Acid
NFLIS	National Forensic Laboratory Information System
NPS	Novel Psychoactive Substances
PBS	Phosphate Buffer Saline
Perk	phosphoExtracellular Signal–Regulated Kinases
PKA	Protein Kinase A
PKC	Protein Kinase C
PTX	Pertussis Toxin
RFU	Relative Fluorescence Unit
rpm	Revolutions Per Minute
RT	Room Temperature
SCs	Synthetic Cannabinoids
SEM	Standard Error Mean
SST	Somatostatin
UNODC	United Nations Office on Drugs and Crime
WT	Wild-Type

LIST OF DRUGS

Δ9-THC	Δ9-tetrahydrocannabinol;(−)-(6aR,10aR)-6,6,9-Trimethyl-3-pentyl-6a,7,8,10a-tetrahydro-6H-benzo[c]chromen-1-ol
WIN55,212	R)-(+)-[2,3-Dihydro-5-methyl-3-(4-morpholinylmethyl)pyrrolo[1,2,3-de]-1,4-benzoxazin-6-yl]-1-napthalenylmethanone
CP 55,940	2-[(1R,2R,5R)-5-hydroxy-2-(3-hydroxypropyl)cyclohexyl]-5-(2-methyloctan-2-yl)phenol
CP 47,497	2-[(1S,3R)-3-hydroxycyclohexyl]-5-(2-methyloctan-2-yl)phenol
JWH-018	1-[(5-Fluoropentyl)-1H-indol-3-yl]-(naphthalen-1-yl)methanone
JWH-072	1-naphthalenyl(1-propyl-1H-indol-3-yl)-methanone
JWH-015	(2-Methyl-1-propyl-1H-indol-3-yl)-1-naphthalenylmethanone
JWH-046	(2-methyl-1-propyl-1H-indol-3-yl)(7-methylnaphthalen-1-yl)methanone
JWH-048	(1-pentyl-2-methyl-1H-indol-3-yl)(7-methyl-1-naphthalenyl)methanone
JWH-073	Naphthalen-1-yl-(1-butylindol-3-yl)methanone
ML297	N-(3,4-Difluorophenyl)-N'-(3-methyl-1-phenyl-1H-pyrazol-5-yl)urea
SR141716	5-(4-Chlorophenyl)-1-(2,4-dichloro-phenyl)-4-methyl-N-(piperidin-1-yl)-1H-pyrazole-3-carboxamide
UR 144	(1-pentylindol-3-yl)-(2,2,3,3-tetramethylcyclopropyl)methanone

*Recently emerged Synthetic Cannabinoids

MDMB-CHMICA	Cyclic-Indole-Leucinate	Methyl(2S)-2-{[1-(cyclohexylmethyl)-1H-indol-3-yl]formamido}-3,3-dimethylbutanoate
MDMB-CHMINACA	Cyclic-Indazole-Leucinate	Methyl(2S)-2-{[1-(cyclohexylmethyl)-1H-indazol-3-yl]formamido}-3,3-dimethylbutanoate
MDMB-FUBINACA	PFB-Indazole-Leucinate	methyl(2S)-2-{[1-[(4-fluorophenyl)methyl]indazole-3-carbonyl]amino}-3,3-dimethylbutanoate
5F-AMB	5F-Indazole-Valinate	Methyl(2S)-2-{[1-(5-fluoropentyl)-1H-indazol-3-yl]formamido}-3methylbutanoate
5F-MDMB-PICA	5F-Indole-Leucinate	Methyl(S)-2-(1-(5-Fluoropentyl)-1H-indole-3-carboxamido)-3-methylbutanoate

- All the Synthetic Cannabinoids were synthesized at the University of Sydney.

ABSTRACT

Introduction. Synthetic cannabinoids (SCs) with indole or indazole cores and featuring L-valinate or L-tert leucinate groups are epidemic recreational drugs in many parts of the world, and are reported to be associated with severe toxicity. We evaluated the cannabimimetic activity of these compounds on human cannabinoid type 1 (CB1) and type 2 (CB2) receptors. We also examined desensitization of CB1 receptor signaling on continued exposure to SCs.

Methods. We used a fluorescence-based membrane potential assay to measure the potassium channel-mediated cellular hyperpolarization of AtT20 cells expressing CB1 or CB2. Compound 101, Trametinib and SCH772984 were used to study the involvement of G Protein-Coupled Receptor Kinase2/3 (GRK), Mitogen activated protein kinase enzyme (MEK) and extracellular signal regulated kinase (ERK) in CB1 receptor desensitization.

Results. All 16 indole and indazole SCs tested activated CB1 and CB2, with a modest preference for CB1. The most potent was 5F-MDMB-PICA, with an EC_{50} of 0.45 nM at CB1 receptor. The desensitization of the CB1 mediated hyperpolarization produced by EC_{50} and EC_{90} concentrations of 5F-MDMB-PICA was $65\pm5\%$ and $78\pm2\%$ after 30 min (n=6). Like CB1 receptor, CB2 receptor also shows a decline in signaling on continuous exposure to EC_{50} and EC_{90} of 5F-MDMB-PICA. A significant change in fluorescence was observed for somatostatin after 30 mins of EC_{90} 5F-MDMB-PICA to that of SST alone at CB2 receptor (P<0.05). Although, the hyperpolarization to a subsequent application of SST (100 nM) after SCs to SST alone was unchanged at CB1 receptor. In cells treated with Cmpd101 (10 µM), we did not observe any difference in the desensitization of CB1 receptor evoked by the EC_{90} concentration of 5F-MDMB-PICA, but at a concentration of 10 µM 5F-MDMB-PICA, Cmpd 101 reduced desensitization from $97\pm3.9\%$ to $77\pm3.5\%$. Inhibition of MEK or ERK had no effect on CB1 receptor desensitization.

Discussion. All SCs tested in this study have greater potency and maximum effect than Δ^9-THC. CB1 receptor desensitization was largely homologous, with little effect on the native SST receptor responses, whereas desensitization at CB2 receptors was found to be both homologous and heterologous. Our data demonstrate a role of GRK2/3 in CB1 receptor desensitization to high concentrations of agonist in AtT20 cells, but suggest that other mechanisms may be recruited by lower concentrations of drug.

PUBLICATION

Samuel D. Banister, Mitchell Longworth, Richard Kevin, **Shivani Sachdev***, Marina Santiago, Jordyn Stuart, James B. C. Mack, Michelle Glass, Iain S. McGregor, Mark Connor, Michael Kassiou"* The pharmacology of valinate and tert-leucinate synthetic cannabinoids 5F-AMBICA, 5F-AMB, 5F-ADB, AMB-FUBINACA, MDMB-FUBINACA, MDMB-CHMICA, and their analogues", ACS Chemical Neuroscience (2016).

ORAL PRESENTATION

Shivani Sachdev*, Marina Santiago, Samuel D. Banister, Mitchell Longworth, James B. C. Mack, Michael Kassiou, Mark Connor.* "Desensitization of CB1 receptor signaling by valinate and tert-leucinate synthetic cannabinoids". NSW Inter-University Neuroscience and Mental Health Conference, 2016.

Shivani Sachdev*, Mark Connor;* "The pharmacology of valinate and tert-leucinate synthetic cannabinoids and their analogues." Sydney GPCR Research Symposium, 2016.

1

INTRODUCTION

CONTENTS

1.1 Cannabis History

Marijuana or Cannabis is the most widely used recreational drug in many parts of the world. Cannabis use originated thousands of years ago in Central Asia and regions of Mongolia and southern Siberia[1]. The intoxicating resin, secreted from the lower portions of the Cannabis was first recorded for its pharmacology attributes as early as third millennium B.C[2,3]. The herb was used for its ability to soothe nausea, anxiety and even as an anesthetic during surgery[3]. Since then Cannabis has found its way to many regions in the world and eventually spreading to United States[4,5]. In 1920 Cannabis was declared by U.S. Federal Bureau of Narcotics as a powerful, addicting substance that would lead users into narcotics addiction[2,6]. By this time, Cannabis was effectively banned and regulated under the Controlled Substances Act as a Schedule 1 drug[2].

1.2 Illicit Synthetic Cannabinoids

1.2.1 Unexpected Invention of Synthetic Cannabinoids

Gaoni et al. 1964, first identified the exact chemical structure of Δ^9-tetrahydrocannabinol (Δ^9-THC), the main psychoactive ingredient of Cannabis[7]. This finding raised the crucial question of whether there were cannabinoid receptors in brain and other tissues by which Δ^9-THC exerted its specific action. Δ^9-THC was explored to develop a binding assay for the CB receptor, however, it failed because of presumably the high lipophilic nature of Δ^9-THC, made any specific binding impossible[8]. Research scientist at the Pfizer Pharmaceutical Company designed a less lipophilic and more potent synthetic cannabinoid agonist CP 55,940 to study the existence of specific cannabinoid receptors by means of radiolabeled ligand binding assay[2,9]. Two types of cannabinoid receptors have been identified, CB1 and CB2 receptors[10]. CB1 receptors are predominantly found at the terminals of central and peripheral neurons, where they inhibit neurotransmitter release, CB2 receptors occurs mainly in T cells of the immune system, macrophages and B cells, and in hematopoietic cells[11,12], but lately it has also been found in the brain, mainly in microglia[13]. Endogenous ligands had been found for CB receptors, primary endogenous ligands are anandamide (AEA) and 2-arachidonylglycerol (2-AG)[14,15].

1.2.2 Emergence of Spice

Synthetic cannabinoids (SCs) are the family of rapidly growing and evolving series of recreational drugs that are assumed to have a similar psychoactive effect as Δ^9-THC[16]. The European Monitoring Centre for Drugs and Drug Addiction (EMCDDA) reports that 134 new SCs have been recognized in the marketed products since 2008, with the emergence of 30 novel SCs officially notified in 2014[17]. Furthermore, 177 different SCs were reported to the United Nations Office on Drugs and Crime (UNODC) Early Warning Advisory (EWA) in 2014[18]. The SCs were first detected in herbal blend towards the end of 2008 under the brand name of "Spice"[19]. Spice was found to contain a C8 homologue of CP 47,497 as well as JWH-018, a drug designed to explore the structural requirements of cannabinoid receptor binding[19]. Although these products are often misleadingly marketed as research chemicals or incense and often labeled "not for human consumption", they were easily accessible in various retail outlets such as tobacconists, petrol stations and adult shops, as well as from online stores[20].

Unlike the psychoactive effects of cannabis like relaxation, anxiety, hallucinations; the adverse effects of SCs are in addition to the pleasant affects, and they differ from THC because they are more intense, and often of a different kind. SCs can cause serious life threatening effects including suicidality, exacerbation of preexisting psychosis, coma, euphoric, paralysis, tachycardia, high blood pressure and rhabdomyolysis [20,21]. Two cases of pneumonia were also reported after SCs consumption[22]. Many of these compounds has also been linked to kidney malfunctions. Other side effects documented in few case studies are increase acidity of blood, incontinence, hot flashes, hemorrhage, blindness and increase of white blood count[22]. These effects of SCs have been accountable for hundreds of hospitalizations and dozens of deaths[23]. SCs are classified as controlled substances in many parts of the world [24]. Because of these restrictions on SCs, creators of Spice moved on to the generation of new cannabimimetic drugs by slightly altering the chemical composition of the active ingredient in the existing SCs. For example, By the end of 2009, 27 new herbal incense arrived on the market as an alternative version to Spice, in one sample the active ingredient in Spice, JWH-018 was replaced by JWH-073[25]. Thus this is how the drug market is continuously flooded with newer progressing series of synthetic CB receptor agonist under brand names like Kronic and Blue Moon Tea, often promoted as easy way to get natural and legal high to circumvent legislation[26].

1.2.3 CB receptor Signaling

THC acts at CB receptors, as a partial agonist. SCs identified to date also seem to act at CB receptors, but they are often more potent or have a higher efficacy. CB1 receptors is expressed mainly in the brain was responsible for the psychoactive effects of cannabinoids[27]. CB1 and CB2 receptors are G protein-coupled receptors (GPCRs) that belong to a large family of rhodopsin like class A GPCRs[28]. Rhodopsin-like receptors are the largest group of GPCRs that comprises of hormones, neurotransmitters, and light receptors, all of which transduce extracellular signals through interaction with G proteins[29]. Activation of CB1 receptors results in inhibition of adenylate cyclase, thereby reducing intracellular cAMP levels[30] and activation of G protein gated inwardly rectifying potassium channels (GIRK) and inhibition of voltage dependent calcium channels (I_{ca})[31,32]. These CB1 receptor signal transduction pathways are blocked by pertussis toxin, which disrupts $G_{i/o}$ mediated signaling further implying $G_{i/o}$ preferring conformation of the CB1 receptor[33]. But in certain circumstances CB1 receptors can also signal via G_s proteins that activates cAMP dependent pathway[34]. There is a considerable evidence of CB1 receptor signaling via G_q, an increase in Ca^{2+} levels was observed in some cells but not others on the activation of CB1 receptor[35,36]. These differences in the CB1 receptor signaling may be due to the G-protein subunit composition in the various cell types or may be due to the interaction of CB receptors with some other receptors in the cells. Activation of CB1 receptor may lead to increase level of ERK1/2[37]. Similar to CB1, CB2 receptors signals primarily through $G_{i/o}$ pathway. Activation of CB2 revealed changes in cAMP levels that result in the inhibition of T cell signaling. This has implications in the treatment of neuropathic pain and inflammation[38]. It has been established that CB_1 receptor activation is largely associated with analgesic and anxiety-related reactions, rewards circuitry, facilitates appetite, and is slightly involved in motor control and hypotension[13]. In contrast to CB2 receptor, that is significantly involved in inflammatory processes, induction of apoptosis and cell migration[39].
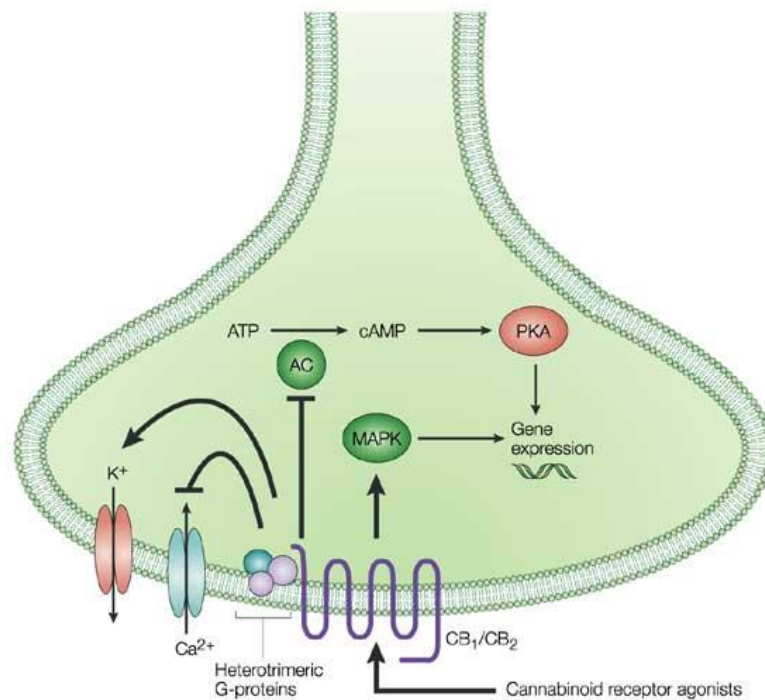
Figure 1. CB receptor signaling transduction pathways; Adapted from Nature reviews 2004 "Endocannabinoids and its therapeutic exploitation", this figure depicts the main signaling pathway of CB1 and CB2 receptor activation through G proteins and their subsequent effectors[40].

1.2.4 Synthetic Cannabinoids: Epidemiology

In recent cases in New York, an increase in adverse events and emergency department's visits was associated with SCs consumption. Between July 11 and July 13 2016, 130 individuals experienced adverse effects like respiratory depression, bradycardia, vomiting, seizures and unconsciousness from the suspected use of SCs. The common short-term effects include paranoia, anxiety, depression, hallucinations, and increased heart rate. Provisional mortality data of New York showed emergency department visits related to SC (K2). According to New York City Department of Mental and Health Hygiene, since 2015, more than 8000 SCs related emergency hospitalizations were reported and of that portion, 90% were males. Also, 99% of the patients are nearly aged 18 or older[41]. A global survey indicated 30 times higher medical emergency department related to SC use than natural Cannabis[42].

Efforts have been made to investigate the reasons for using SCs over Cannabis. Surveys have shown that the most common reasons for cannabis use is relaxation and relief of body pain. On the other hand, data showed that 19% of the population preferred SCs over natural cannabis for its "more intense" effect, 12% of the surveyed population cited the use of SCs to avoid screening positive on drug test and 10% of the users claimed that SCs are legal (which is not the case now) as opposed to natural cannabis. Therefore, this has increased the desirability of people using SCs[43].

1.2.5 Structural classes of Synthetic Cannabinoids

Cannabinoids has been previously classified into four main structural groups: classical, non-classical, aminoalkylindoles and eicosanoids (Figure 2). Classical are represented as cannabinoids with dibenzopyran scaffold that constitutes Δ^9-THC, while the non-classical cannabinoids include compounds invented by Pfizer such as CP-55,940, which were loosely based on the THC structure. The third group includes WIN-55,212 and a series of compounds synthesized by J.W Huffman. Finally, eicosanoids comprise entirely of endocannabinoids, AEA and 2-AG[44]. Although, with the rapid evolution of SCs, their classification into four groups is becoming increasingly unhelpful. Most of these SCs consists of at least four structural components: an indole or indazole core; an ester, amide or ketone linker; a ring containing quinolinyl, napthhyl, adamantly, tetramethylcyclopropyl or other moiety; a hydrophobic "side chain" linked to the nitrogen of indole or indazole system[45]. However, many SCs are unidentified prior to first detection by forensic chemists, and nothing is known of their activity in humans. Thus, the insufficiency of the data regarding its pharmacology and toxicology poses an ongoing challenge for scientists, healthcare workers, and lawmakers across the globe and requires an immediate attention.
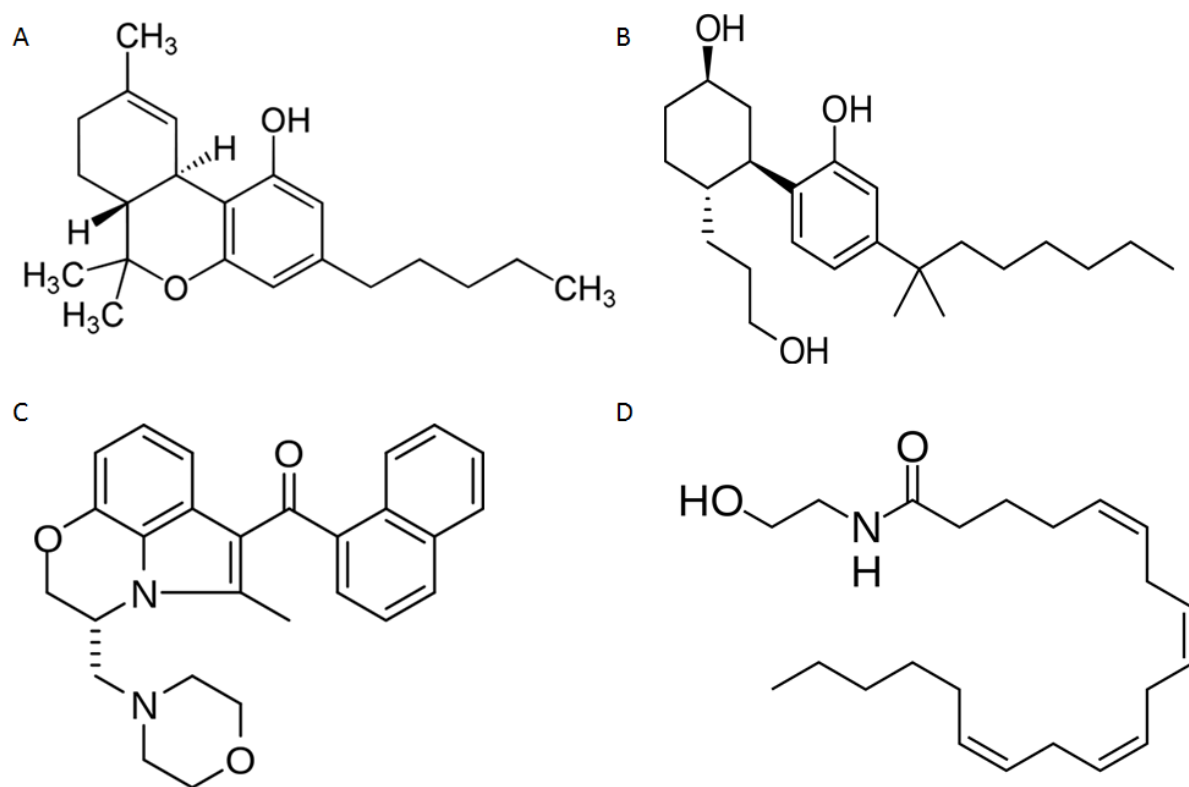
Figure 2 Four main Classification of Cannabinoid structural group, A) Classical Cannabinoid Δ^9-THC; B) Non-Classical, CP-55,940; C) Aminoalkylindoles, WIN-55,212; D) Eicosanoids Anandamide; This figure represents an example chemical structure from each group. Chemical structures were compiled in one frame, taken from different sources[46,47].

1.2.6 Pharmacology of existing Synthetic Cannabinoids

In 30 years since the elucidation of the structure of CB receptors, many structurally diverse compounds have been developed. WIN 55,212 has a common pharmacophore (napthyl ring and cyclohexene ring, the carbonyl and the phenolic hydroxyl) as that of Δ^9-THC[48]. WIN 55,212 has been shown to act through CB1 receptor, as the pharmacology effects of WIN was reversed upon the addition of SR141716, which is an antagonist of CB1 receptor[49]. The elimination of oxygen bridge and aminoalkyl groups in WIN 55,212 resulted in cannabimimetic indoles that were equally effective at CB1 receptors. The first series of cannabimimetic indoles including JWH-072, JWH-015, JWH-046 and JWH-048 had a higher binding affinity at CB2 receptor to that of CB1 receptors[50,51]. Studies have also revealed the correlation of the length of carbon chain and certain structural groups (morpholinoethyl and napthoyl) to the potency and affinity for CB1 receptors[52]. The structure-activity relationship of these compounds has also been studied *in vivo.* As reviewed by Wiley 2013, the most critical factor affecting the *in vivo* potency at CB1 receptors was the substituent's position in indole derived cannabinoids[53]. Another important inference was "good CB1 affinity" across a wide array of structurally diverse substituents of WIN 55,212[53]. In 2011, the *in vivo* data of phenylacetylindoles was shown to share many pharmacological properties to THC based on its good CB1 binding affinity in mice[54]. Another trend that followed in 2011 was the incorporation of fluorine in the terminal position of newer evolved SCs[55]. It is suggested that terminal fluorination of N-pentyl substituent of SCs usually enhances the potency of CB1 receptor activation. A second most prevalent SC, RCS-4 was identified in the same year[56]. In 2013, the pharmacology of SCs with indazole in its core structure was determined. They found that all the indazole SCs have cannabimimetic affect parallel to those of Δ^9-THC, but with greater potency[57]. One of the most dominant and recent group of Indole and indazole synthetic cannabinoids (SCs) featuring L-valinate or L-*tert*-leucinate were identified, and their use has been associated with serious adverse health effects[58].

A detailed study on the pharmacology of recently emerged SCs is discussed in Chapter 3.

1.2.7 Study of CB receptor Pharmacology using different Assays

A number of different bioassays have been used to study the pharmacology of receptor-ligand interaction. Some of the *in vivo* assays that has been used to study the CB receptor activation includes dog static ataxia, drug discrimination techniques, overt behavior in monkeys, and the mouse tetrad model[59]. These assays are more important in assessing the behavioral effects of SCs but it would be difficult to determine the detailed signaling pathways following the receptor activation[60]. However, *in vivo* assays are essential to demonstrate that the molecules are biologically active in an animal, and to give an idea of which sort of behavioural effect may predominate. In our case, we were interested in the pharmacological properties of rapidly evolving SCs and how the continuous presence of these drugs affects the CB receptor signaling. This presented the need for high-throughput *in vitro* assays to generate the pharmacological data on emerging trends of SCs.

In vitro studies for assessing the molecular pharmacology of these SCs can be achieved using various commercially available assays. The key techniques available are classified as ligand binding assay, measurement of agonist stimulated GTPase activity, guanine nucleotide exchange (GTPγS) and functional activity assays. The radiologand binding assays are generally used to characterize the binding of a radioactively labeled drug to its target receptor. But the binding affinity data from this does not provide information of the ligand being tested as agonist, antagonist or inverse agonist[61]. Thus, the emphasis has been shifted from the radiometric to functional assays. For CB receptors, this can be achieved using cell lines expressing G proteins that couple to downstream signaling molecules such as intracellular calcium ([Ca]i) mobilization, cAMP-dependent gene transcription, or more traditional assays of adenylyl cyclase (AC) activity, which require harvesting or lysing of cells[62]. All the assays mentioned above are laborious technically, although a few cAMP assays have been automated. But these assays are likely to be measuring the combined effects of receptor activation and desensitization[63]. Thus, this has led to the emergence of more rapid and less invasive assay to readily measure the agonist stimulated receptor signaling in an intact cell at an effector level similar to neurons for extended periods. In AtT20FlpIn cells heterologously expressing CB receptors, the agonist-induced activity is readily detected by inhibition of native voltage dependent calcium channels (Ica) and activation of GIRK channel[31]. We accessed the pharmacology of the recently emerged SCs *in vitro* based on FLIPR membrane potential assay via FlexStation 3, measured as hyperpolarization of cell on activation of GIRK channel.

1.3 Regulation of GPCR Signaling

The continuous stimulation of the receptor with agonist generally results in the decline in the activity of receptor[64,65]. We do not know the effect on the signaling of CB receptor in the continuous presence of SCs. Desensitization is the uncoupling of the receptor from G protein, which results in the termination of G-protein dependent signaling. Desensitization has been studied for many different receptors and it is classified as:Homologous desensitization and Heterologous desensitization.

The term homologous desensitization is defined as the agonist induced decline in the activity of the receptor with no significant effect on the signaling of other receptors present in the same cell, whereas we define heterologous desensitization as the attenuation of signaling at different receptors or through the pathways common to different receptors in the same cell mediated by an agonist[66].

The mechanism underlying desensitization has been widely studied in the β-adrenergic receptor and μ-opioid receptor (MOR). The essential steps involved in the receptor desensitization is explained here by taking MOR as an example (Figure 3). First, the agonist binds to the receptor and leads to receptor activation. Second, when this receptor is stimulated with the agonist for a prolonged period, GPCR kinases are translocated to the membrane where they phosphorylates the C terminal of the receptor. Third, once the receptor is phosphorylated by GRK, it facilitates the binding of β-arrestin to the receptor. β-arrestin recognizes both the active confirmation of the receptor and the phosphorylation site on the receptor. Fourth, β arrestin recruits another protein called clathrin, thus initiating the receptor internalization through clathrin mediated endocytosis, Lastly, the receptor is either recycled to the membrane or trafficked to the lysosomes for degradation[67-70]. MOR are also phosphorylated by non-GRK kinases such as JNK, PKC, PKA, CAMKII and MAPK but the consequences of these phosphorylation events have not been completely defined[71-73]. A number of mechanism underlying β-adrenergic receptor short term and long-term desensitization has been studied. Phosphorylation by PKA and βARK attributes largely to the β-adrenergic receptor short-term desensitization. But the similar mechanism was not involved in the long term desensitization of the same receptor[74]. Thus, the desensitization mechanism may vary for the same receptors, which often makes the comparison between studies difficult.
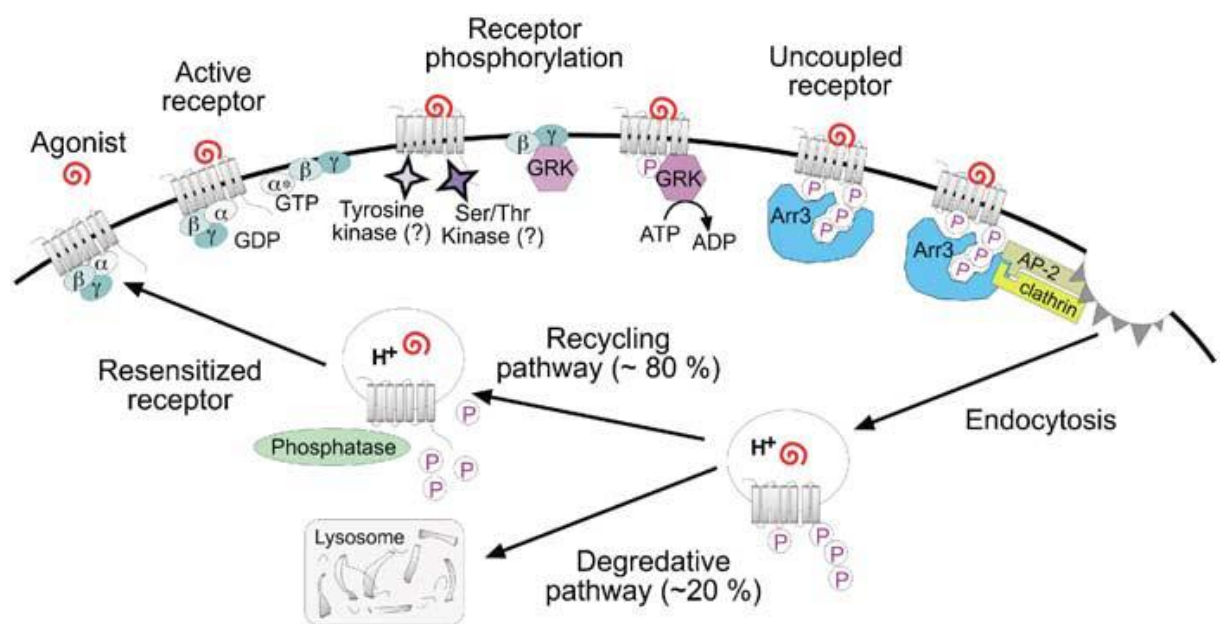
Figure 3: General Scheme of regulatory pathway following binding of an agonist. Summary of the classical pathway adopted for MOR desensitization coupled with resensitization. Surprisingly, almost all the CB receptors are degraded rather than recycled[75]. Figure reprinted from, μ-Opioid receptor desensitization: Is morphine different?[68]

1.3.1 Regulation of CB receptors: Desensitization, phosphorylation and Internalization

Drug tolerance is define as subjects reduced response to drug following its repeated use. In other words, subjects take higher dose of drug to achieve the same level of drug effectiveness as achieved intially[76]. Tolerance to drug is developed by many different mechanisms such as desensitization, a reduction in receptor density or changes at level of cellular targets[77]. Tolerance development to cannabinoids by chronic administration might involve receptor desensitization or uncoupling, as one of the molecular events underlying this complex phenomenon[78,79]. The effect of repetitive administration to Δ^9-THC did not significantly altered the receptor binding or mRNA levels of CB1 receptors in mice[80]. Other studies have showed the changes in binding sites or mRNA levels of CB receptors in rat brain on exposure to cannabinoids for a prolonged period of time[81,82]. CB1 receptor desensitization has been studied in rat brain, measured as the ability of cannabinoid agonist to activate G proteins by [^{35}S]GTPγS. They showed that repeated administration of THC shows region specific downregulation of CB1 receptor in different brain regions[83]. More recently age and sex dependent differences in CB1 receptor desensitization was studied following repetitive administration with THC. They found that degree of desensitization was highest in adolescent female rodents to that of adult female and male rodents, which might be because of the interference of THC with endocannabinoids system in brain[84]. However, downregulation of CB1 receptors following chronic administration of drug has been widely studied, but there is no strong evidence of the exact pattern of CB receptor desensitization in the continuous presence of SCs. Thus, the mechanism underlying CB receptor desensitization needs to be closely elucidated.

Mackie et al 1999 first studied the mechanism underlying desensitization of CB receptor; they suggested that CB1 receptors and opioid receptors shows a similar trend in signal transduction. Consistent with the results of δ opioid receptor desensitization in *Xenopus oocytes,* it was found that even CB1 receptor desensitization is GRK 3 and β arrestin 2 dependent[85]. Thus, they determined that different domains in the receptor may have a distinct role in receptor desensitization and internalization[85]. The role of β-arrestin2 was also examined in regulation of CB1 signaling mediated by several cannabinoid receptor agonists including Δ^9-THC, CP 55,940 and JWH-073. These studies indicated that the *in vivo* effects of Δ^9-THC was selectively influenced in the β-arrestin2 knockout mice, implying agonist selective involvement of β-arrestin2 in CB1 regulation[86].

Recent studies have shown that a significant proportion of CB1 receptor is found in the cytoplasm in addition to those of plasma membrane[87-89]. This observation combined with the receptor internalization, trafficking and recycling back to the surface has been of considerable interest. Studies have suggested that intracellular CB1 receptors does not co-localize with the cellular machinery, which is responsible for the recycling of the CB1 receptor back to the plasma membrane in HEK 293 cells[89]. Although prior studies have shown rapid CB1 receptor internalization and constitutive recycling of CB1 receptors on continuous stimulation with an agonist[89,90], but the evidence for recycling of CB1 receptor is very limited . However, a recent study indicates that constitutive delivery of CB1 receptor back to the cell membrane is the result of receptor synthesis and not the recycling of CB1 receptor. They also found that intracellular CB1 receptor have traversed the synthetic pathway, which is that these receptors are fully glycosylated[75]. A question then arises that if this mature and proficient CB1 receptor resides in an intracellular pool with no apparent function or whether it involves some different mechanism, has not been determined.

Chapter 4 will further discuss the mechanism underlying the desensitization of CB receptors in details.

1.4 AIMS

The main aim of this research is to determine the pharmacology of recently emerged SCs and their analogues. Consumption of these SCs has been found to be associated with adverse health reactions. By studying the activity of these SCs on CB receptor, we aimed to assess the structural activity relationship of these SCs and how the functional activity of these SCs attributes to its toxicological properties. In addition to this, we also investigated the effect of these SCs on CB receptor signaling for a prolonged period.

Aim 1: Examine the pharmacology of recently emerged SCs with indole and indazole in its core structure featuring valinate and tert leucinate groups and its analogues, by evaluating its activity on human CB1 and CB2 receptor.

Aim 2: Determine if there is any desensitization of CB receptor or not in the presence of SCs in AtT20 cells. This chapter also examines the effect of kinase modulators on the signaling of CB1 receptors in the continuous presence of most potent SC.

2

METHODS

CONTENTS

2.1 Cell Culture

We used immortalised mouse pituitary adenoma (AtT20FlpIn) cells heterologously expressing human CB1 and CB2 receptors to study the pharmacology of recently emerged SCs. We chose this cell type for our project because it expresses native G protein-coupled inwardly rectifying potassium channels. Two GIRK channel subunits are expressed in AtT20 cells: GIRK1 (Kir3.1), GIRK2 (Kir3.2)[91]. GIRKs play an important role in the regulation of membrane potential of the cell, activated in response to GPCRs[91], which is crucial for the main signaling assay performed during this work. AtT20 cells also natively express somatostatin receptors[92], which has allowed us to study heterologous desensitization at CB receptors. SST receptors also couple to Gi/Go-type G proteins and activate GIRK[91], therefore provides a way of testing for unspecific effects of the novel drugs on K channels and other elements of signaling cascades in WT cells.

2.1.1 Transfection:

The AtT20 cell line with FlpIn system was used for the expression of HA tagged human CB1 or CB2 receptor. This system allows the integration and expression of different CB receptors at a specific genomic location and under the same transcriptional control. The FlpIn system was created by the incorporation of Flp recombinase target (FRT) into the genome of AtT20 WT cells as previously described[94]. This FlpIn AtT20 host cell line was cotransfected with pcDNA5-FRT-HA-hCB1 and pOG44 expression vector, which encodes for the hemagglutinin (HA) tagged human cannabinoid type 1 receptor and Flp recombinase respectively. The HA tagged human CB1 was synthesized by Genescript Piscataway, NJ and the complete procedure of transfection was carried out with transfectant Fugene (Promega). The selection for AtT20FlpIn cells stably expressing hCB1 was completed using hygromycin B (500 ug/ml) and grown to confluency. The same procedure was followed for the expression of HA tagged human cannabinoid type 2 receptor in mouse AtT20FlpIn cells[95]. Cells were created by Dr Marina Santiago, as part of a project funded by the Lambert Initiative for Cannabis Therapeutics. Clones expressing cannabinoid receptors was assayed for the SC response after it has gone through few passages and then the cells were frozen down for future use.

2.1.2 Growing and subculturing of cells:

The cryovials containing frozen AtT20FlpIn-CB1 or CB2 cells were quickly thawed in 37ºC water bath. Cells were cultured in Dulbecco's modified Eagle's media (DMEM) containing 10% Fetal bovine serum (FBS) and 100 U penicillin/streptomycin ml^{-1} without selection antibiotics and incubated at 37ºC, 5% CO_2 for 24 hours. After 24 hours of incubation the old media was aspirated and replaced by DMEM supplemented with 10% FBS, 100 U penicillin/streptomycin ml^{-1} and 80 µg/ml hygromycin. Cells were grown to 80% confluence in 75 cm^2 flask and were ready to be passaged. The cells were subcultured only at its log phase, where it proliferates exponentially. The old media was removed and the cells grown as monolayer in the flask was rinsed with 4 ml of Phosphate buffer saline (PBS). The cells were detached from the flask using 3 ml trypsin, incubated for two minutes to ensure the full release of the cells. This was followed by the addition of DMEM to stop the enzymatic reaction of trypsin. The cells were then spun down at 1000 rpm for 5 minutes and resuspended to the new T75 flask in DMEM media with selection antibiotics. The cells were adapted and maintained under these conditions for atleast one week before being used in experiments.

Likewise, AtT20FlpIn-WT cells, which do not express CB1 or CB2 were cultured in DMEM supplemented with 10% FBS, 100 U penicillin/streptomycin ml^{-1} and 100 µg/ml zeocin.

2.1.3 Plating cells for assay

Cells for assay were grown in 75cm^2 flasks and used at its 90% confluency. The day before the assay, cells were detached from the flask by trypsinization as described above. The cells were spun down at 1000 rpm for 5 minutes and the pellet was resuspended in 10 ml of Leibovitz's L-15 media supplemented with 1% FBS, 100 U penicillin/streptomycin ml^{-1} and 15 mM glucose. The cell suspension was transferred in volume of 90 µl in each well in black walled, clear bottomed 96 well plates and incubated overnight at 37ºC.

The similar procedure was followed for the plating of cells treated with Pertussis toxin (PTX). The stock solution of PTX was diluted in L15 to make the final concentration to 200 ng/ml. The cell suspension was transferred in the volume of 90 µl in odd wells and 80 μl in the even wells in 96 well plates. The even wells were subsequently treated with 10 μl of PTX so as to make the total volume to 90 µl. The assay plate holding 90µl of cells treated with PTX and control (non-PTX treated) was incubated overnight at 37°C.

2.2 Membrane potential Assay

The membrane potential of AtT20 FlpIn cells transfected with HA tagged human CB1 or CB2 was measured using FLIPR membrane potential assay kit (blue) via FlexStation3 as described in Knapman et al, 2013[96]. This kit detects the ion channel modulation and cellular membrane potential reflected by decrease or increase in fluorescent signal (Figure 4). When the cell is in hyperpolarized state, the fluorescence intensity decreases as the dye flows outside the cells, and vice versa. The dye was reconstituted in low potassium Hank's Balanced Salt Solution containing (in mM) NaCl 145, HEPES 22, Na_2HPO_4 0.338, $NaHCO_3$ 4.17, KH_2PO_4 0.441, $MgSO_4$ 0.407, $MgCl_2$ 0.493, $CaCl_2$ 1.26 and glucose 5.56 with pH of 7.4 and osmolarity of 315 ± 5. Cells were loaded with 90 µl dye solution without the removal of L-15 to make the initial volume to 180 µl per well. This was followed by 60 mins incubation at 37ºC in FlexStation3 and the plate was left uncovered for the last 10 mins of final incubation. The drug was made up in HBSS buffer containing 0.01% BSA and 1% DMSO, known as assay buffer. The stock solution of drug was diluted every time in the assay buffer to achieve the desired concentration, which is 10 times the final concentration. The final concentration of drug results from the end dilution of drug in FlexStation3 run. The FlexStation3 has appropriate drawers for placing the drug plate and 96-well black FlexStation pipette tips named as source and tip rack respectively. The setting for the instrument was made in SoftMax Pro with respect to the wells to read, drug plate and pipette tip layout. The Fluorescence was then recorded using Flexstation 3 microplate reader with cells being excited at wavelength of 530 nm and emission at 565 nm recorded, with a filter at 550 nm. The baseline reading was taken for at least 120 seconds after which 20µl of vehicle or drug was added to the cells. The change in Fluorescence was recorded for all the selected wells and analysed using Graph Pad prism.

Figure 4 (following page) FLIPR membrane potential assay kit: Fluorescence intensity increases or decreases with change in cellular membrane potential. Blue circle represents fluorescent dye[97]
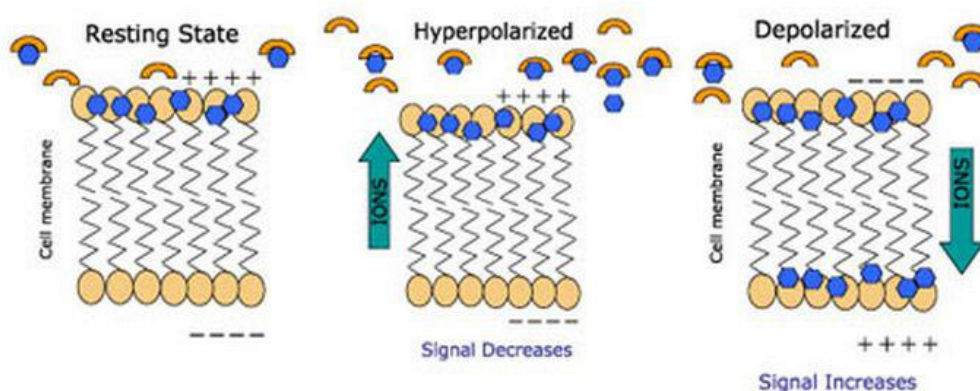
Table 1 represents the setup parameters for membrane potential Assay

Read Mode	Fluorescence (RFUs) and Bottom Read
Wavelength (nm)	530 (Ex) 565 (Em) 550 (Cutoff)
Sensitivity	Reading: 6 (normal) PMT sensitivity: Medium
Timing Interval	2 sec
Assay Plate Type	96 well Costar blk/clrbtm
Compound Source	Greiner 96 Vbtm plate
Auto Calibrate	On
Auto Read	Off

2.2.1 Experimental Setup for Concentration response curve

The drug solution (SCs) of different concentrations as made above was loaded in duplicate onto 96 well V-bottomed drug plate. It was made sure each time that every column of drug had well occupied for blank (assay buffer) and CP-55,940 as a reference standard. The run time for this assay was kept to 5 minutes. Once the run started, the data was collected every two seconds for 5 minutes per well. The entire data for each experiment (n=6) was then analysed.

The similar protocol was followed for the MPA assay in AtT20FlpIn-WT cells except that this time the run was for 10 minutes. SCs was added to the WT cells after 2 mins of baseline recording, followed by the second addition of maximal effective concentration of somatostatin (obtained from CRC of SST previously reported for this assay), upon SC for the latter half of 10 mins (Figure 4).

For the PTX-treated cells challenged with SCs (10 µM), the change in fluorescence was compared with those produced by SCs administration to cells in adjacent columns not treated with PTX.
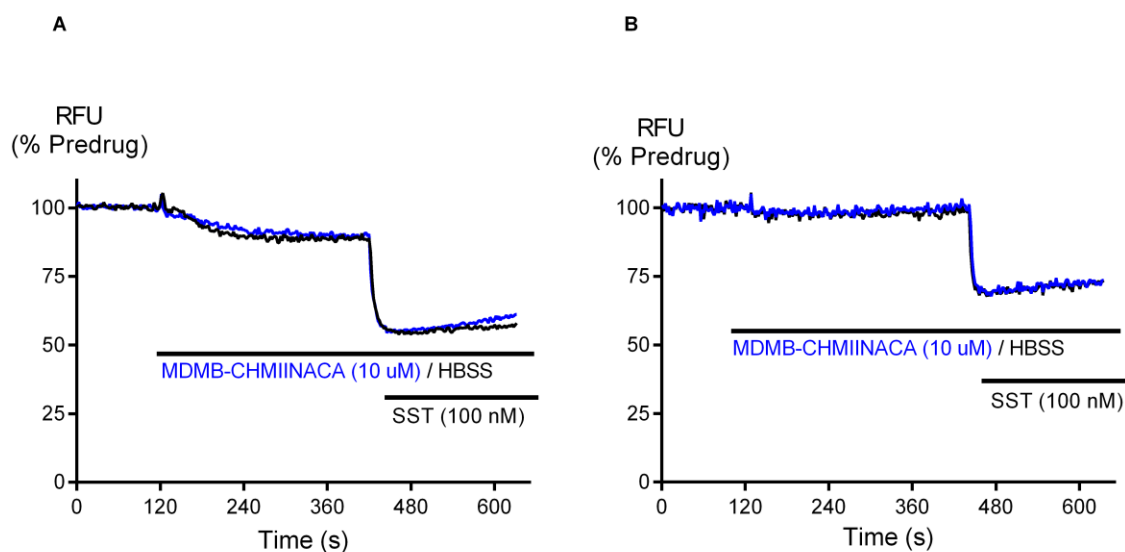
Figure 5: Representative traces showing MDMB-CHMINACA on AtT20FlpIn-WT cells. Trace A is normalized to the percentage baseline, where SST is added 5 min after MDMB-CHMINACA. Trace B is the blank corrected data (of A), that eliminated the slightest drop in the fluorescence, results from the DMSO in the blank.

2.2.2 Experimental Setup for Desensitization

The desensitization assay was performed for selected SCs (MDMB-CHMICA, MDMB-CHMINACA, 5F-AMB and MDMB- FUBINCA). For this, EC_{50} and EC_{90} concentration of SCs were used to precisely measure the degree of desensitization in AtT20FlpIn-CB1/CB2 cells.

The experimental procedures designed for desensitization assay is very much similar to the setup followed up for the CRC of SCs, except for the few changes in the parameters. SC was added to the cells after two minutes of baseline recording and the data was collected every 2 seconds To quantify homologous desensitization, maximal effective concentration of CP-55,940 (reference standard) was added upon SC after 30 mins. Whereas to quantify the heterologous desensitization, a high concentration of SST (100 nM) was added.

2.3 Kinases in CB1 receptor desensitization

2.3.1 Inhibition of GRK 2/3

Compound 101, a potent inhibitor of GRK2/3 was used at this step to determine the involvement of GRK2/3 in CB1 receptor desensitization caused by EC_{90} (3 nM) and at saturating concentration (10 µM) of 5F-MDMB-PICA. AtT20FlpIn-CB1 cells were pre-incubated with 10 µM of Cmpd 101 in parallel to the control cells (incubated with assay buffer) for 60 mins. The desensitization was assessed in the similar way as described above. The percentage change in fluorescence was measured for the control cells and cells treated with Cmpd 101. We also performed this assay to investigate the role of GRK2/3 in SST receptor desensitization.

The involvement of GRK2/3 was also examined for DAMGO induced MOR desensitization in AtT20 cells transfected with human MOR[95]. All the conditions for this was kept exactly the same as previously described.

2.3.2 Inhibition of ERK

Trametinib, a potent MEK inhibitor was used here to determine the potential involvement of ERK via MAPK pathway in CB1 receptor desensitization[98]. AtT20FlpIn-CB1 cells were pre-incubated with 100 nM of Trametinib in parallel to the control cells (incubated with assay buffer) for 60 mins in the continued presence of EC_{90} (3 nM) and saturating concentration (10 µM) of 5F-MDMB-PICA. The percentage change in fluorescence was measured for the control cells and trametinib treated cells. The similar assay was performed exactly for the same concentration of Cmpd 101 and Trametinib in combination.

SCH772984, a direct inhibitor of ERK activity was used to study the involvement of ERK, independent of the upstream MAPK pathway in CB1 receptor desensitization at EC_{90} and at saturating concentration of 5F-MDMB-PICA. AtT20FlpIn-CB1 cells were pre-incubated with 100 nM of SCH772984 in parallel to the control cells (incubated with assay buffer) for 4 hours. The experimental design for desensitization assay was kept same for each run[99].

2.4 Data Analysis:

2.4.1 For Concentration Response Curve

The data collected from SoftMax Pro was analysed using Microsoft excel. The analysis was carried out for each of the SC in duplicate. In the first step, the baseline was calculated by taking an average of the last 20 seconds prior to the SC addition and data expressed as a percentage of this baseline. Subsequently, the vehicle (blank) for that particular column was normalized and subtracted from the changes produced by the drug (Figure 4). Thus the minimum fluorescence that corresponds to the maximum hyperpolarization was determined for each concentration of SCs. The changes in fluorescence were expressed as a percentage of that produced by 1 µM CP55940, which was included in each column of each assay to allow ready comparisons across different days and cell passage numbers.

Data was plotted using GraphPad Prism to obtain CRC containing standard error mean. The pooled data was fitted by non-linear regression to a 4 parameter logistic equation of the form $[Y = minimum + (maximum - minimum)/(1 + 10^{((LogIC50 - X) * HillSlope)}]$, where X is concentration and Y is response. The maximum, EC50 and Hill slope were allowed to vary, but for consistency the minimum was constrained to zero for all fits.

2.4.2 For Desensitization

The data analysis for desensitization was done in similar way as of CRC. Desensitization of CB1 responses was determined in 2 ways. Firstly, the degree of reversal of the hyperpolarization in the continued presence of SC was quantified by comparing the % change in RFU at the peak of drug effect and at 30 minutes, a complete reversal of the drug effect at 30 minutes represents 100% desensitization.

Homologous and heterologous desensitization were calculated by comparing the response to CP-55,940 or SST added after 30 minutes of SC with that of CP or SST added after 30 minutes of vehicle.

Statistical comparisons between groups were made using a 2-way Unpaired Students T-test, with a value of $P < 0.05$ being considered significant.

2.5 Immunocytochemistry

In this project, we used immunocytochemistry technique to assess the ability of (a) Cmpd 101 to inhibit GRK 2 or 3 in AtT20FlpIn-hMOR cells (b) trametinib to inhibit MEK in AtT20FlpIn-CB1 cells.

2.5.1 Experimental procedures

Sterile coverslips coated with poly-D-lysine was placed carefully in 24-well plate. Cells supplemented in DMEM was seeded in low confluency to the 24-well plate and incubated overnight at 37°C. On the day of the assay, inhibitor (Cmpd 101/ trametinib) was prepared in DMEM, followed by an hour of incubation. Subsequently, drug was added onto these wells, keeping the parameters similar to that of MPA assay. Then, plate was placed in ice for a couple of minutes to which 4% PFA solution was added. Fixation was performed on ice for 5 mins followed by 10 more mins of incubation at RT, before washing three times with ice cold PBS. Cells were permeabilized with 0.25% Triton-X in PBS (called PBS-T) for 10 mins. Cells were washed with PBS-T for 5 mins with gentle agitation. These cells were then incubated in the blocking solution (1% BSA in PBS-T) for at least 30 mins, after which the cells were loaded with primary antibody diluted in blocking solution (pSer^{377} for Cmpd 101/ pERK for trametinib) for 1 hour at RT. Then, three washes with PBS-T were performed followed by incubation with Secondary Antibody diluted in blocking solution (anti rabbit Cy3 for Cmpd 101/ anti mouse Cy3 for trametinib). Last, wells were rinsed five times with PBS-T and the coverslips were mounted on slides with Prolong Gold with DAPI and allowed for drying in the dark before imaging. Coverslips were cleaned and images were obtained using Zeiss microscope.

2.5.2 Data Analysis

Images were analyzed using ZEN lite software and no statistical tests was performed as for the objective of this experiment was only to visually compare the controls with the treated.

3

Pharmacology of Valinate and tert- Leucinate Syntetic Cannabinoids

This chapter presents the pharmacology of recently emerged SCs with indole or indazole core featuring pendant-valinamide and tert-leucinamide groups. These SCs including MDMB-CHMICA, MDMB-CHMINACA, 5F-AMB and MDMB-FUBINACA and their analogues have become increasingly widespread and are reported to be associated with severe adverse health reactions. In spite of the extensive use of these SCs, a very little is known about their pharmacological and toxicological properties. In this chapter, we determined the activity of these SCs on human CB1 and CB2 receptors. This was achieved using high throughput fluorescence-based membrane potential assay (MPA) to measure potassium channel activation and subsequent cellular hyperpolarization in AtT20FlpIn-CB1/CB2 cells. The majority of work presented in this chapter has been recently published as a part of "The pharmacology of valinate and tert-leucinate synthetic cannabinoids 5F-AMBICA, 5F-AMB, 5F-ADB, AMB-FUBINACA, MDMB-FUBINACA, MDMB-CHMICA, and their analogues" (*Samuel D. Banister, Mitchell Longworth, Richard Kevin, Shivani Sachdev, Marina Santiago, Jordyn Stuart, James B. C. Mack, Michelle Glass, Iain S. McGregor, Mark Connor, Michael Kassiou*). This chapter represents my contribution to the paper, the concentration response curves for the other compounds were generated by Mark Connor in parallel experiments to mine.

3.1 Introduction

Many SCs have been reported in the past few years and the structural diversity of these compounds is growing incredibly[100-102]. For example, EMCDDA reported over 3600 MDMB-CHMICA seizures between 2014 and 2016[103]. MDMB-CHMICA was responsible for 29 deaths and 42 people were admitted to the hospital's emergency ward in European countries[103,104]. The recently emerged indole and indazole SCs featuring pendant-valinaminde and tert-leucinamide groups (Figure 5) appeared to be among the most prevalent in US over the last 12 months[105,106]. MDMB-FUBINACA was reported to be the most lethal SC till date as it accountable for more than 1000 hospitalization and 40 deaths in 2015[107,108]. 5F-AMB, first identified in Japan has recently topped the list of SCs extensively reported in U.S, stated in National Forensic Laboratory Information System (NFLIS) 2015[109]. MDMB-CHMICA, first recognized in Hungary, but has since been reported to EWA in France, U.K, Mauritius and Turkey[110]. Moreover, a recent report on clinical toxicity associated with exposure to MDMB-CHMICA has been issued[111]. They recorded clinical details of seven males on exposure to MDMB-CHMICA, which involved acidosis, unconsciousness or coma, mydriasis, heart rate disturbances and convulsions[111]. MDMB-CHMINACA was more closely related to MDMB-FUBINACA than other SCs, which caused dozens of deaths and hundreds of hospitalizations in Russia as a result of intoxication[112]. In this chapter we have also presented the pharmacology of 5F-MDMB-PICA, most potent of the SCs we identified in this series. This chapter aims at providing the pharmacological data for selected members (MDMB-CHMICA, MDMB-CHMINICA, 5F-AMB and MDMB-FUBINACA) of this class of SCs on human CB1 and CB2 receptors.

5F-AMBICA (**10**: R = H; X = CH)
5F-MDMB-PICA (**11**: R = CH$_3$; X = CH)
5F-AMB (**12**: R = H; X = N)
5F-ADB (**13**: R = CH$_3$; X = N)

AMB-FUBICA (**14**: R = H; X = CH)
MDMB-FUBICA (**15**: R = CH$_3$; X = CH)
AMB-FUBINACA (**16**: R = H; X = N)
MDMB-FUBINACA (**17**: R = CH$_3$; X = N)

AMB-CHMICA (**18**: R = H; X = CH)
MDMB-CHMICA (**19**: R = CH$_3$; X = CH)
AMB-CHMINACA (**20**: R = H; X = N)
MDMB-CHMINACA (**21**: R = CH$_3$; X = N)

AMBICA (**22**: R = H; X = CH)
MDMB-PICA (**23**: R = CH$_3$; X = CH)
AMB-PINACA (**24**: R = H; X = N)
MDMB-PINACA (**25**: R = CH$_3$; X = N)
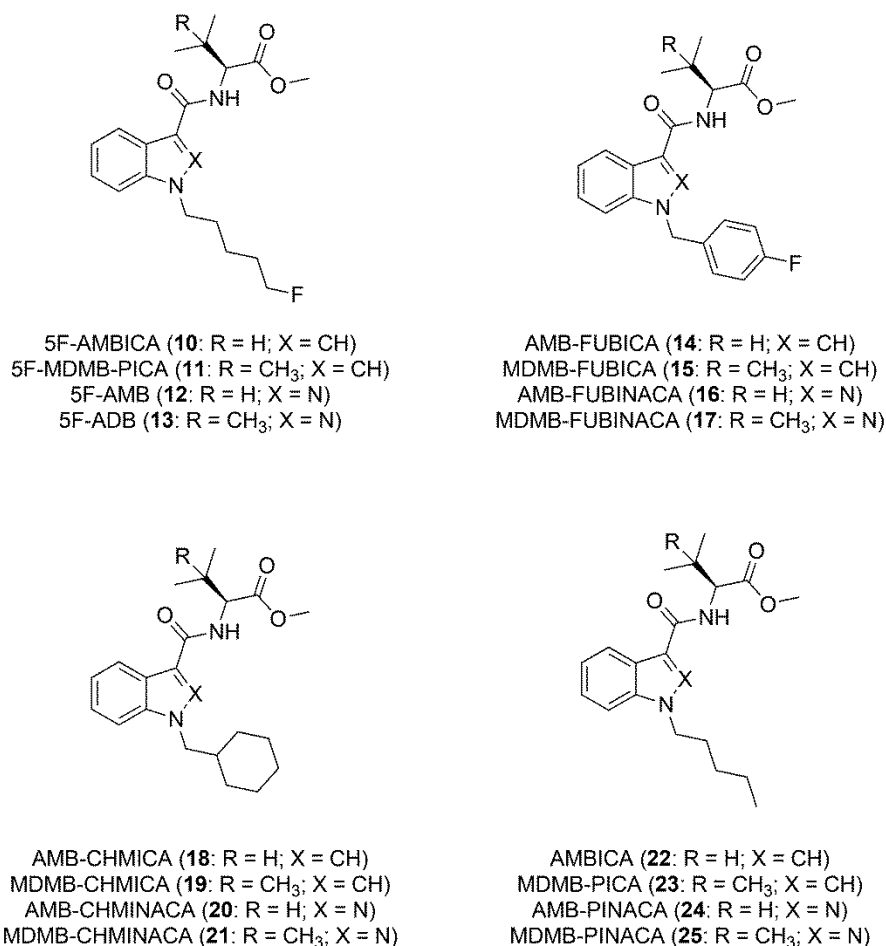
Figure 6: This figure represents the chemical structure of newly evolved SCs featuring pendant methyl-valinate and methyl tert-leucinate functional groups. As shown in figure 10, 11, 14 15, 18, 19, 22 and 23 are SCs with indole core; while 12, 13, 16, 17, 20, 21, 24 and 25 have indazole core. Each of them either has 5-fluoropentyl, 4-fluorobenzyl, cyclohexylmethyl or pentyl substiutuent at the 1 position, and valinate or tert leucinate methyl ester side chains, at the 3-position (-R)[58].

3.2 Results

3.2.1 Activity of SCs on CB1 and CB2 receptor

The SCs caused a rapid, concentration-dependent decrease in fluorescence when applied on AtT20FlpIn-CB1 or CB2 cells loaded with MPA dye, reflecting hyperpolarization of cell on activation of GIRK channel. Example traces are illustrated in Figure 6. Data from each of the experiment (n=6) was then analysed as outlined in the methods and normalized to the maximal effective concentration of CP-55,940 (1 µM).

A set of concentration response curve of all cannabinoids including $\Delta 9$ -THC, CP-55,940 and SCs is shown in Figure 7.

 It was found that CP-55,940 (1 µM) decreased fluorescence by 31±1% in AtT20FlpIn-CB1 cells, and 26±1% in AtT20FlpIn-CB2 cells (Figure 7).

Figure 6 (following page): Representative traces showing the change in fluorescence normalized to the predrug baseline, produced by SCs on activation of CB receptor as a result of potassium channel mediated cellular hyperpolarization. This figure illustrates the response of A) MDMB-CHMICA, B) MDMB-CHMINACA, C) 5F-AMB, D) MDMB-FUBINACA; on AtT20FlpIn-CB1 and AtT20FlpIn-CB2.

AtT20FlpIn-CB1

A

RFU (% Predrug) — MDMB-CHMICA
- 1 μM
- 10 nM
- 100 pM
- CP (1μM)

B

RFU (% Predrug) — MDMB-CHMINACA
- 1 μM
- 3 nM
- 1 nM
- CP (1μM)

C

RFU (% Predrug) — 5F-AMB
- 1 μM
- 1 nm
- 100 pm
- CP (1μM)

D

RFU (% Predrug) — MDMB-FUBINACA
- 100 nM
- 3 nM
- 10 pM
- CP (1μM)

AtT20FlpIn-CB2

A

RFU (% Predrug) — MDMB-CHMICA
- 10 μM
- 100 nM
- 10 nM
- CP (1μM)

B

RFU (% Predrug) — MDMB-CHMINACA
- 1 μM
- 100 nM
- 1 nM
- CP (1μM)

C

RFU (% Predrug) — 5F-AMB
- 1 μM
- 30 nM
- 100 pM
- CP (1μM)

D

RFU (% Predrug) — MDMB-FUBINACA
- 1 nM
- 30 nM
- 100 pM
- CP (1μM)

A

Δ Fluorescence (%)

CB1, EC$_{50}$ 42 nM
CB2, EC$_{50}$ 68 nM

log [CP 55,940]

B

% CP 55,940 (1 μM)

CB1, EC$_{50}$ 171 nM
CB2

log[Δ^{9}THC]

C

% CP 55,940 (1 μM)

CB1, EC$_{50}$ 10 nM
CB2, EC$_{50}$ 71 nM

log [MDMB-CHMICA]

D

% CP 55,940 (1 μM)

CB1, EC$_{50}$ 10 nM
CB2, EC$_{50}$ 128 nM

log [MDMB-CHMINACA]

E

% CP 55,940 (1 μM)

CB1, EC$_{50}$ 1.9 nM
CB2, EC$_{50}$ 10 nM

log [5F-AMB]

F

% CP 55,940 (1 μM)

CB1 EC$_{50}$ 3.9 nM
CB2, EC$_{50}$ 55 nM

log [MDMB-FUBINICA]

G

% CP 55,940 (1 μM)

CB1, EC$_{50}$ 0.45 nM
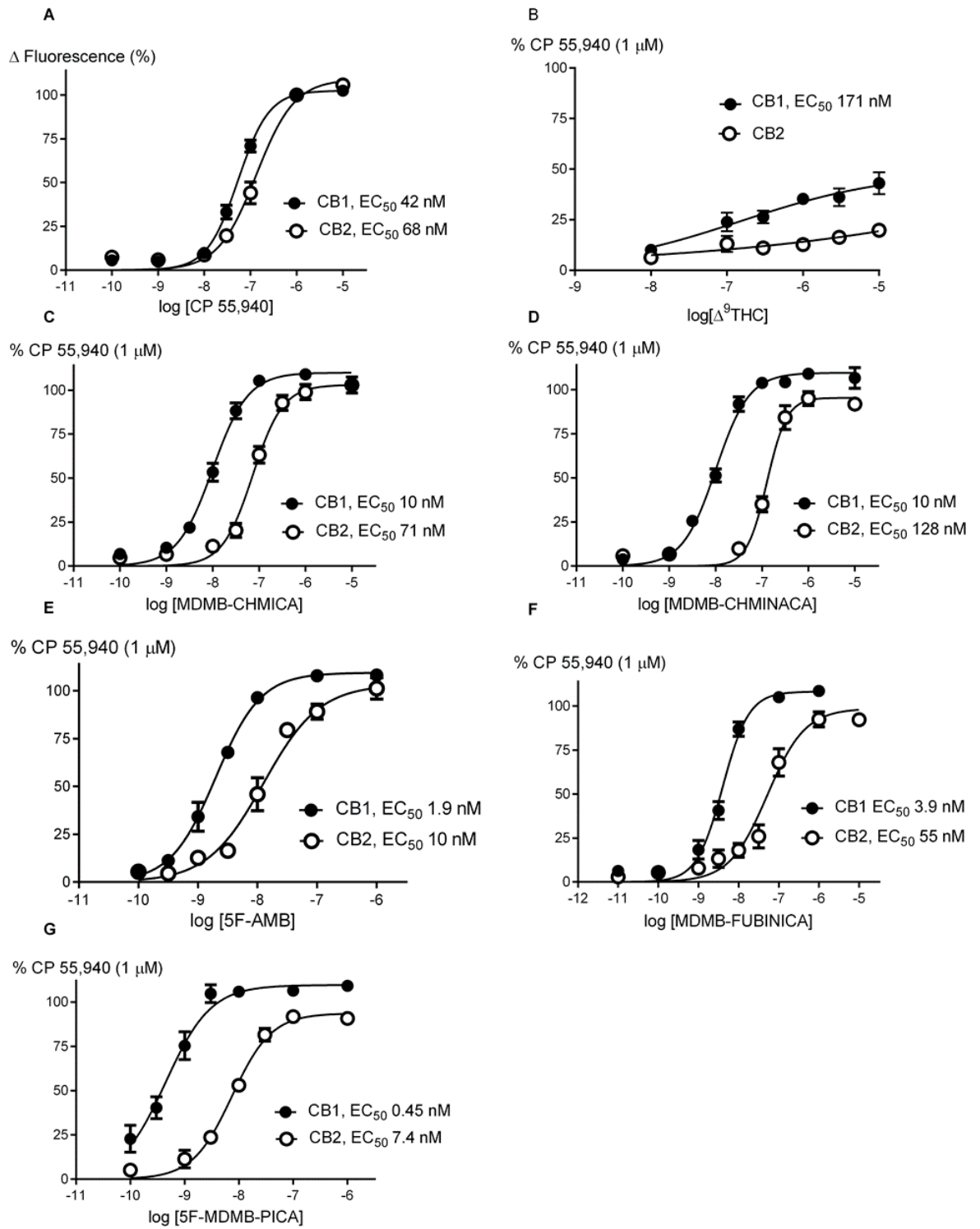CB2, EC$_{50}$ 7.4 nM

log [5F-MDMB-PICA]

29

Figure 7: Concentration response curve (CRC) for changes in fluorescence of AtT20FlpIn-CB1/CB2 cells induced by A) CP-55,940; B) Δ^9-THC; C) MDMB-CHMICA; D) MDMB-CHMINACA; E) 5F-AMB; F) MDMB-FUBINACA, G) 5F-MDMB-PICA; Data is expressed as a percentage of fluorescence produced by maximal effective concentration of CP-55,940 (1 µM). Each point represents the mean ± SEM of 6 independent determinants, performed in duplicate. Data was fitted with four parameters logistic equation, bottom constrained to zero in GraphPad Prism.

As shown in Table 2, all the SCs had a higher potency (0.45 to 10 nM) than either Δ^9-THC (171 nM) or CP-55,940 (42 nM) at CB1 receptor. The most potent SC, 5F-MDMB PICA, was 380 times more potent than Δ^9-THC and 90 times more potent than CP-55,9540. As previously reported for this assay, Δ^9-THC was found to be a low efficacy agonist at CB2 receptors[43-45]. The maximum hyperpolarization of AtT20-FlpIn-CB2 cells induced by Δ^9-THC at 10 µM was 20 ± 3% of that mediated by the maximal effective concentration of CP-55,940. At CB2 receptor MDMB-CHMICA and MDMB-CHMINACA were less potent than CP-55,940. However, MDMB FUBINACA and 5F-MDMB-PICA were slightly more potent than CP-55,940 at CB2. Thus, all the SCs activated CB1 and CB2 receptor, with a mild preference for CB1 over CB2. 5F-MDMB-PICA showed 16 times higher selectivity for CB1 to that of CB2 receptors. Moreover, all the SCs had a similar E_{max} to that of CP-55,940, indicating that all these SCs are also high efficacy agonists.

Compound	hCB$_1$	hCB$_1$	hCB$_2$	hCB$_2$	CB$_1$ sel.
	pEC$_{50}$ ± SEM (EC$_{50}$, nM)	Max ± SEM (% CP 55,940)	pEC$_{50}$ ± SEM (EC$_{50}$, nM)	Max ± SEM (%CP 55,940)	(EC$_{50}$CB1/ EC$_{50}$CB2)
Δ^9-THC	6.77 ± 0.05 (171)	50 ± 11	-	20 ± 3 at 10 μM	-
CP 55,490	7.47 ± 0.05 (42)	-	7.17 ± 0.07 (68)	-	1.6
MDMB-CHMICA	8.00 ± 0.05 (10)	112 ± 3	7.15 ± 0.05 (71)	103 ± 3	7.1
MDMB-CHMINACA	7.99 ± 0.04 (10)	111 ± 2	6.89 ± 0.04 (128)	96 ± 3	12.8
5F-AMB	8.71 ± 0.04 (1.9)	109 ± 3	7.99 ± 0.13 (10)	103 ± 7	5.3
MDMB-FUBINACA	8.41 ± 0.04 (3.9)	108 ± 3	7.26 ± 0.14 (55)	101 ± 9	14.1
5F-MDMB-PICA	9.35 ± 0.07 (0.45)	110 ± 4	8.13 ± 0.05 (7.4)	94 ± 3	16.4

Table 2 represents the functional activity of Δ^9-THC, CP-55,940 and SCs at CB1 and CB2 receptors. Data represents mean value ± SEM for 6 experiments, each in duplicate.

3.2.2 Effects of SCs on AtT20FlpIn-WT cells:

The activity of these SCs was assessed on AtT20FlpIn-WT cells. When applied at 10 µM, none of these SCs produced a significant change in the membrane potential of AtT20FlpIn-WT cells, which do not express CB1 or CB2 receptors (Figure 8). A substantial drop in fluorescence was observed for maximal effective concentration of SST (100 nM). We also found that the change in membrane potential of WT cells induced by SST, was unaffected by SCs.
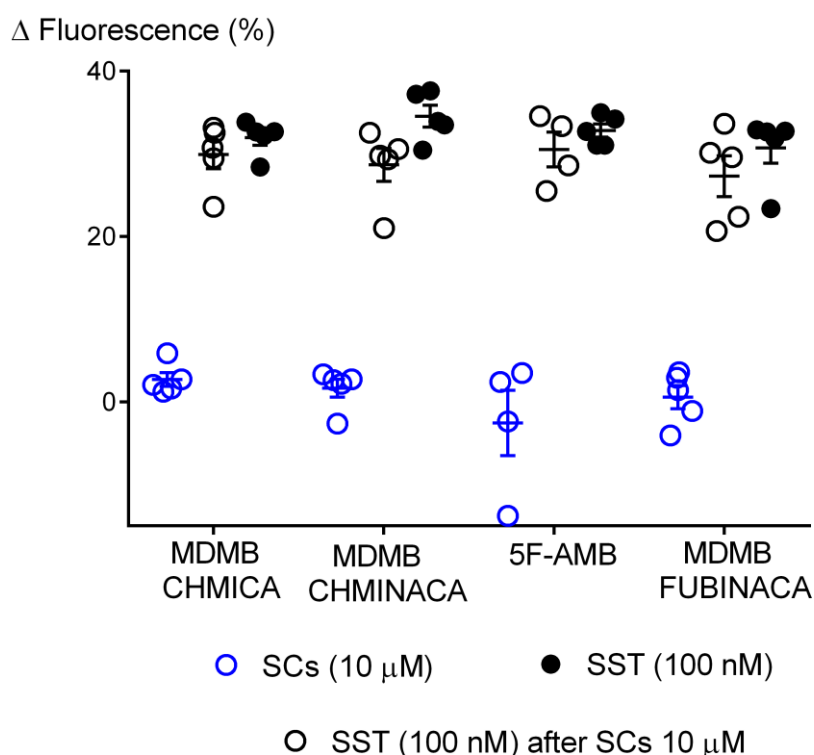

Figure 8: Scatter dot plot representing the percentage change in fluorescence for SC's (10 µM), SST (100 nM) alone and SST in the continued presence of SCs in AtT20FlpIn-WT cells. SCs showed no significant drop in fluorescence. The percentage change in fluorescence between SST alone and SST after SCs was not different. Data represents mean ± SEM, n=4-5.

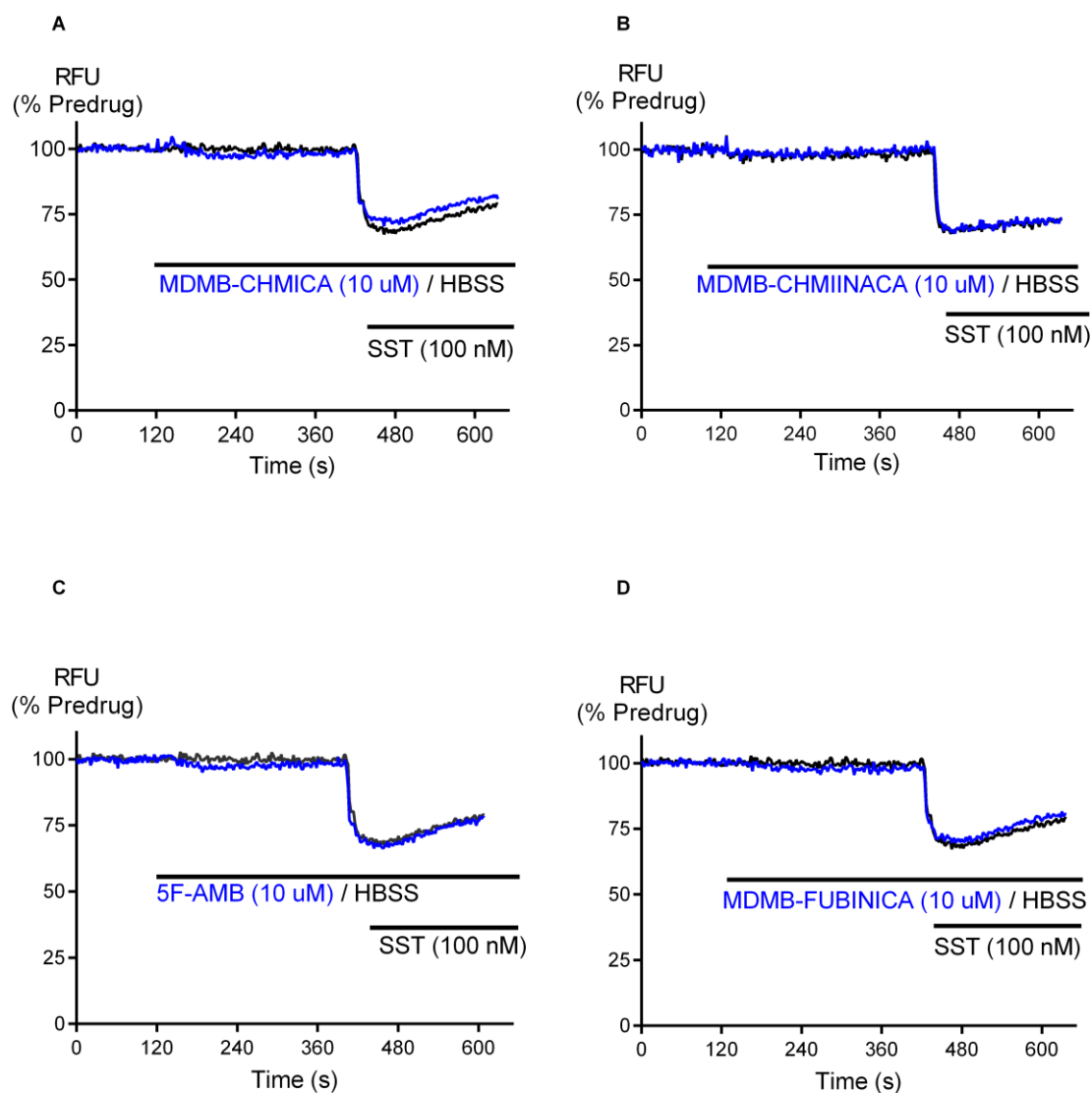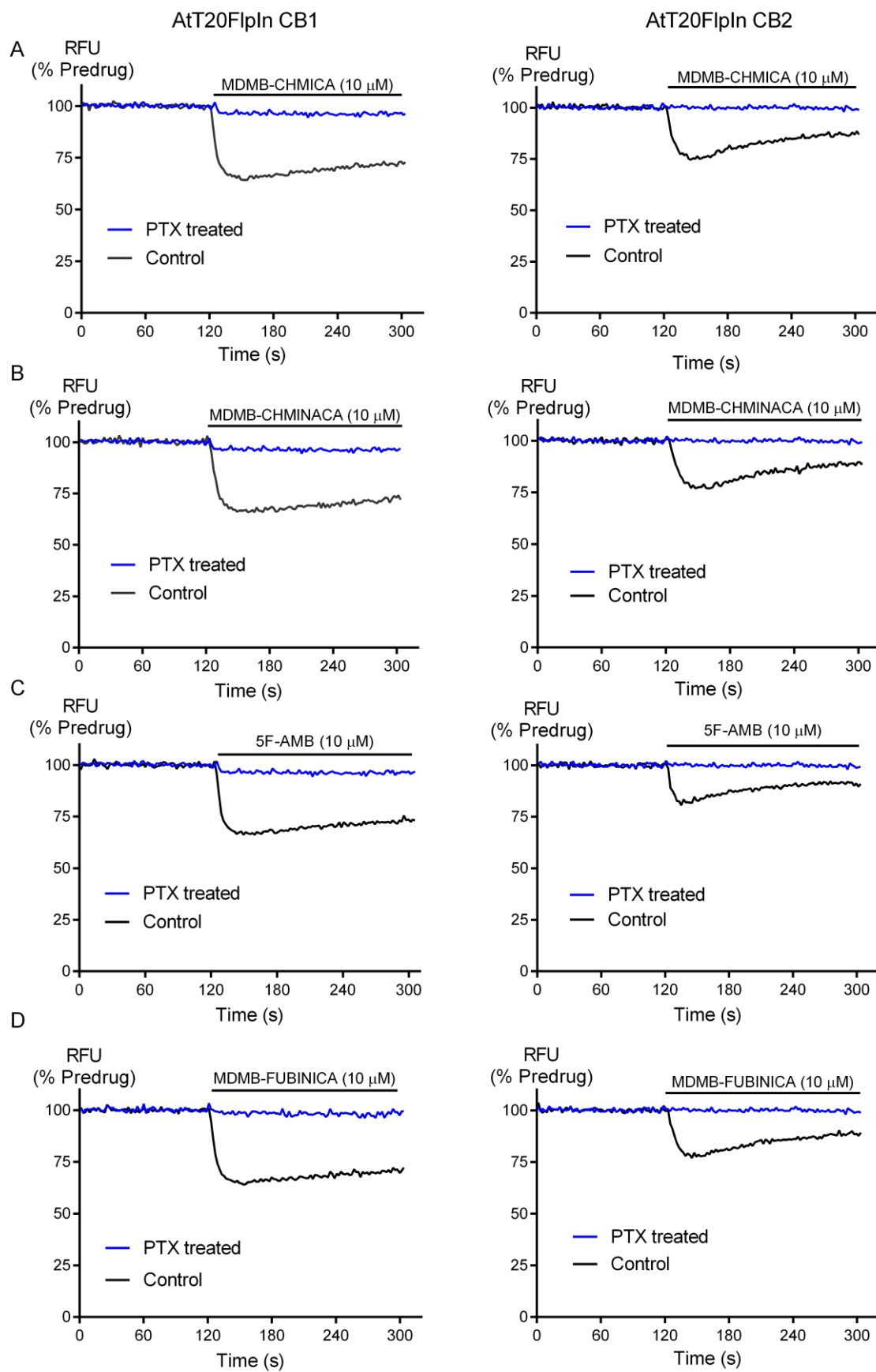Figure 9: Trace of fluorescent signal from AtT20FlpIn-WT cells exposed to 10 µM of A) MDMB-CHMICA, B) MDMB-CHMINACA, C)5F-AMB, D) MDMB-FUBINACA followed by SST upon it for 5 minutes. The traces represented are normalized to the predrug baseline followed by blank subtraction. No drop in fluorescence was observed for SCs on WT cells, although a significant drop in fluorescence was observed for SST (100 nM).

3.2.2 Effect of SCs on AtT20FlpIn-CB1/CB2 cells treated with Pertussis toxin:

Cells were incubated overnight with 200 ng/ml PTX, adjacent to the control cells (untreated). We observed that SC induced hyperpolarization was abolished by the treatment with PTX to that of control cells which showed normal hyperpolarization on exposure to high concentration of SCs (Figure 10).

In addition to this 4 compound characterized in this Chapter, I also determined the effects of 12 related SCs in AtT20FlpIn-WT cells and AtT20FlpIn-CB1 and CB2 treated with PTX. This data is summarized in the Appendix.

Figure 10 (following page): Representative traces showing the change in fluorescence normalized to the predrug baseline for A) MDMB-CHMICA, B) MDMB-CHMINACA, C) 5F-AMB, D) MDMB-FUBINACA at 10 μM on AtT20FlpIn-CB1 and AtT20FlpIn-CB2 with and without PTX treatment. PTX treated cells (blue trace) shows no drop in the fluorescence than that of control cells.

AtT20FlpIn CB1 | AtT20FlpIn CB2

A. RFU (% Predrug) — MDMB-CHMICA (10 μM); PTX treated; Control

B. RFU (% Predrug) — MDMB-CHMINACA (10 μM); PTX treated; Control

C. RFU (% Predrug) — 5F-AMB (10 μM); PTX treated; Control

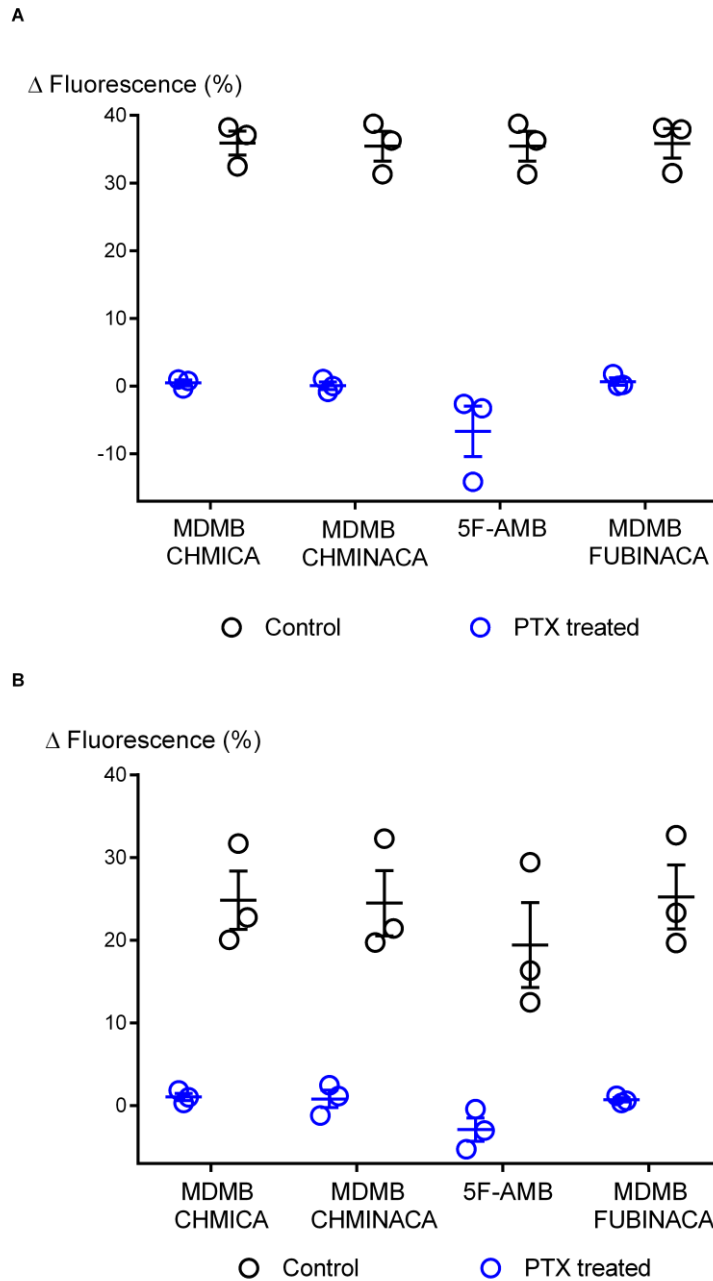D. RFU (% Predrug) — MDMB-FUBINICA (10 μM); PTX treated; Control

Figure 11: Scatter dot plot representing the percentage change in fluorescence of SCs on AtT20 cells expressing A) CB1, B) CB2, treated with PTX and control (HBSS). The PTX treated cells abolished the response of SCs completely as compared to control, signifying PTX sensitive $G\alpha_i$ mediated signaling. Data represents mean ± SEM, n=3, each in duplicate.

3.3 Discussion

In this study, we have used real time assay to determine the pharmacology of recently emerged illicit synthetic cannabinoids by evaluating their activity on human CB1 and CB2 receptors. All the indole and indazole SCs featuring a valinate or tert-leucinate group activated CB1 and CB2 receptor. These consistent observations have confirmed that SCs are likely to act through CB1 and CB2 receptors. Our data demonstrate that all the SCs had a greater efficacy and potency than that of Δ^9-THC or CP-55,940 for CB1 receptor mediated hyperpolarization. Thus, the more pronounced effects of SCs in comparison to Δ^9-THC could have a correlation to the high potency of these SCs at CB receptor, if a higher relative dose of SCs are consumed than Δ^9-THC. A recent report issued by EMCDDA on July 2016 suggests that a range of doses of MDMB-CHMICA from 0.1 to 15 mg has been used in self-prepared preparations, although a dose above 1 mg could potentially cause severe toxicity[113].

Agonist efficacy depends on the relationship between the degree of the physiological response produced by the drug to the number of receptors occupied in the system. Over past decades, researchers have established that CP-55,940 exhibits higher efficacy at CB receptors as compared to that of Δ^9-THC, which is a lower efficacy CB1 agonist[114]. Our results suggested that all the SCs showed a similar maximal effect (E_{max}) to CP-55,940 at CB receptors indicating that these SCs are also high efficacy agonists. SCs may activate CB1 receptor with higher efficacy than that of CP-55,940 is yet to be determined.

CB receptor agonists affect the central nervous system (CNS), which includes disruption of psychomotor behavior, short-term memory loss, intoxication, stimulation of appetite, antiemetic effects, and antinociceptive actions[115]. There is substantial evidence on the psychoactive effects of the cannabinoids attributable to CB1 receptor activation. The low doses of cannabinoids was found to produce a mixture of stimulatory and depressant effects, whereas higher dose of this may lead to tranquillity and distortions in both hearing and vision[116]. As seen in table 2, all SCs showed a modest preference for CB1 receptor as compared to CB2 receptors. Our findings are consistent with the role of the CB1 receptor for the psychoactive effects of SCs, although some abused SCs have been reported to be relatively non-selective or even CB2-preferring. For example, UR-144 was found to have a higher affinity towards CB2 receptor to that of CB1[117]. Wiley et al. 2013, demonstrated that UR-144 activated CB1 and CB2 receptors with similar pharmacological profile as other abused indole-derived cannabinoids, suggesting the psychoactive properties of UR 144[118].

Consistent with this, our group showed that UR 144 activated CB2 receptor with a greater potency than CB1 receptor *in vitro*[55].

This study also explored the structure-activity relationship of this class of SCs at human CB1 and CB2 receptors. It has been shown that the addition of fluorine group in the terminal position of SCs increases the binding affinity at both CB1 and CB2 receptors[55]. Consistent with this observation, our findings highlight that 5F-MDMB-PICA with 5-fluoropentyl moiety is the most potent at CB1 and CB2 receptors. This group of SCs also differ from each other by presence of L-valinamide or L-tert-leucinamide at position 3. The addition of an extra methyl group increased the potency of SCs with L-tert-leucinamide (5F-MDMB-PICA, MDMB-FUBINACA, MDMB-CHMINACA) compared to its L-valinamide counterparts at both CB1 and CB2 receptors. Furthermore, our data show that SCs with indazole in its core structure has proved to have a higher potency at CB1 receptors than that of its corresponding indole analogues, similar to the previously published results with cannabimimetic indole and indazole derivatives[119].

As suggested by J.W Huffman 2005, the CB receptor activation by its ligand considerably depends on hydrophobicity and aromatic-aromatic interactions for binding[120]. Although this recent group of SCs with amino acid in its side chain have higher potency and efficacy than earlier indole or indazole SCs with aromatic character. This proves that an aromatic entity at position 3 of indole or indazole SCs is not essential for ligand interaction to take place at CB receptors. It has been shown that indole or indazole based SCs binds to different residue in the binding pocket of CB receptor than classical cannabinoids[121]. It might be possible that this particular group of indole or indazole SCs, which lacks the aromatic character, has unique way of binding to CB receptors. The activation of CB receptors with these high efficacy SCs can be attributed to the difference in the binding to CB receptor as compared to earlier indole or indazole SCs with aromatic character, but this clearly needs much more study.

Having demonstrated that these SCs are potent and efficacious at CB receptors, we sought to examine any off target activity of SCs on AtT20-FlpInWT cells, which do not express CB1 and CB2 receptors but have native somatostatin receptors. We found that there is no effect of SCs on WT cells. Our data also indicate that these SCs, even at its high concentration, do not interfere with GIRK as observed from the unchanged response of SST, which activate the same channel as SCs. Thus, it seems very unlikely that this factor

contributes to SCs-related toxicity. Perhaps future research is needed to determine the pharmacology of these compounds at other off target to see if SCs promiscuity has detrimental contribution to its severe toxicity.

To confirm that the observed signaling was mediated via Gi coupling to CB1 or CB2 receptors, we determined the activity of SCs on AtT20FlpIn-CB1/CB2 cells treated with PTX. Our data shows that the response of SCs was completely blocked by overnight treatment with PTX, suggesting that SCs mediated PTX sensitive hyperpolarization was $G\alpha_i$ coupled, further implicating GIRK mediation. Thus, our studies have found that these SCs follows the similar signaling pathway as the existing cannabinoids with the most obvious difference between SCs that had higher potency and efficacy, at both CB1 and CB2 receptors[122].

4

Desensitization of CB1 and CB2 receptor Signaling by valinate and tert-leucinate Synthetic Cannabinoids.

CONTENTS

In this chapter we have examined (homologous and heterologous) desensitization of SCs (MDMB-CHMICA, MDMB-CHMINACA, 5F-AMB, MDMB-FUBINACA and 5F-MDMB-PICA) on CB1 and CB2 receptor. We have also investigated the multiple mechanisms that underlie desensitization of CB1 receptor in the presence of 5F-MDMB-PICA, most potent of these SCs. We investigated the effect of inhibiting GRK 2 or 3 and ERK1/2 on CB1 receptor desensitization. Acute desensitization has been extensively studied in the context of opioid and β-adrenergic receptor but much less is known about the signaling pathway regulating desensitization of CB1 receptors. The work presented in this chapter has not been published.

4.1 Introduction

Signaling via GPCR is a highly regulated process. Following activation, the receptor often undergoes desensitization when exposed to a ligand for a prolonged period of time. Desensitization is a complex phenomenon, defined as a rapid loss in the responsiveness of receptor function. Receptor desensitization is often mediated via phosphorylation by GRK, this phosphorylation facilitates the binding of β-arrestin to the receptor and promotes internalization[67-69]. However, the mechanism underlying desensitization of receptor is not entirely regulated by GRKs. Other non-GRKs like PKC, PKA, MEK, ERK1/2, JNK and CAMKII, which may as well contribute to the homologous and heterologous desensitization has been intensely studied for different receptors[73]. Few data are available to address the role of β-arrestin and GRKs in CB1 receptor desensitization. Jin et al. in 1999, provided first evidence of the involvement of GRK3 and β-arrestin2 in CB1 receptor desensitization in *Xenopus* oocytes[85]. The coexpression of GRK3 and β-arrestin2 in *Xenopus* oocytes significantly enhanced desensitization compared with cell expressing either GRK3 or β-arrestin2 alone. It has also been reported that the expression of dominant negative β arrestin2 and GRK3 in hippocampal neurons reduced the CB1 receptor desensitization[122]. Moreover, it has been established that the C terminus of CB1 receptor is required for desensitization in AtT20 and HEK 293 cells[85,123]. Phosphorylation of serine residues 426 and 430 in C terminus of the CB1 receptor was found to be involved in GRK3 and β-arrestin2 dependent CB1 receptor desensitization; however, mutation of these residues was found to make no difference in the internalization of CB1Rs in HEK 293 and AtT20 cells[80]. On the other hand, Daigle et al. in 2008 showed that serine and threonine residues in the extreme C-terminus of CB1 receptor are involved in both desensitization and internalization[124]. It remains unclear whether the desensitization of CB1 receptor is affected by GRK 2 or 3, furthermore there is no robust evidence for the role of GRK 2 or 3 in SCs mediated CB1 receptor desensitization.

There has been considerable interest in the role of MAPK pathways in CB1Rs activation. The classical pathway of ERK activation is via MAPK pathways, however ERK can be activated through different pathways that is MAPK independent, as reported for MOR[125,126]. It has been known that cannabinoids activate p38 MAPK but not JNK in rat hippocampal slices[127,128]. Whereas Downer et al. 2003, showed that JNK was activated, when stimulated with THC in cultured cortical neurons[129]; however, no ERK1/2 p38 MAPK and JNK activation was observed for another agonist HU-210[130]. It was also reported that HU-210 activated only ERK1/2, independent of MAPK pathway in Neuro2a cells[131], which

endogenously expresses cannabinoid receptor. Although another study revealed the activation of JNK via Src kinase in Neuro2a cells[132]. Daigle et al. in 2008, evaluated the parameters affecting ERK1/2 activity in HEK 293 cells expressing CB1 receptor. This study indicates that there was rapid inactivation of ERK1/2 activity during prolonged stimulation of CB1, regulated by receptor desensitization. Also, ERK1/2 activation (or inactivation) was unaffected by CB1 receptor internalization[123]. Thus, from the data available till date, a potential role of ERK1/2 in CB1 receptor desensitization remains to be elucidated. The activation of ERK1/2 also seems to depend on the cell type and different agonist that can activate ERK1/2 via different pathways, adding more complexity than clarity. We used AtT20 cells for all the experiment, reported to have high basal level of ERK1/2; taking advantage of this cell type, we examined the role of ERK1/2 in CB1 receptor desensitization.

4.2 Results

4.2.1 Desensitization of CB receptor signaling in AtT20 cells mediated by SCs

Prolonged application of SCs at their EC_{50} and EC_{90} concentration produced a hyperpolarization that slowly reversed over time when applied on AtT20FlpIn-CB1 cells for 30 minutes. We observed that trace for SC induced hyperpolarization of AtT20 cell plateaued after about 20 mins (Figure 12)

CB1 receptor activity declined more in the continued presence of EC_{90} (3 nM) than that of EC_{50} (1 nM) of 5F-MDMB-PICA (Figure 12). The percentage decline in CB1 receptor signal mediated by EC_{50} and EC_{90} of 5F-MDMB-PICA was found to be $65 \pm 5\%$ and $78 \pm 1.5\%$ respectively. A second addition of CP-55,940 (1 μM) or SST (100 nM) was used to assess the homologous or heterologous desensitization of CB1 receptor. The response of CP-55,940 was significantly reduced on continuous application of 5F-MDMB-PICA at EC_{90} concentration when compared to CP-55,940 alone (Figure13), whereas no significant change in the fluorescence was observed for SST (100 nM) after 30 mins of 5F-MDMB-PICA to that produced by SST alone (Figure 13). Also no significant desensitization of the SST response was detected after 30 minutes of the EC_{50} concentration of 5F-MDMB-PICA (Figure 13). There was a significantly larger inhibition of the CP 55,940 response produced by EC_{90} than EC_{50} 5F-MDMB-PICA (Figure 13).

Like CB1 receptor, CB2 receptor also shows a decline in the hyperpolarization produced by continuous exposure to EC_{50} (10 nM) and EC_{90} (30 nM) of 5F-MDMB-PICA (Figure 14). The percentage desensitization for EC_{50} ($41\pm9.1\%$) of 5F-MDMB-PICA is half to that produced by its EC_{90} ($80\pm1.1\%$) concentration (Figure 16). A similar pattern of homologous desensitization was observed for CB2 receptors as that of CB1 receptors; although CB2 receptor also mediates heterologous desensitization presented as a significant change in the fluorescence of SST (100 nM) after 30 mins of EC_{90} 5F-MDMB-PICA to that produced by SST alone (Figure 15).
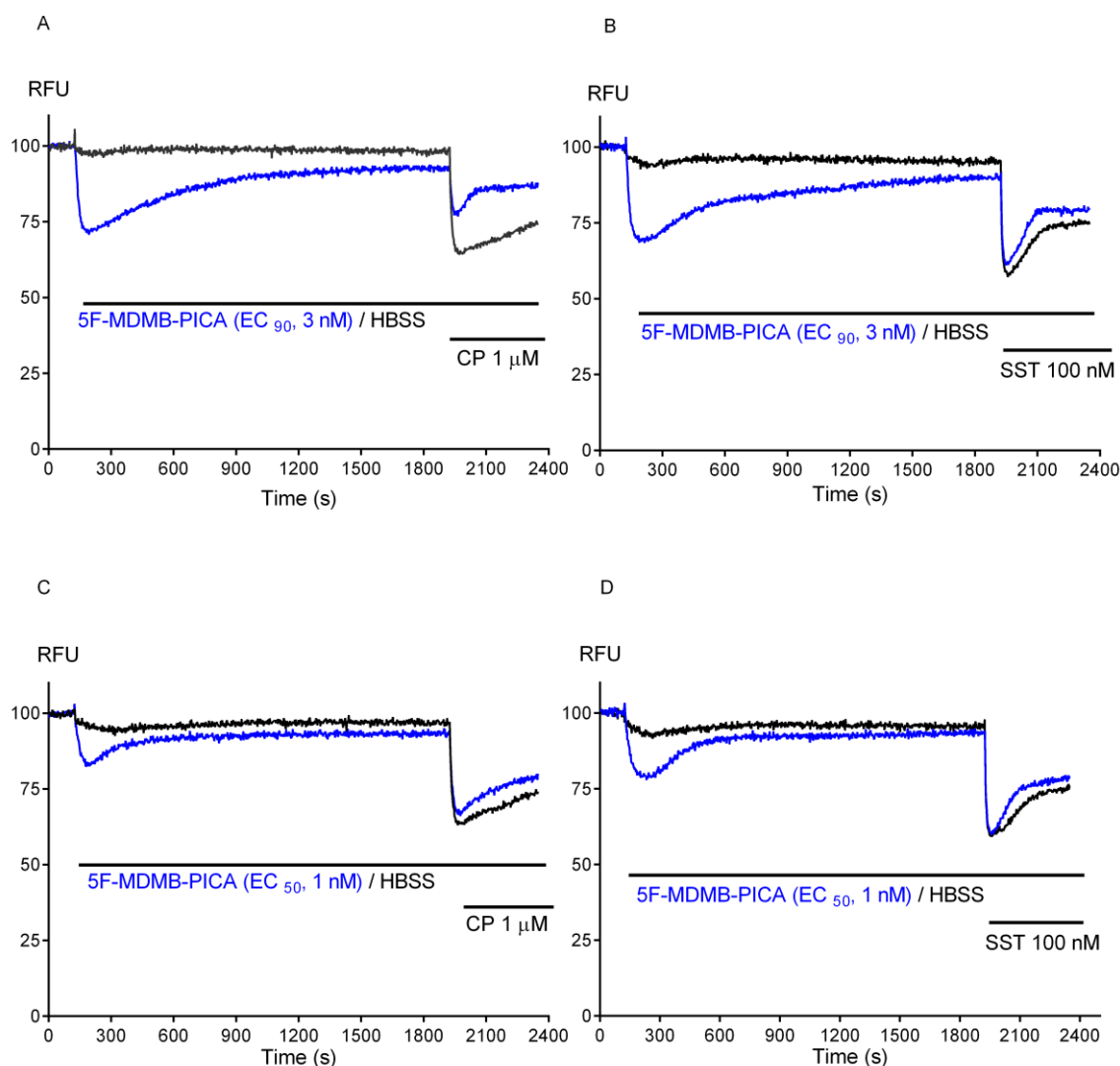
Figure 12 : Homologus and heterologus CB1 receptor desensitization in AtT20 cells. Represntative normalized traces showing the changes in fluorescence produced by 5F-MDMB-PICA on activation of CB1 receptor as a result of cellular hyperpolarization for 30 minutes. This figure shows that the continuous application of A) 5F-MDMB-PICA (EC$_{90}$, 3 nM) and B) 5F-MDMB-PICA (EC$_{50}$, 1 nM) reduces the response to a subsequent addition of CP-55,940 or SST. Traces A and C represents the homologous desensitization, challenged with CP-55,940 (1 μM) in the continuous presence of 5F-MDMB-PICA to that of CP-55,940 alone, trace B and D shows heterologous desensitization, challenged with SST (100 nM) after 30 minutes of 5F-MDMB-PICA.
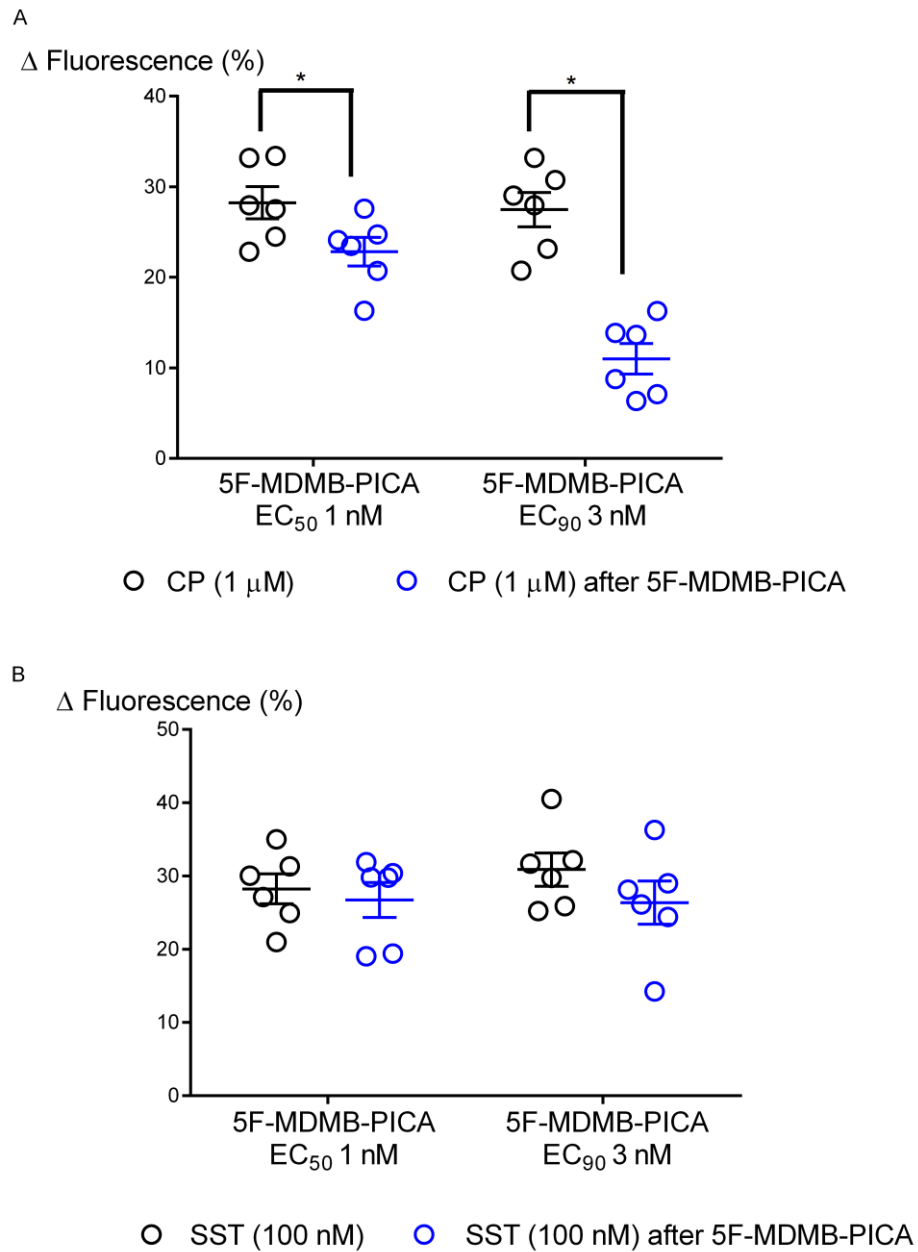
Figure 13: Scatter dot plot representing the percentage change in fluorescence reflecting (A) homologous and (B) heterologous desensitization of CB1 receptor mediated by EC_{50} (1 nM) and EC_{90} (3 nM) of 5F-MDMB-PICA. This figure shows the hyperpolarization of AtT20FlpIn-CB1 cells stimulated with 5F-MDMDB-PICA/HBSS (vehicle) for 30 minutes to the subsequent addition of A) CP-55,940 (1μM); B) SST (100 nM); Data represents mean ± SEM, of n=6, * indicates *P*-value < 0.05
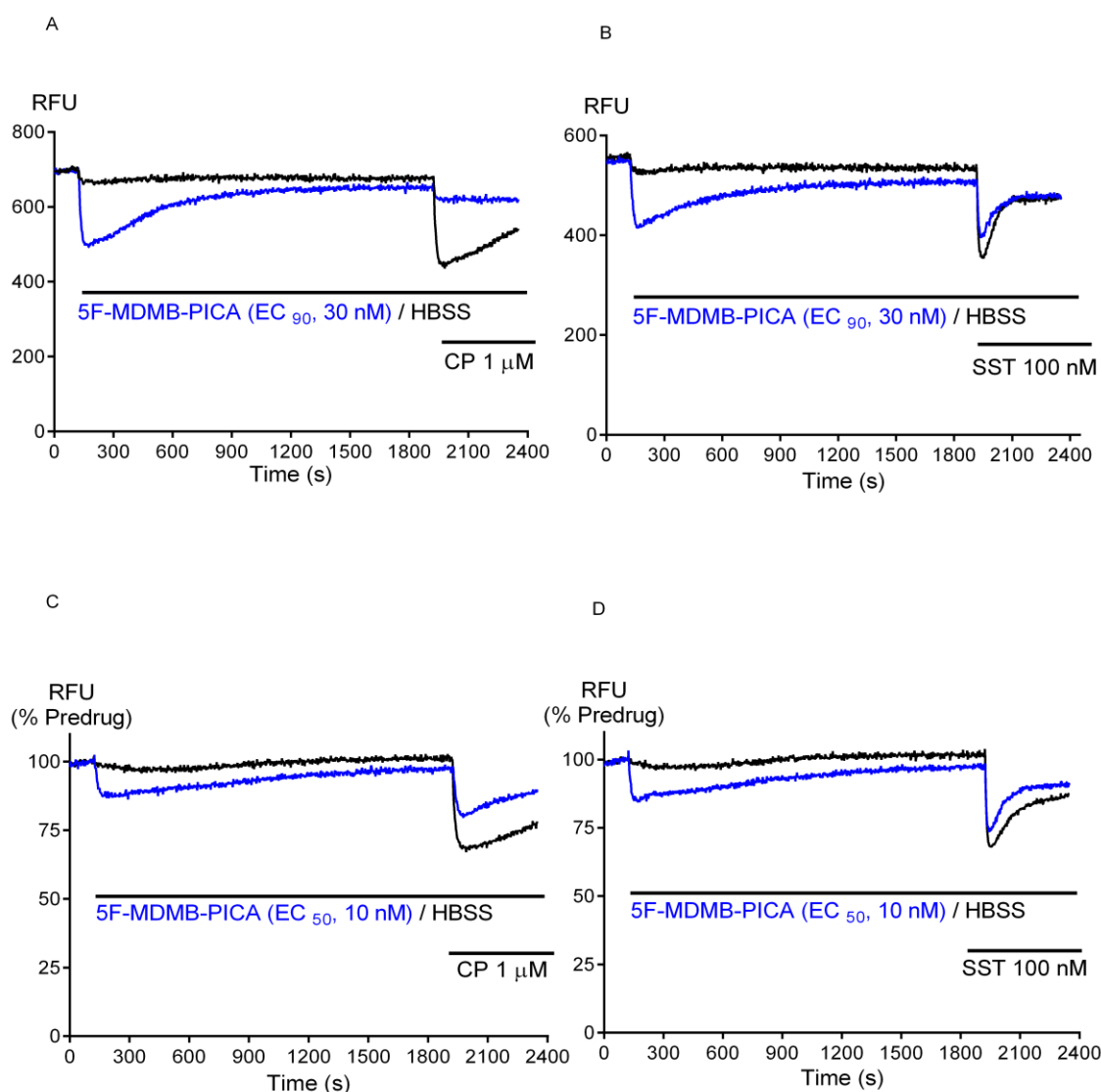
Figure 14: Homologous and heterologous CB2 receptor desensitization in AtT20 cells. Representative raw trace (AandB), and normalized trace (CandD) showing the changes in fluorescence produced by 5F-MDMB-PICA on activation of CB2 receptor as a result of cellular hyperpolarization for 30 minutes. This figure shows that the continuous application of A) 5F-MDMB-PICA (EC_{90}, 30 nM) and B) 5F-MDMB-PICA (EC_{50}, 10 nM), reduces the response to a second addition of CP-55,940 or SST. Traces A and C represents the homologous desensitization, challenged with CP-55,940 (1 µM) in the continuous presence of 5F-MDMB-PICA to that of CP-55,940 alone, traces B and D shows heterologous desensitization, challenged with somatostatin (100 nM) after 30 minutes of 5F-MDMB-PICA.
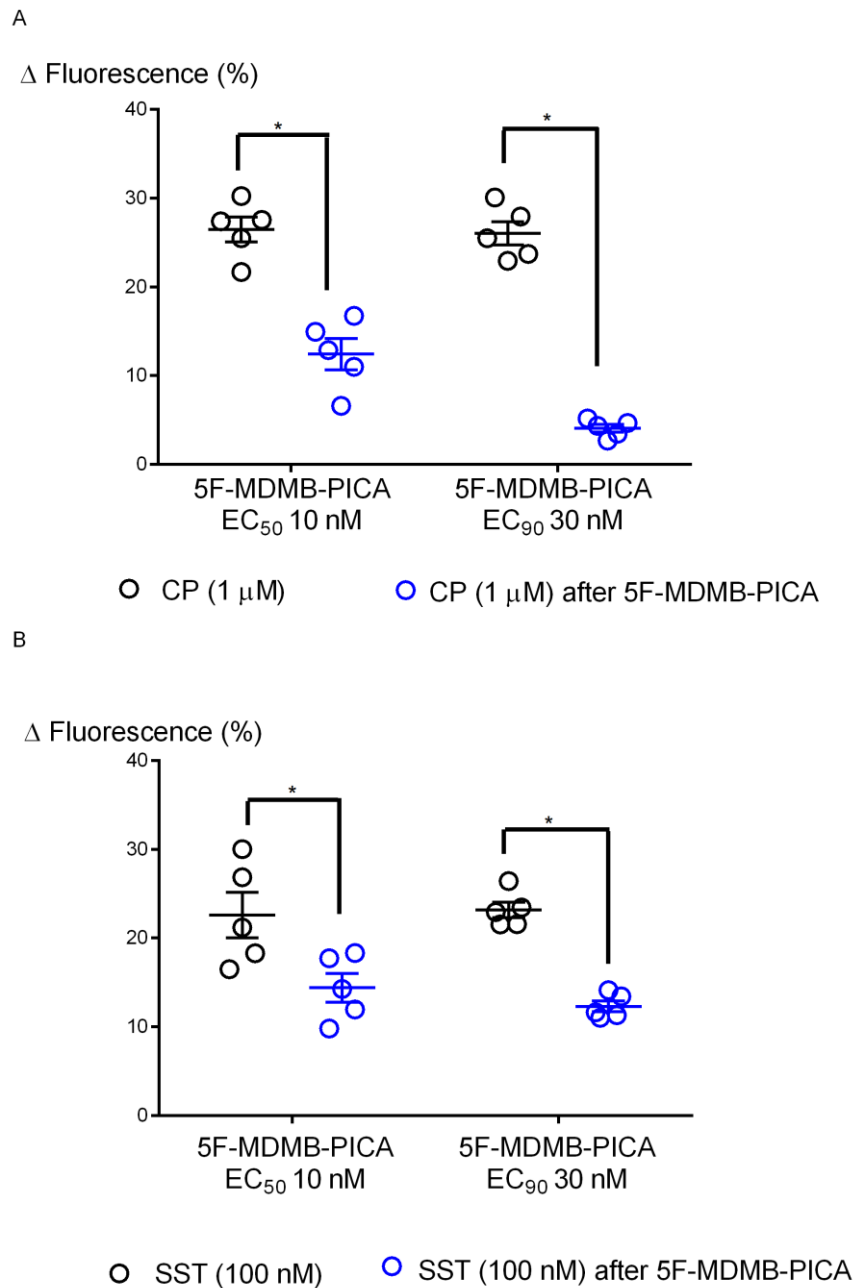
Figure 15: Scatter dot plot representing the percentage change in fluorescence reflecting homologous (A) and heterologous (B) desensitization of CB2 receptor mediated by EC_{50} (10 nM) and EC_{90} (30 nM) of 5F-MDMB-PICA. This figure shows the hyperpolarization of AtT20FlpIn-CB2 cells stimulated with 5F-MDMDB-PICA/HBSS (vehicle) for 30 minutes to the subsequent addition of A) SST (100 nM) B) CP-55,940 (1µM); Data represents mean ± SEM, of n=5, * indicates *P*-value < 0.05.

A

% Desensitization

B

% Desensitization

Figure 16: Scatter dot plot representing desensitization of AtT20 cells expressing A) CB1, B) CB2 receptors on stimulation with 5F-MDMB-PICA for a prolonged period of time. 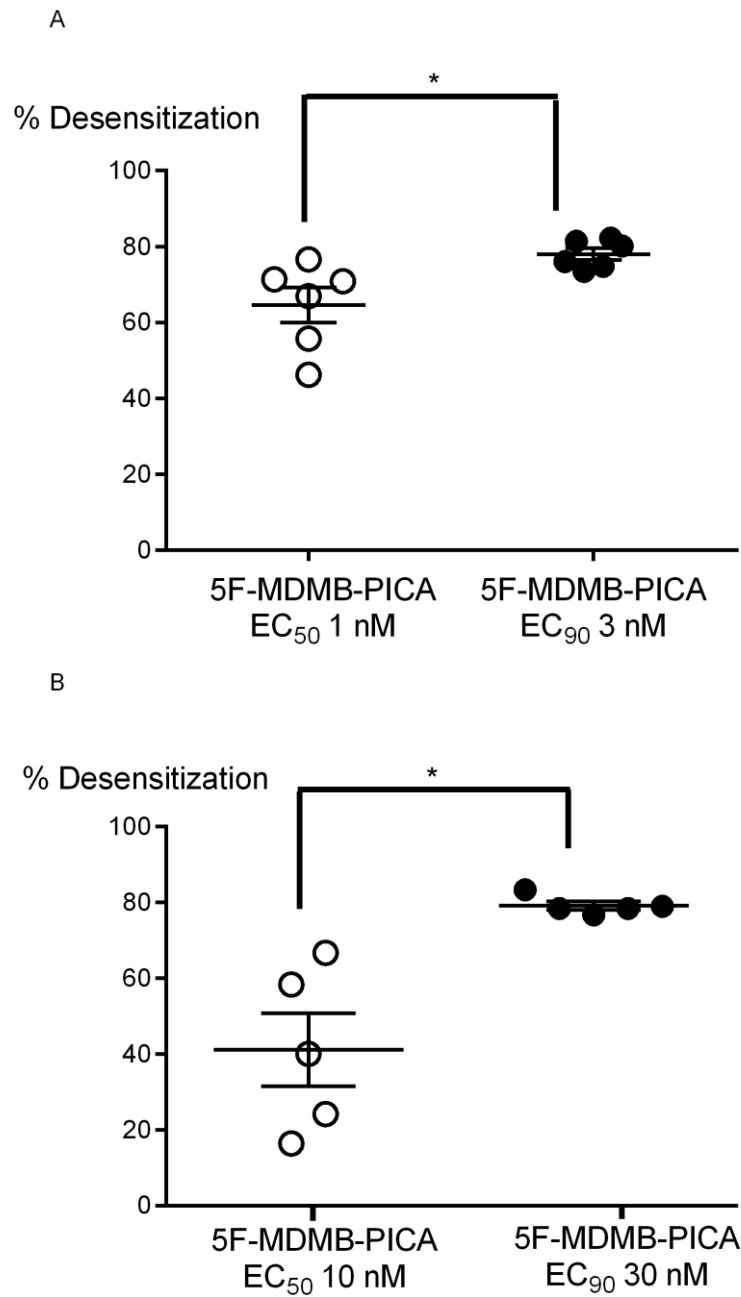This plot shows percentage desensitization comparing peak fluorescence after the addition of SC and 30 mins post addition. Data represents mean ± SEM, n= 5to 6, * indicates P-value < 0.05

To determine whether the decline in signaling of CB1/CB2 was due to the receptor or GIRK channel desensitizing because of prolonged opening, we exposed the AtT20FlpIn-CB1 cells to ML297, a direct activator of GIRK channel[125]. We did not observe any decline in the hyperpolarization on application of ML297 (10 µM) for 30 mins (Figure 17). This implies that the decline in the signaling of cells expressing CB or CB2 receptor in the continuous presence of SCs was due to receptor itself or downstream signaling pathways (potentially affecting the channel), and not a consequence of prolonged activation of GIRK channel.
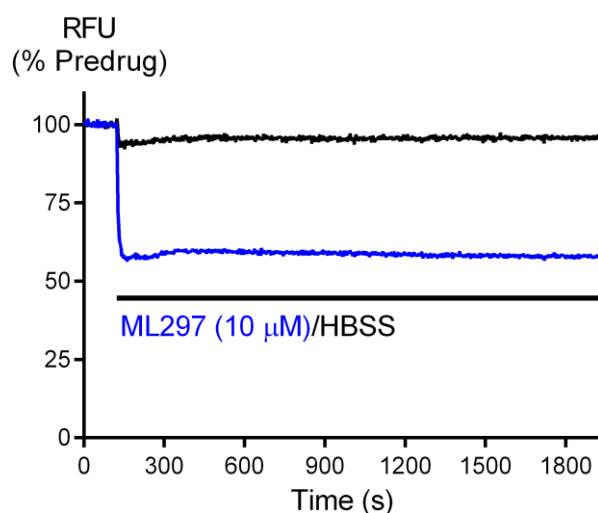

Figure 17: Representative trace showing fluorescence normalized to the predrug baseline, produced by 10 µM of ML297 on activation of GIRK channel for 30 mins.

CB1 receptor desensitization was also assessed for the four SCs (MDMB-CHMICA, MDMB-CHMINACA, 5F-AMB and MDMB-FUBINACA) in AtT20 cells (Figure 18). To investigate this, we examined the homologous and heterologous desensitization expressed as the percentage change in fluorescence of CP-55,940/SST in continued presence of SCs and CP-55,940/SST alone. Like 5F-MDMDB-PICA, application of 100 nM of SST after 30 min of these SCs produced a hyperpolarization that was not significantly different to that produced by SST alone, except for MDMB-CHMINACA that has little effect on the native SST receptor response, ($P<0.05$, Figure 19). Both EC_{50} and EC_{90} of SCs produced a significant homologous desensitization (similar to that of 5F-MDMB-PICA) expressed as percentage change in fluorescence of CP-55,940 after SCs to that of CP-55,940 alone in AtT20FlpIn-CB1 cells (Figure 19). No significant difference was observed for the percentage decline in the signaling of CB1 mediated by EC_{50} of MDMB-CHMINACA and 5F-AMB to its EC_{90} (Figure 20), although EC_{50} of MDMB-CHMICA and MDMB-FUBINACA was different from its to its EC_{90}.

The representative traces for the SCs not shown in this chapter can be found in the Appendix.

The desensitization of CB1 receptor was also accessed on exposure to Δ^9-THC for 30 mins. We observed similar decline in signaling of CB1 receptor with Δ^9-THC as that of other SCs (Figure 21). The percentage CB1 receptor desensitization mediated by Δ^9-THC was $60\pm5\%$ (Figure 21).
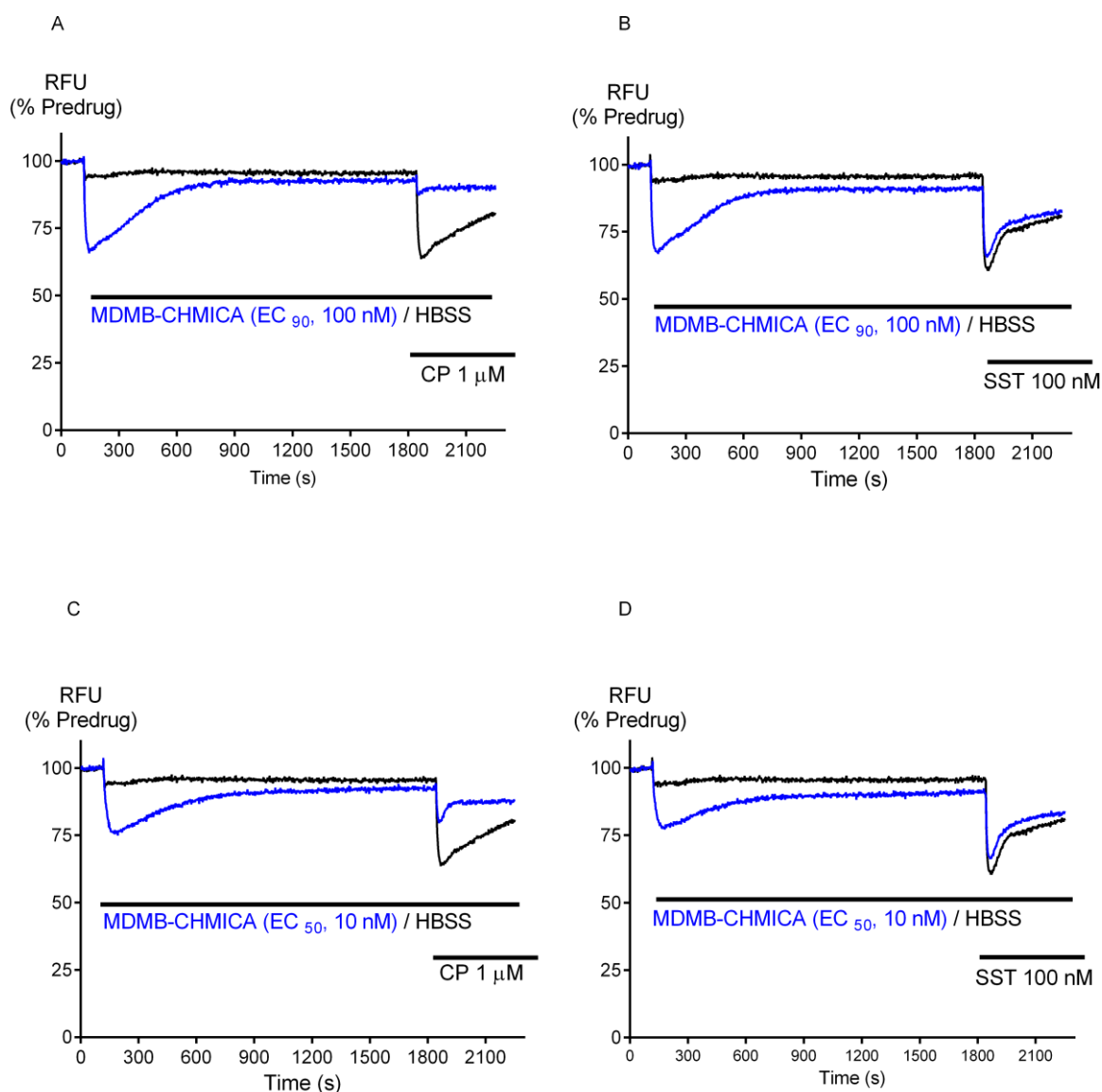
Figure 18: Homologus and heterologus desnsitization of CB1 receptor in AtT20 cells mediated by other 4SCs Representative traces showing the change in fluorescence normalized to the predrug baseline, produced by SCs on continuous stimulation of CB1 receptor as a result cellular hyperpolarization. This figure shows that the continuous application of A) SCs $EC_{90,}$ and B) SCs EC_{50} reduces the response to a following addition of CP-55,940 or SST, Trace A and C represents homologous desensitization expressed as decline in response of CP-55,940 (1 µM) in the continued response of SCs to that of CP-55,940 alone, trace B and D, shows heterologous desensitization, challenged with SST (100 nm) 30 minutes after the desensitizing concentration of SCs.
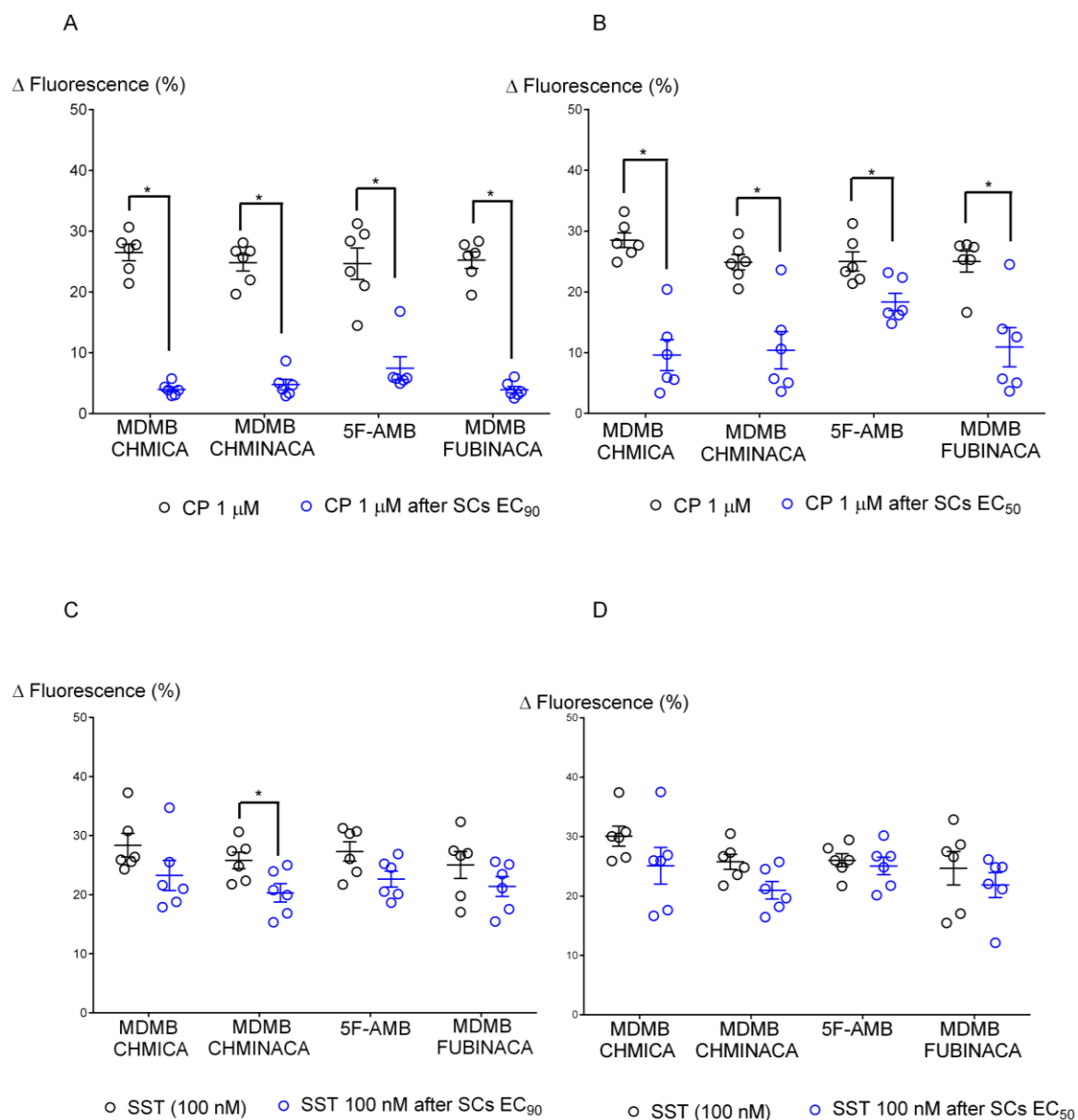
Figure 19: Scatter dot plot representing the percentage change in fluorescence represented as (A and B) homologous and (C and D) heterologous desensitization. This figure shows the hyperpolarization of AtT20FlpIn-CB1 cells stimulated with EC_{90} of SCs, EC_{50} of SCs for 30 minutes to the subsequent addition of SST (100 nM) or CP-55,940 (1µM); Data represents mean ± SEM of n=6, * indicates P-value < 0.05
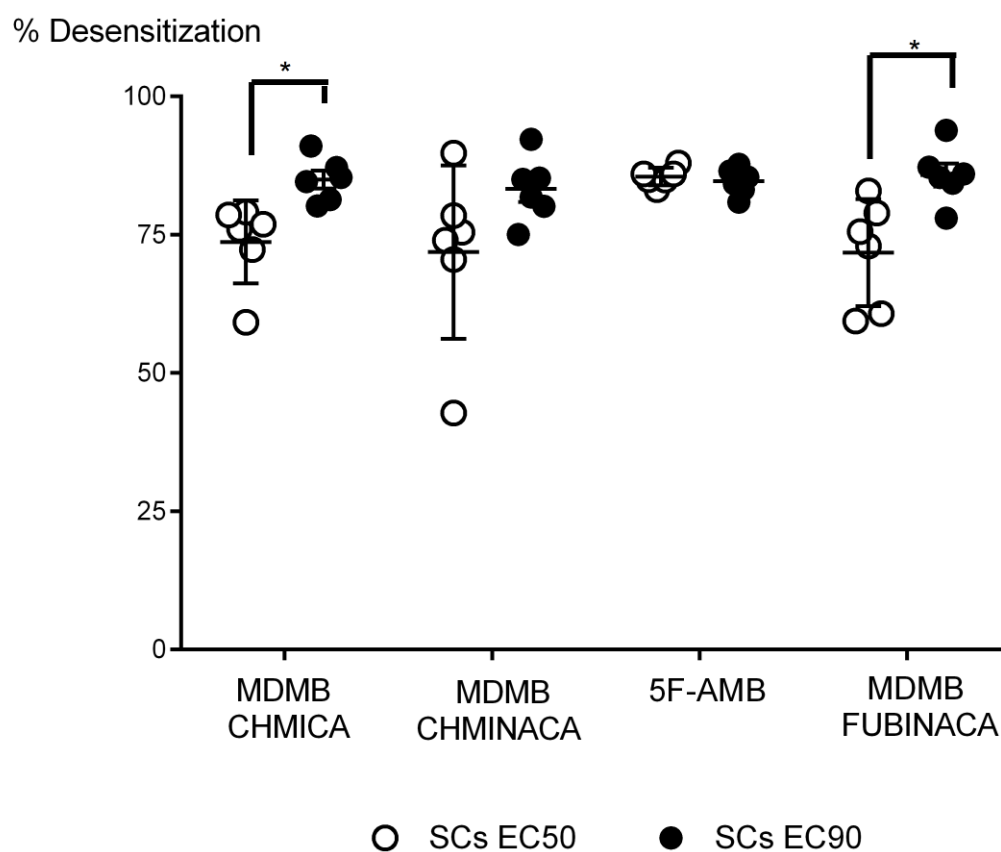
Figure 20 : Scatter dot plot representing desensitization of AtT20 cells expressing CB1 receptors on stimulation with SCs for a prolonged period of time. This plot shows percentage desensitization comparing peak fluorescence after the addition of SCs and 30 mins post addition. Data represents mean ± SEM,n=6, * indicates *P*-value < 0.05

A

B
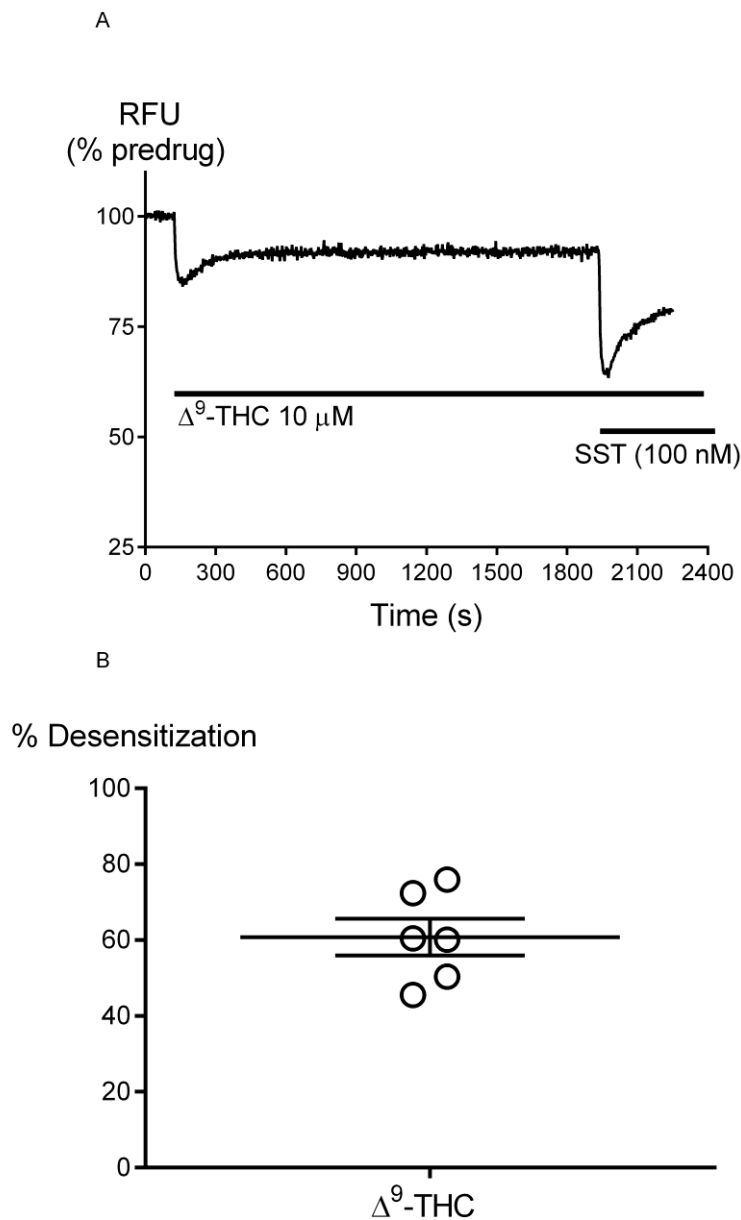
Figure 21: CB1 receptor desensitization mediated by 10 µM Δ^9-THC. A) representative trace of Δ^9-THC induced CB1 receptor desensitization. Activation of CB1 receptor by Δ^9-THC for a prolonged period of time follows the similar pattern of desensitization as SCs, B) Scatter dot plot representing desensitization of CB1 receptors on exposure to Δ^9-THC for 30 mins. This plot shows percentage desensitization comparing peak fluorescence after the addition of SCs and 30 mins post addition. Data represents mean ± SEM,n=6.

4.2.2 Effect of G Protein-Coupled Receptor Kinase 2 or 3 at CB1 receptor desensitization:

To examine the effect of GRK2/3 inhibitor on CB1 receptor desensitization mediated by the submaximal concentration of 5F-MDMB-PICA (3 nM), AtT20FlpIn-CB1 cells were pretreated with Compound 101 (10 µM), which is reported to be a potent and selective inhibitor of GRK2/3 and which was previously reported to inhibit the desensitization of MOR in rat and mouse coeruleus (LC) neurons[133]. In cells treated with Cmpd 101, we found that CB1 receptor desensitization (homologous and heterologous) was unaffected at submaximal concentration of 5F-MDMB-PICA in AtT20 cells (Figure 23). From this experiment, it was concluded that probably GRK 2 or 3 has no role to play in desensitization of CB1 receptor. But this experiment was performed at submaximal concentration of 5F-MDMB-PICA and we then investigated the effect of Cmpd 101 on desensitization produced by a saturating concentration (10 µM) of 5F-MDMB-PICA at CB1 receptor. At saturating concentration of 5F-MDMB-PICA (10 µM), the desensitization was reduced from 97±3.9% to 77±3.5% in the cells treated with Cmpd 101. (Figure 23). As shown in the example trace (Figure 22), the hyperpolarization produced by 5F- MDMB-PICA (10 µM) in the presence of Cmpd 101 reversed rapidly after about 10 minutes to that of control (untreated). Thus we also measured the percentage desensitization of AtT20 cells expressing CB1 receptor at 10 min for Cmpd 101 treated and control, which was found to be significantly different (Figure 23).
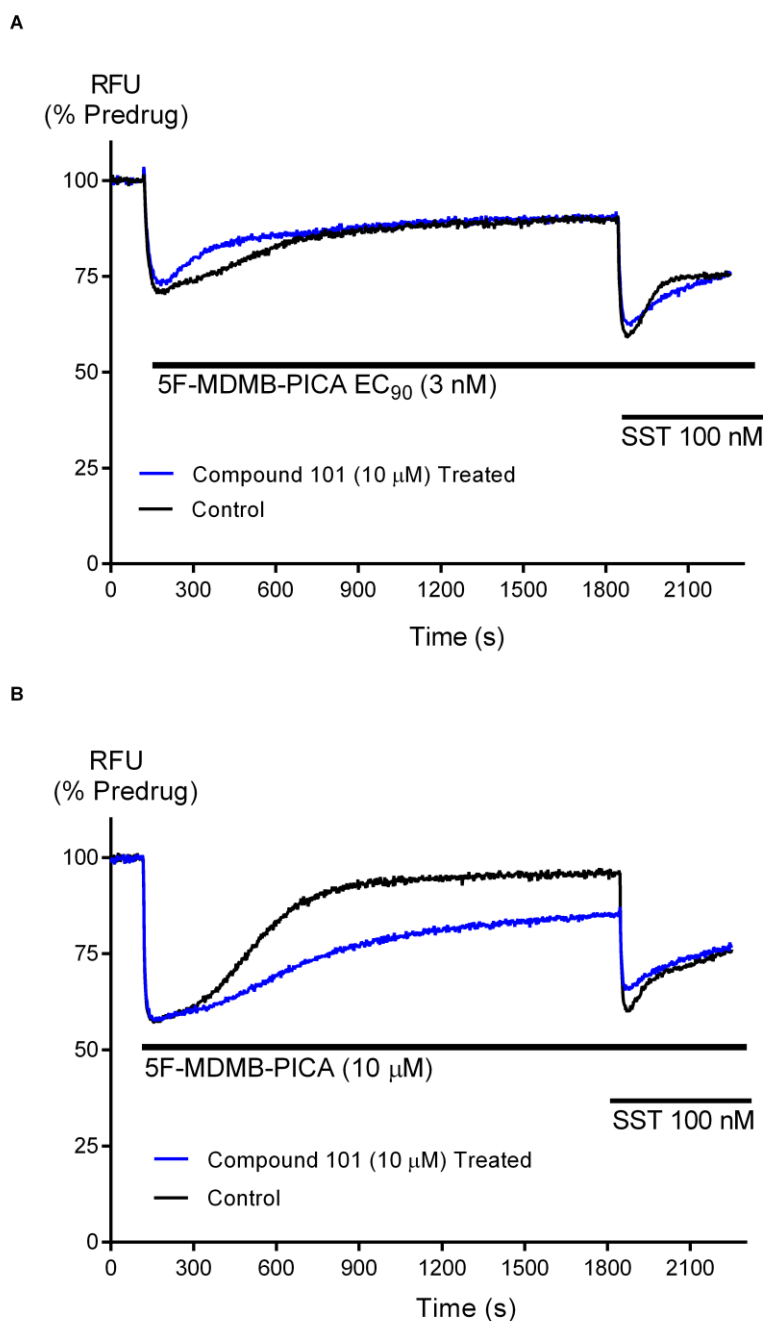
Figure 22: Inhibition of CB1 receptor desensitization by Cmpd 101 in AtT20 cells. Representative traces showing the change in fluorescence normalized to the predrug baseline, in response to A) EC_{90}, 3nM of 5F-MDMB-PICA, B) receptor saturating concentration of 5F-MDMB-PICA (10 μM) in the AtT20 cells treated with Cmpd 101 (blue trace) or control (black trace). Cmpd 101 significantly inhibited the desensitization of 5F-MDMB-PICA (10 μM).

56

A

% Desensitization
(at 30 mins)

5F-MDMB-PICA
10 μM

5F-MDMB-PICA
EC$_{90}$ 3 nM

B

% Desensitization
(at 10 mins)

5F-MDMB-PICA
10 μM

○ Control   ○ Cmpd 101 (10 μM) Treated

C

Δ Fluorescence (%)

SST

5F-MDMB-PICA
10 μM

5F-MDMB-PICA
EC$_{90}$ 3 nM

● SST (100 nM)   ○ SST (100 nM) after 5F-MDMB-PICA

○ Compound 101 (10 μM) treated

Figure 23: Role of GRK 2 or 3 in CB1 receptor desensitization. Desensitization of AtT20FlpIn-CB1 after A) 30 mins B) 10 mins of stimulation with 5F-MDMB-PICA, treated with Cmpd 101 or untreated. This plot shows percentage desensitization comparing peak fluorescence after the addition of SC and 30 min/10 min post addition. Cmpd 101 significantly reversed the desensitization caused by saturating concentration of 5F-MDMB-PICA (10 μM) more significantly after 10 mins. C) Scatter dot plot represents the heterologous desensitization expressed as percentage change in fluorescence. This figure shows the hyperpolarization of AtT20FlpIn-CB1 cells stimulated with 5F-MDMB-PICA for 30 minutes to the subsequent addition of SST (100 nM), The heterologous desensitization of CB1Rs was not different in Cmpd 101 treated cells compared with that of untreated cells. Data represents mean ± SEM n=6, * indicates P-value < 0.05

To determine whether prolonged inhibition of GRK 2/3 affected agonist mediated hyperpolarization of AtT20FlpIn-CB1, we pre-treated the cells with Cmpd 101 (10 μM) and performed CRC. The pEC_{50} ± SEM of 5F-MDMB-PICA on AtT20FlpIn-CB1 cells was found to be 8.97±0.2 for Control and 8.96±0.1 for Cmpd 101 treated. Thus the pre-treatment of cells with Cmpd 101 did not affect the potency or maximal effect of 5F-MDMB-PICA. (Figure 24).
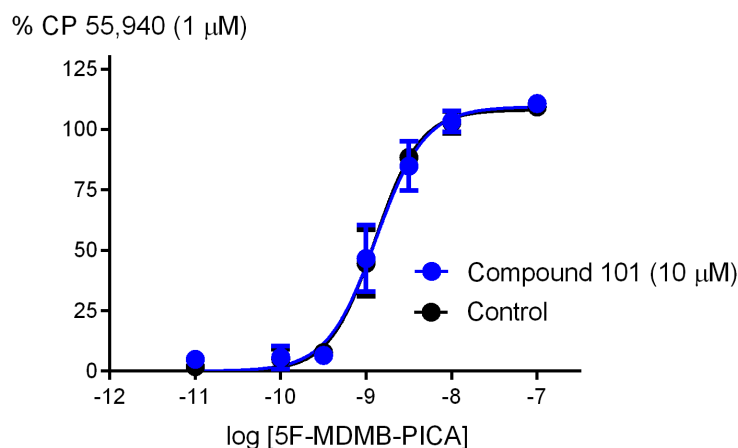
Figure 24: 5F-MDMB-PICA concentration response curve, obtained as a result of hyperpolarization of AtT20FlpIn-CB1 cells, treated with Cmpd 101 (blue trace) or control (black trace). Data represents mean ± SEM for 3-4 experiments.

GRK 2 or 3 has previously shown to play a role in the desensitization of MOR and SST receptor[133,134], we therefore examined the effect of Cmpd 101 on desensitization of AtT20 cells expressing MOR or SST receptors. To determine this, AtT20FlpIn cells expressing MOR or SST were pretreated with Cmpd 101 (10 µM). We found that the hyperpolarization induced by continued presence of DAMGO (10 µM) treated with Cmpd 101 was similar to that of untreated cells (Figure 25). DAMGO induced desensitization measured after 30 minutes was not different in the cells untreated or treated with Cmpd 101 (Figure 25). Likewise, the desensitization of SST receptor was same for both AtT20 cells treated with Cmpd 101 or untreated (Figure 26).

A

B

Figure 25: Effect of GRK 2 or 3 in MOR desensitization, A) Representative traces showing the change in fluorescence normalized to the predrug baseline, in response to DAMGO (10 µM) in the AtT20FlpIn-MOR cells treated with Cmpd 101 (blue trace) and control (black trace). B) Desensitization of AtT20 cells expressing MOR in the continuous presence of DAMGO, treated with Cmpd 101 or untreated. This plot shows percentage desensitization comparing peak fluorescence after the addition of drug and 30 min post addition. The desensitization of MOR was not different in Cmpd 101 treated cells compared with that of untreated cells (75 ± 5%). Data represents mean ± SEM n=3.
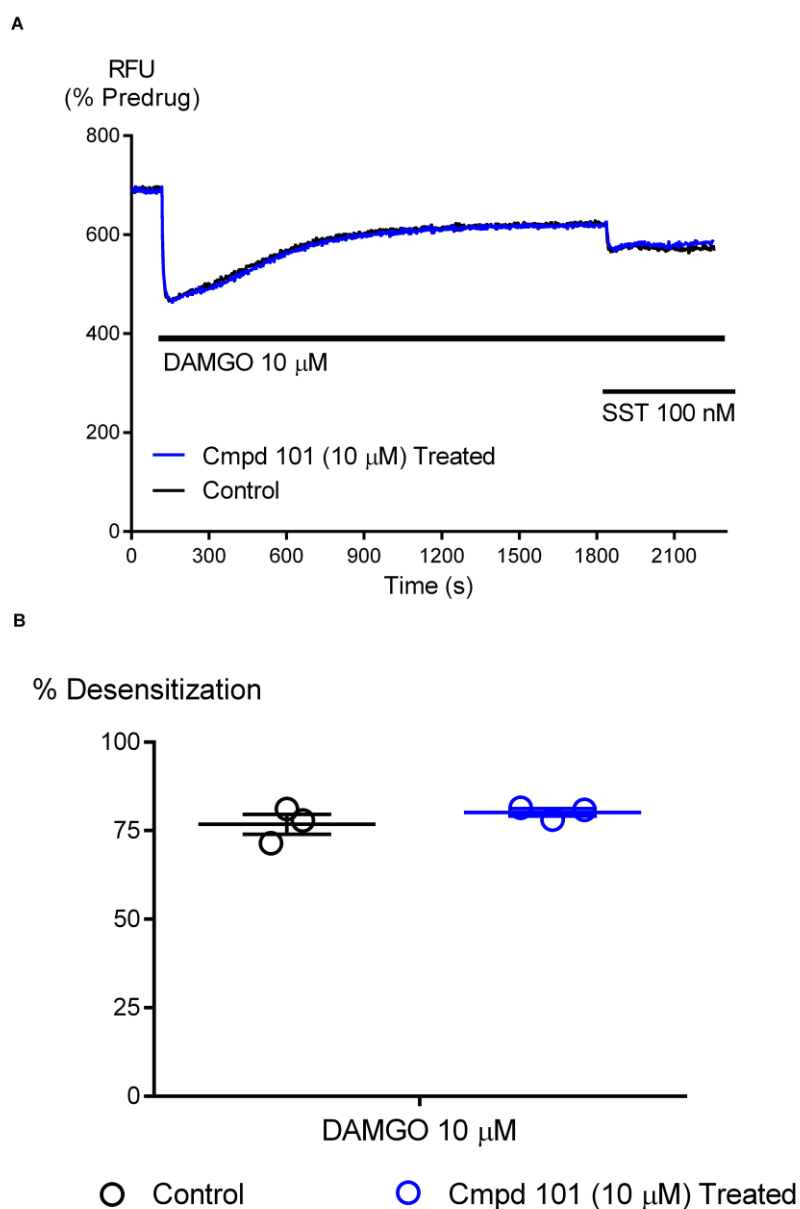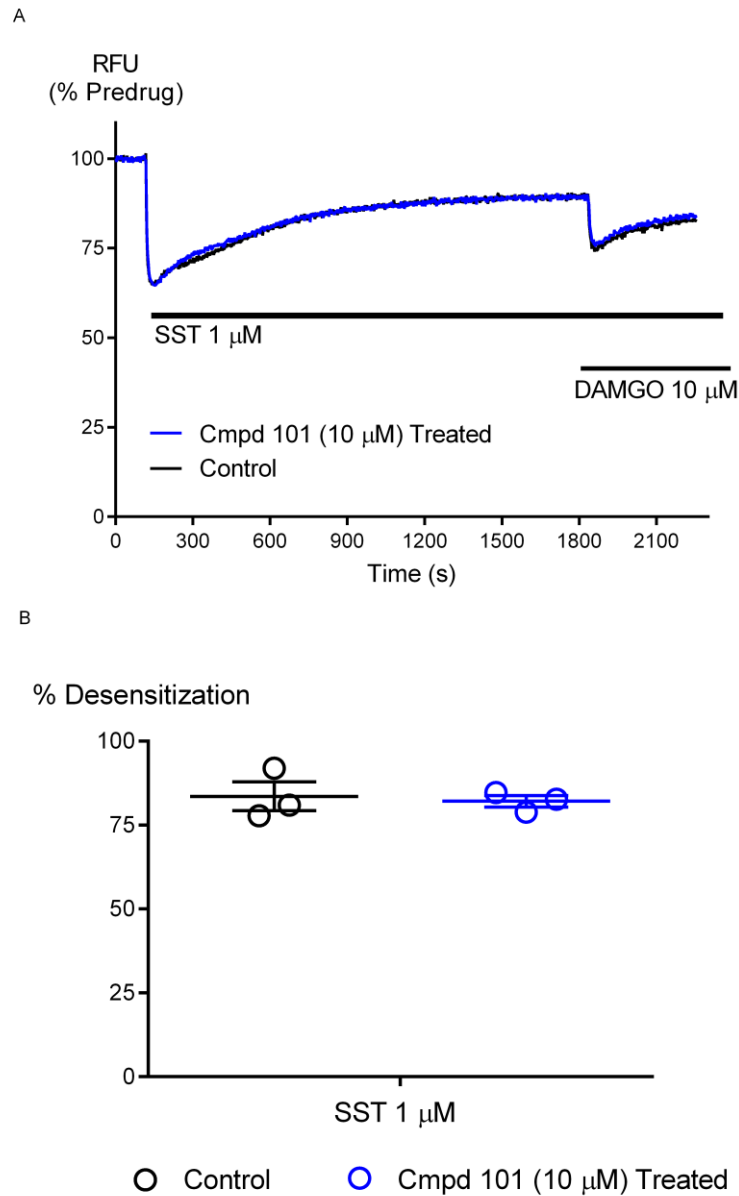
Figure 26: Effect of GRK 2 or 3 in SST receptor desensitization, A) Representative traces showing the change in fluorescence normalized to the predrug baseline, in response to SST (10 µM) in the AtT20 cells treated with Cmpd 101 (blue trace) and control (black trace). B) Desensitization of AtT20 cells expressing endogenous SST receptor, treated with Cmpd 101 or untreated. This plot shows percentage desensitization comparing peak fluorescence after the addition of SST and 30 min post addition. The desensitization of SST receptor was same for cells treated with Cmpd 101 compared with that of untreated cells. Data represents mean ± SEM n=3.

4.2.2.1 Inhibition of MOR phosphorylation by Cmpd 101

To confirm the ability of Cmpd 101 to inhibit GRK2/3 in an intact cell, we tested the Cmpd 101 inhibition of DAMGO induced phosphorylation of Serine 377 residue in the C terminal of MOR. It is well established that that GRK2 is responsible for the DAMGO induced phosphorylation of Ser^{377}[135]. We studied this by immunocytochemistry, using the commercially available antibody that binds specifically to the phosphorylated Ser^{377}. Application of DAMGO (10 µM) for 10 mins (10 µM) to the AtT20FlpIn-MOR cells shows a strong phosphorylation of Ser^{377} (Figure 27) that was partially inhibited by treatment of Cmpd 101 (10 µM).
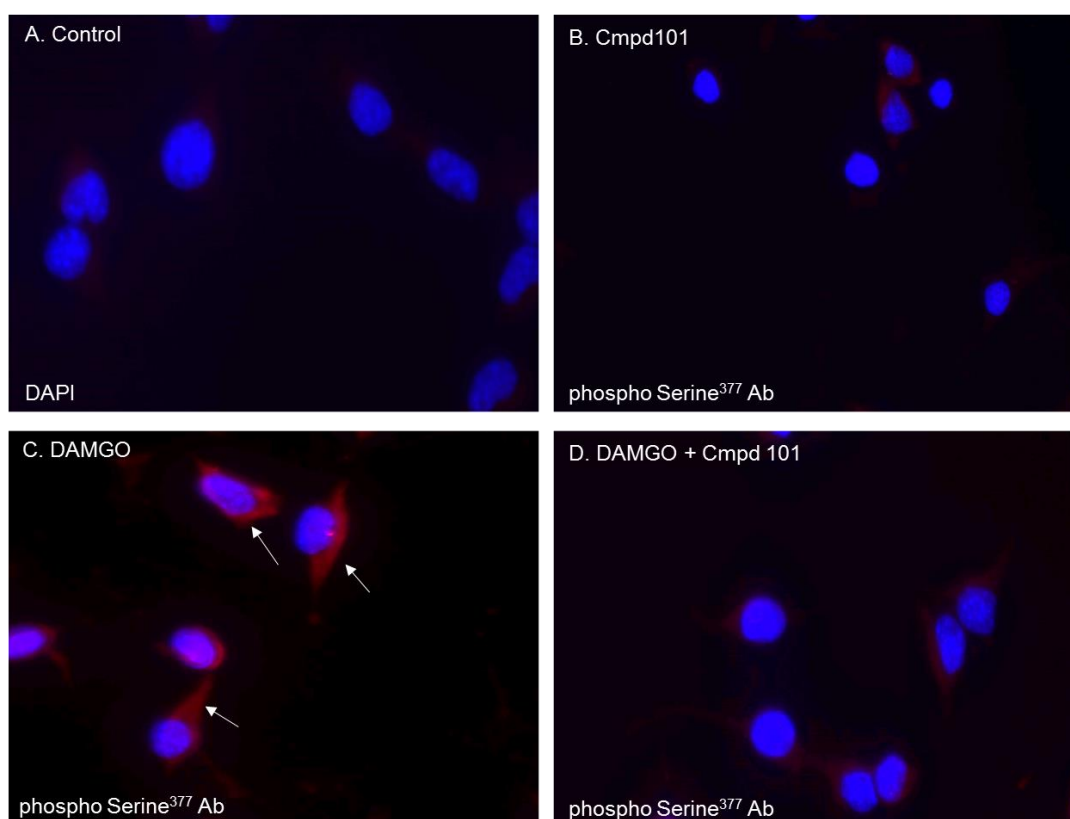
Figure 27: Inhibition of DAMGO induced phosphorylation by Cmpd 101. Figure represents the Fluorescent Carl Zeiss images of AtT20FlpIn-MOR A) Control (no treatment), B) Cmpd 101 10 µM, C) DAMGO 10 µM, D) DAMGO 10 µM plus Cmpd 101 10 µM, following incubation with primary antibody targeting phospho-Ser^{377} and secondary Goat-Anti Rabbit Cy3 (red), counterstained with DAPI (blue), Images are from single experiment repeated 3 times, Magnification 40x.

4.2.3 Effect of ERK1/2 on CB1 receptor desensitization:

We have also determined that if there is any role of ERK1/2 in CB1 receptor desensitization via MAPK pathway. The cells were treated with MEK inhibitor, trametinib (100 nM), which has been reported as a targeted therapy for melanoma cells[98]. To determine the role of ERK1/2 in the 5F-MDMB-PICA induced desensitization of CB1 receptors, AtT20FlpIn-CB1 cells were preincubated with trametinib for 60 mins. We did not observe any difference in the desensitization mediated by EC_{90} or at saturating concentration (10 µM) of 5F-MDMB-PICA (80 ± 5%), in trametinib treated cells compared to control (Figure 28).

To demonstrate the positive control for this, we assess the ability of trametinib to block the basal ERK phosphorylation in AtT20 cells by Immunocytochemistry. As seen in figure 29, the basal level of ERK was found to be really high in AtT20 cells, which was partially blocked by the treatment with MEK inhibitor, Trametinib.

Figure28, (following page) : Effect of ERK1/2 on CB1 receptor desensitization, Representative traces showing the change in fluorescence normalized to the predrug baseline, in response to A) saturating concentration of 5F-MDMB-PICA (10 µM) B) $EC_{90,}$ 5F-MDMB-PICA, in the AtT20 cells treated with MEK inhibitor, trametinib 100 nM (blue trace) and control (black trace). C) Desensitization of CB1 receptor after 30 mins of stimulation with 5F-MDMB-PICA, treated with Trametinib or untreated. This plot shows percentage desensitization comparing peak fluorescence after the addition of SC and 30 mins post addition. The desensitization of CB1 receptor was unaffected by MEK inhibitor, Trametinib. D) Scatter dot plot showing heterologous desensitization expressed as percentage change in fluorescence. This figure shows change in fluorescence represented as the hyperpolarization of AtT20FlpIn-CB1 cells stimulated with 5F-MDMB-PICA for 30 minutes to the subsequent addition of SST (100 nM), The %change in fluorescence for CB1Rs was not different in Trametinib treated cells compared with that of untreated cells. Data represents mean ± SEM, n=3.

A

RFU
(% Predrug)

5F-MDMB-PICA EC$_{90}$ 3 nM

SST 100nM

— Control
— Trametinib 100 nM

Time (s)

B

RFU
(% Predrug)

5F-MDMB-PICA 10 μM

SST 100nM

— Control
— Trametinib 100 nM

Time (s)

C

% Desensitization

5F-MDMB-PICA
10 μM

5F-MDMB-PICA
EC$_{90}$ 3 nM

○ Control

○ Trametinib 100 nM treated

D

Δ Fluorescence (%)

SST

5F-MDMB-PICA
10 μM

5F-MDMB-PICA
EC$_{90}$ 3 nM

● SST (100 nM)   ○ Trametinib 100 nM treated

○ SST (100 nM) after 5F-MDMB-PICA

64
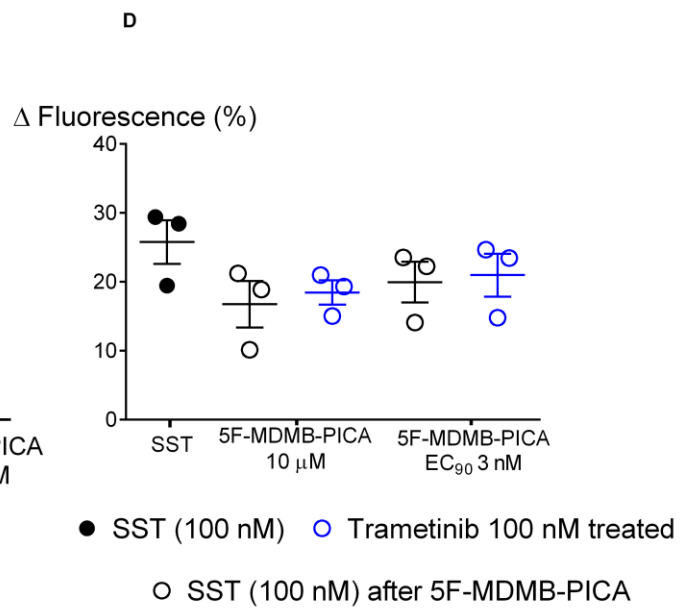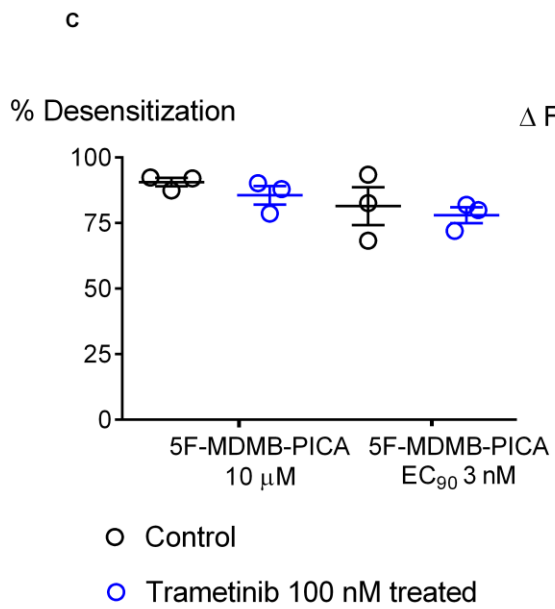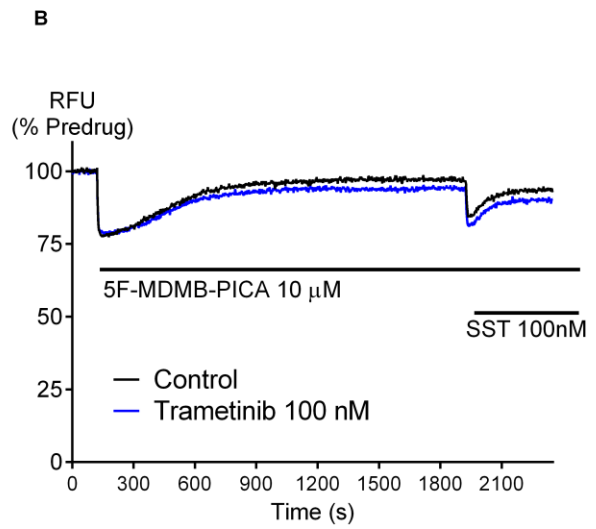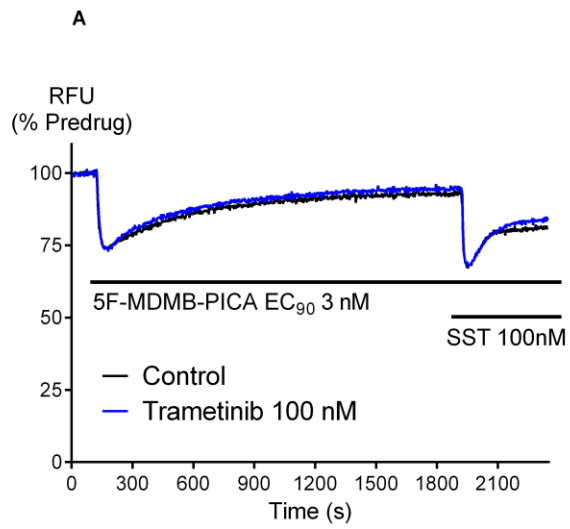
Figure 29: Inhibition of basal ERK phosphorylation in AtT20 cells. Figure represents the Fluorescent Carl Zeiss images of AtT20FlpIn-CB1 A) Control (no primary Ab), B) No drug C) Trametinib (100 nM) treated, following incubation with primary antibody (B and C) targeting phospho-ERK and secondary anti mouse Cy3 (red), counterstained with DAPI (blue), Images are from one experiment (n=1), Magnification 40x.

It has previously been reported that ERK1/2 can be activated via MAPK independent pathway, mostly GRKs and arrestins, as observed for MOR[126]. To determine whether there was any role of ERK1/2 in CB1 receptor desensitization via MAPK independent pathway, we pretreated the cells with selective and potent inhibitor of ERK1/2, SCH772984 (100 nM), which has been reported recently as a novel specific kinase inhibitor with prolonged on-target activity[99]. We assess the role of ERK1/2 in the 5F-MDMB-PICA induced desensitization of CB1Rs in AtT20FlpIn-CB1 cells preincubated with SCH772984 for 4 hours. We did not observe any difference in the desensitization mediated by EC_{90} or at saturating concentration (10 μM) of 5F-MDMB-PICA, in SCH772984 treated cells compared to control (Figure 30). Thus, there was no reduction in desensitization (homologous and heterologous) of CB1Rs in the presence of direct inhibitor of ERK1/2 (Figure 30).

Figure 30, (following page) : Role of ERK1/2 on CB1 receptor desensitization via MAPK independent pathway, Representative traces showing the change in fluorescence normalized to the predrug baseline, in response to A) saturating concentration of 5F-MDMB-PICA (10 μM) B) EC_{90}, 5F-MDMB-PICA in the AtT20 cells treated with ERK1/2 inhibitor, SCH772984 100 nM (blue trace) and control (black trace). C) Desensitization of CB1 receptor after 30 mins of stimulation with 5F-MDMB-PICA, treated with SCH772984 or untreated. This plot shows percentage desensitization comparing peak fluorescence after the addition of drug and 30 min post addition. The desensitization of CB1 receptor was unaffected by ERK1/2 inhibitor, SCH772984 D) Scatter dot plot showing heterologous desensitization expressed as percentage change in fluorescence. This figure shows change in fluorescence represented as the hyperpolarization of AtT20FlpIn-CB1 cells stimulated with 5F-MDMB-PICA for 30 minutes to the subsequent addition of SST (100 nM), The % change in fluorescence for CB1Rs was not different in SCH772984 treated cells compared with that of untreated cells. Data represents mean ± SEM, n=3.
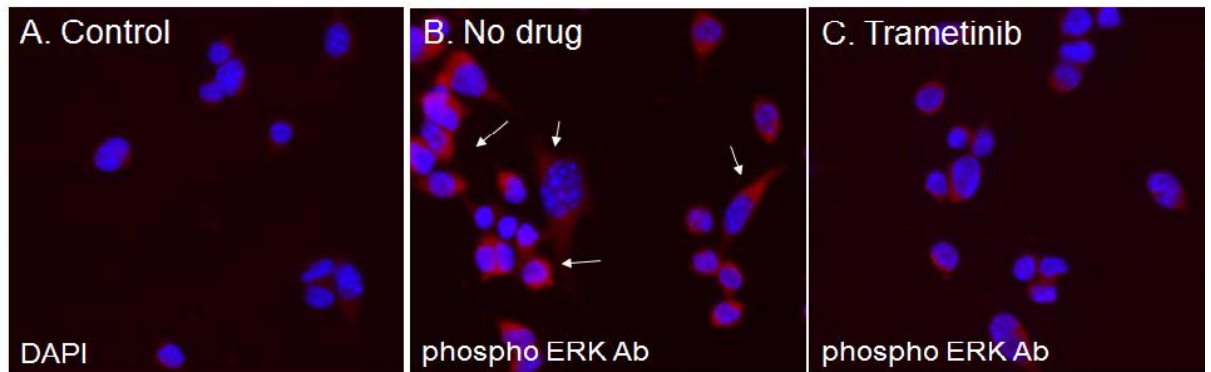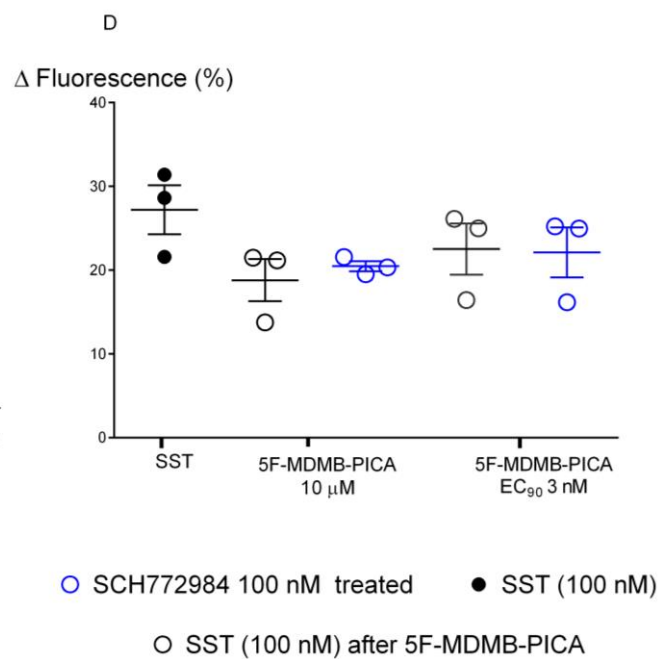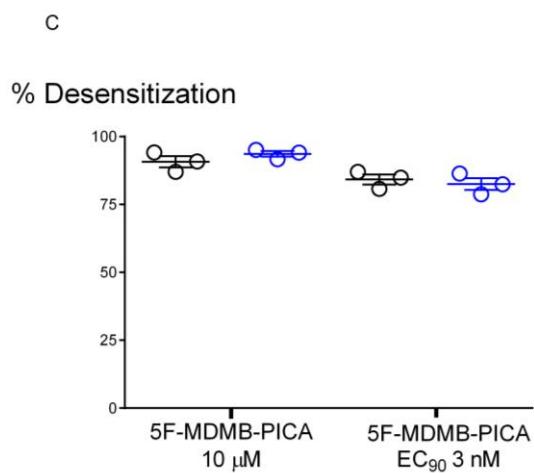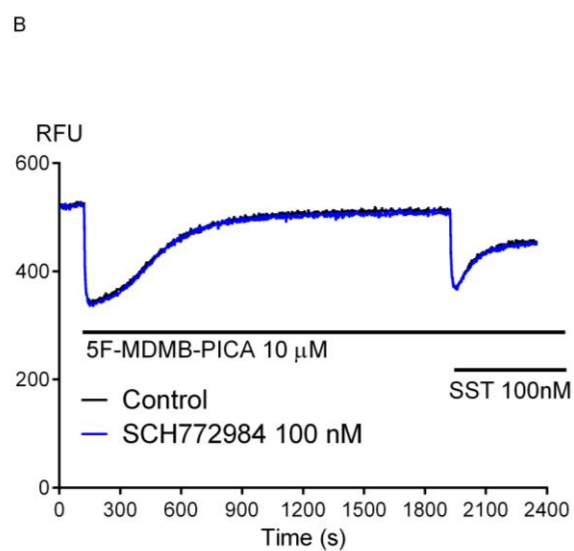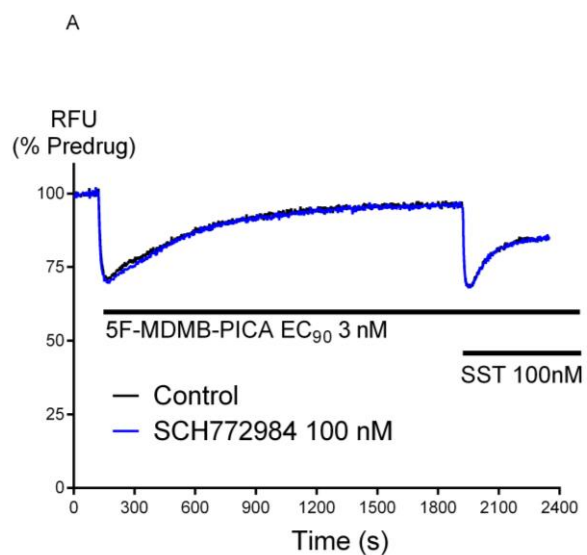
A

RFU
(% Predrug)

5F-MDMB-PICA EC_{90} 3 nM

SST 100nM

Control
SCH772984 100 nM

B

RFU

5F-MDMB-PICA 10 μM

SST 100nM

Control
SCH772984 100 nM

C

% Desensitization

5F-MDMB-PICA
10 μM

5F-MDMB-PICA
EC_{90} 3 nM

○ Control

○ SCH772984 100 nM treated

D

Δ Fluorescence (%)

SST

5F-MDMB-PICA
10 μM

5F-MDMB-PICA
EC_{90} 3 nM

○ SCH772984 100 nM treated   ● SST (100 nM)

○ SST (100 nM) after 5F-MDMB-PICA

4.2.3.1 To investigate ERK1/2 mediated GRK2/3 phosphorylation in CB1 receptor desensitization:

Based on previous reports that showed ERK1/2 influences receptor desensitization by phosphorylating GRKs[136], we examined 5F-MDMB-PICA (10 µM) induced desensitization of AtT20FlpIn-CB1 cells treated with Cmpd 101 (10 µM) and trametinib (100 nM) together and in parallel to Cmpd 101 alone and trametinib alone for 60 mins. We did not found any change in CB1 receptor desensitization mediated by 5F-MDMB-PICA in cells treated with Cmpd 101 (10 µM) and trametinib (100 nM) together compared to Cmpd 101 alone or trametinib alone (Figure 31). Thus, Cmpd 101 and trametinib together did not affect the percentage decrease in desensitization (homologous and heterologous) any further than that caused by cells treated with Cmpd 101 alone (Figure 31).

Figure 31, (following page) : Effect of ERK1/2 on CB1 receptor desensitization mediated via GRKs phosphorylation, Representative traces showing the raw fluorescence, in response to saturating concentration of 5F-MDMB-PICA (10 µM) in the AtT20 cells treated with ERK1/2 inhibitor (trametinib) and GRK2 inhibitor (Cmpd 101) together (red trace), trametinib alone (grey trace), Cmpd 101 alone (blue trace) and control (black trace). C) Desensitization of CB1 receptor after 30 mins of stimulation with 5F-MDMB-PICA, treated with Cmpd101 and trametinib treated or Cmpd 101 alone or trametinib alone or untreated. This plot shows percentage desensitization comparing peak fluorescence after the addition of SC and 30 min post addition. D) Scatter dot plot showing heterologous desensitization expressed as percentage change in fluorescence. The %change in fluorescence for CB1Rs treated with Cmpd101 and trametinib together was not different to that of Cmpd 101 alone. Data represents mean ± SEM, n=3 * indicates P-value < 0.05

A

B

% Desensitization

5F-MDMB-PICA
10 μM
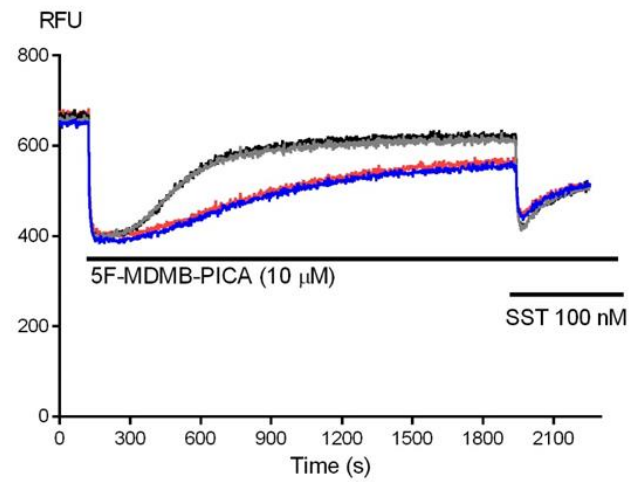
○ Control   ○ Cmpd 101 (10 μM)

○ Trametinib 100 nM treated   ○ Cmpd 101 and trametinib treated

C

Δ Fluorescence (%)

SST   SST 100 nM after 5F-MDMB-PICA 10uM
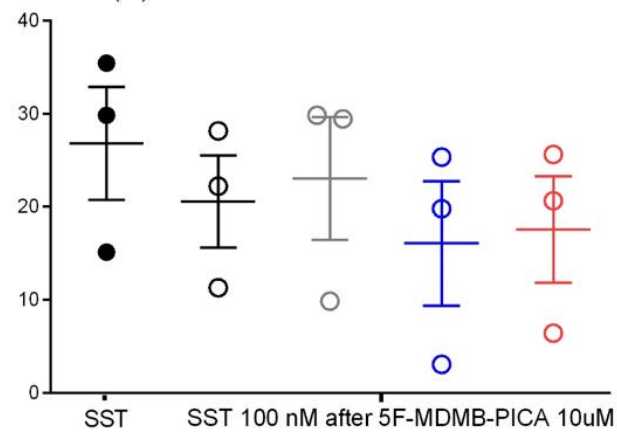
● SST 100 nM   ○ Control   ○ Trametinib treated 100 nM

○ Cmpd 101 treated 10 μM   ○ Cmpd 101 & Trametinib treated

4.4 Discussion

The main finding of this chapter is that the cannabinoid receptors desensitization mediated by recently emerged indole and indazole SCs involves multiple regulatory mechanisms. Using real time assay, we demonstrated that desensitization of CB1 receptor was largely homologous, with little effect on the native somatostatin receptor responses, although desensitization at CB2 receptors was found to be both homologous and heterologous. To date all the studies regarding CB receptor desensitization was demonstrated by chronic administration of Δ^9-THC, CP-55,940 or WIN-55,212 in animal model or cellular model or neurons[137]. The current work represents the first in detailed mechanism of SCs induced CB receptor desensitization in AtT20 cells. The desensitization of CB1 receptor has been reported to be GRK3 and βarrestin-2 dependent[85,107]. Our result support this finding that GRK2/3 do play a role in CB1 receptor desensitization at high concentrations of SC. However, we were unable to detect any role of GRK2/3 at submaximal concentration of SC induced CB1 receptor desensitization, it is certainly possible that other mechanisms may be recruited by lower concentrations of drug. We should also note that more than one mechanism may be involved in CB1 receptor desensitization. The only previous study of CB1 receptor activation of ERK1/2 was on stimulation with HU-210 in Neuro2a cells[113], although there is no clear evidence that suggests the role of ERK1/2 in CB1 receptor desensitization. We were unable to detect any role of ERK1/2 in CB1 receptor desensitization in AtT20 cells. Indeed, it may be anticipated that GPCR signaling may vary between different cell lines and this might display differences in the mechanism involved in desensitization of receptors. Our result clearly demonstrates the role of GRK2/3 but not ERK1/2 in the desensitization of CB1 receptor.

Continual administration of cannabinoids can result in rapid development of tolerance in both animals and humans[71-72]. The earlier studies using autoradiography showed that the chronic administration of Δ^9-THC has significantly reduced the basal level of WIN 55,212 stimulated $[^{35}S]GTP\gamma S$ binding, suggesting CB receptors desensitization in the continuous presence of Δ^9-THC[138]. In this study, we used membrane potential assay to measure SCs induced desensitization of CB1 and CB2 receptors in AtT20 cells. We found that at EC_{90} concentration of 5F-MDMB-PICA, the hyperpolarization reversed rapidly over time to a subsequent addition of CP-55,940. This has been suggested to be due to the decline in the activity of CB1 receptor on continuous exposure to an agonist for a prolonged period of time. A question then arises as to whether this decline in the CB1 signaling is due to the receptor

desensitizing or its the GIRK channel desensitizing. We addressed this question directly by applying ML297 on AtT20 cells for 30 mins, we found that ML297, direct activator of GIRK channel[139], displayed normal hyperpolarization throughout the assay for 30 mins. As seen in Figure 17, no decline in the CB1 signaling was detected in AtT20 cells on continuous application of ML297. Thus further confirming that the decline in the signaling of CB1 receptor mediated by SCs was predominantly due to the desensitization of CB receptor and not the GIRK channel.

In addition to showing decline in the activity of receptor, we also demonstrated homologous and heterologous desensitization of CB receptors. As stated, homologous desensitization of receptor is a central mechanism to an agonist induced decline in the activity of receptor, often initiated by phosphorylation of receptor via GRK or other second messenger dependent kinases[139]. On the other hand, heterologous desensitization is caused due to the decline in the signaling of different receptors or through the pathway common to these receptors in the same cell[55]. We tested whether addition of maximal effective concentration of CP-55,940 after 30 mins of 5F-MDMB-PICA was different from that of CP-55,940 alone in AtT20 cells expressing CB1 receptor. Our data show a significant reduction in hyperpolarization for CP-55,940 in the continuous presence of 5F-MDMB-PICA to that of CP-55,940 alone, strongly suggesting the homologous desensitization of CB1 receptor. We confirmed that this likely represents the decline in the activity of CB1 receptor by demonstrating the decrease in hyperpolarization of CP-55,940 in response to the desensitizing concentration of 5F-MDMB-PICA.

We were able to determine the heterologous desensitization of CB1 receptors by making use of endogenous SST receptor in AtT20 cells to detect if the maximal hyperpolarization at SST receptor was affected by the continuous application of 5F-MDMB-PICA. We found that the response of SST after 30 mins of 5F-MDMB-PICA was similar to that of SST alone, suggesting that CB1 receptor desensitization was unaffected by the signaling of SST receptors. Taken together, these data strongly point that the desensitization of CB1 receptor is mainly homologous and not heterologous in AtT20 cells. Our data also demonstrate the decline in the signaling of CB2 receptor on continuous stimulation with 5F-MDMB-PICA. Unlike CB1 receptors, CB2 receptor involves a significant level of heterologous desensitization at submaximal concentration of 5F-MDMB-PICA (EC_{90}). It is interesting to recall MOR desensitization in AtT20 cells, our group previously demonstrated that a similar pattern of both homologous and heterologous desensitization has been observed for the

DMAGO induced MOR desensitization[117]. Our data combined with this, might therefore suggests that the desensitization of CB1 receptors in continuous presence of SCs is different from that of CB2 receptors, but this clearly needs much more study.

The effect of agonist induced desensitization has been extensively studied in context to MOR[67,140]. For example, morphine and DAMGO exerts desensitization differentially[68]. Mackie at al. 2004, compared agonist efficacy and rate of desensitization, by studying the effect of agonist with different efficacies on CB1 receptor desensitization[114]. They suggested that the rate with which CB1 receptor desensitizes is independent of agonist efficacy[114]. Consistent with this observation, our data showed that cannabinoids, including Δ^9-THC and other 4 SCs (MDMB-CHMICA, MDMB-CMINACA, 5F-AMB and MDMB-FUBINACA) follows a similar pattern of decline in the activity of CB1 receptor when applied for 30 mins as that of 5F-MDMB-PICA. Thus, CB1 receptor desensitization does not depend on structure or nature of ligands, which activates the CB receptor with different potency and efficacy. Also, we have determined the desensitization at EC_{50} and EC_{90} of SCs as seen in figure 12 -15, the extent of desensitization was found to be concentration dependent.

Continuous application of agonist usually results in desensitization of receptor, a complex phenomenon that may involve phosphorylation by GRKs, which usually facilitates the binding of β-arrestin to the phosphorylated receptor and thus promotes receptor internalization[67-70] Mackie et al in 1999, examined the role of GRK and arrestin in CB1 receptor desensitization and found that different domains are involved in GRK and arrestin dependent desensitization and internalization of CB1 receptor[85]. Connecting the dots between GRK and CB1 receptor desensitization, we studied the effect of Cmpd 101, a membrane permeable, selective and potent inhibitor of GRK2 and GRK3[133,140,141], on 5F-MDMB-PICA induced desensitization of CB1 receptor in AtT20 cells. Cmpd 101 has been previously reported to inhibit the desensitization of β₂-adrenoreceptors in HEK 293 cells in a concentration dependent manner[140]. A recent report from Bailey et al. 2015, showed that Cmpd 101 inhibited agonist induced desensitization of MOR in LC neurons, implying the role of GRK 2/3 in MOR desensitzation[116]. Our data demonstrate that Cmpd 101 inhibited the desensitization partially at the highest concentration of 5F-MDMB-PICA, but the desensitization at EC_{90} of 5F-MDMB-PICA remains unchanged. AtT20 cells have been previously shown to express substantial amount of GRK2[142]. Consistent with these observations, our results highlight the role of GRK2/3 in CB1 receptor desensitization to high concentrations of agonist in AtT20 cells, but suggest that other mechanisms may be

recruited by lower concentrations of drug. Several groups have previously demonstrated the role of kinases in receptor desensitization and internalization at saturating concentration of agonist and assume that same mechanism is employed for its lower concentration, which is not always the case. To this end, it is worth noting that GRK2/3 may also have a role in SCs induced CB1 internalization, but it has yet to be determined.

It is important to note that we had positive controls for this experiment to assess the ability of Cmpd 101 to inhibit GRK2/3[95,135]. Many groups have previously demonstrated that GRK2 and GRK3 rapidly phosphorylate the C-terminal of the MOR. Chen et al. reported that GRK 2 phosphorylates Serine[375] in the C terminal of mouse MOR that corresponds to Serine[377] in human MOR[135]. Consistent with this, our immunocytochemistry studies showed DAMGO induced phosphorylation of GRK 2 or 3 in hMOR was partially blocked by Cmpd 101. While, GRK 2 or 3 mediated MOR phosphorylation was blocked by Cmpd 101, this does not necessarily mean that GRK 2 or 3 affects the desensitization of MOR. For example, previous studies showed that disruption of GRK 2 function in neurons failed to affect the MOR desensitization[143]. However, the disruption of both GRK2 and ERK1/2 nearly abolished the desensitization of MOR, so one could hypothesize that the synergistic effect of kinases is required to induce MOR desensitization in AtT20 cells.

Role of GRKs in the desensitization has been described previously in relation to MOR and SST receptor[133,134]. To further assess the ability of Cmpd 101 to inhibit GRK2 or 3, we investigated the effect of Cmpd 101 on DAMGO induced desensitization of hMOR in AtT20 cells. Our observation has been different from what has been reported previously, we were unable to detect the role of GRKs in MOR desensitization in contrast to Bailey 2015[133]. They found that Cmpd 101 fully reversed the MOR desensitization induced by DAMGO in LC neurons. Additional support that the GRK2 is not involved in MOR desensitization comes from the observation that complete deletion of the Serine/Threonine sites in the C-terminal tail of MOR failed to block desensitization of the receptor in AtT20 cells (Santiago and Connor, unpublished observations)[95]. Thus providing corroborating evidence for the lack of involvement of GRK2/3 in MOR desensitization in the GRK assay in AtT20 cells, as well as indicating that the cells also have other mechanisms for regulating GPCR activity. Further, we have been unable to obtain any evidence to support the view that GRKs are involved in the desensitization of SST, as proposed by Stefan 2007[114]. This discrepancy could result from the different mechanisms involved in the desensitization of receptor based on the differences in internal machineries adopted by cell types. For example HEK 293 cells have

significant levels of mRNA for β-arrestin 1 and 2, GRK 3-5 as compared to other cell types like AtT20, N18 cells[144]. Also, the discrepancy in the mechanism underlying receptor desenitization could be the result of the differences in the experimental strategies.

Our studies with Cmpd 101 showed that GRK 2 or 3 may play a role in desensitization of CB1 receptor. Perhaps more surprising Cmpd 101 reverses the amount of desensitization only back to the level of the EC_{90}, which was insensitive to the inhibitor, suggesting that GRK2/3 may not be involved in the greatest part of the CB1 receptor desensitization. Furthermore, this also suggests that might be multiple mechanisms are involved in the desensitization of CB1 receptor signaling. We specifically investigated the effect of ERK1/2 in CB1 receptor desensitization as the basal level of ERK1/2 was found to be significantly high in AtT20 cells (Karunaratne, Santiago and Connor, unpublished observations). Taking advantage of this cell type, we investigated the role of ERK1/2 in CB1 receptor desensitization in AtT20 cells. Indeed, MEK inhibitor, Trametinib, had no impact on the desensitization of CB1 receptor. However, ERK 1/2 is not always activated via MAPK pathways[145], ERK has been previously shown to be phosphorylated by PKC/PKA pathway and β-arrestin pathway in β2-adrenergic receptor[136]. It is possible that ERK 1/2 activation via MAPK independent pathway has a role to play in desensitization of CB1 receptor. However, the present results suggest that SCH772984, direct inhibitor of ERK1/2 did not affect CB1 receptor desensitization. One potential alternative mechanism of receptor desensitization involves a combination of GRK 2 or 3 and ERK 1/2. Dang et al 2009, found that there was overlap and redundancy between GRK 2 or 3 and ERK1/2 in MOR desensitization[143]. We tested whether ERK1/2 mediates the phosphorylation of GRK 2 or 3 in AtT20FlpIn-CB1 that might affect the CB1 receptor desensitization indirectly. However, the inhibition of GRK 2 or 3 and MEK together did not reduce the CB1 receptor desensitization further compared to that of GRK 2 or 3 inhibitor alone. Thus the present study suggests that if there is a multiple mechanism underlying CB1 receptor desensitization in AtT20 cells, it does not involve ERK 1/2.

SUMMARY AND PROSPECTS

In summary, our results indicate that all the recently appeared indole and indazole SCs featuring valinate and tert-leucinate group activated human CB1 and CB2 receptors. All the SCs tested had a higher efficacy and potency than Δ^9-THC. Our studies suggest overall preference of these SCs for CB1 receptor. CB1 activation by Δ^9-THC causes alterations in neuronal function, psychomotor control, heart rate disturbances and vasoconstriction of blood flow[146]. Within the indole and indazole derivatives, MDMB-CHMICA were linked to cardiotoxicity and neurotoxicity[99]; MDMB-FUBINANCA and MDMB-CHMINACA has been linked to growing number of deaths[112]. All these records are consistent with our results obtained with the real time activation of potassium channel mediated cellular hyperpolarization that point towards CB1 receptor activation attributable to SC toxicity. Thus, pharmacological evaluation of recently emerged SCs is essential for providing the data to the lawmakers to keep pace with an evolving series of SCs.

Outside of these findings, our data do not address directly the efficacy of these SCs, which we will be looking into next. To develop a better understanding of the pharmacological profile of these SCs, activity at other targets remains to be determined. These include, Gα modulation of AC, Gq-mediated mobilization of Intracellular calcium and assays measuring the activation of MAPK. Finally, other off target receptor pathways need to be identified. A well-known non-cannabinoid target is GPR55, which was found to be activated by numerous cannabinoid ligands[147]. It has been suggested that indole structure of SCs may prefer its interaction with serotonin receptors, is yet to be determined [53]. Given that SCs continue to evolve and high prevalence associated with it demands further pharmacological assessment essential to develop a medical intervention.

The SCs-related toxicity can be differentiated as acute effects and chronic effects on CB receptors. The subtle effects of SCs may go unnoticed in the short term, only detectable cumulatively in the long term use of drug. There is a compelling evidence that chronic use

of Δ^9-THC can lead to morphological and physiological changes in the brain's cannabinoid system[148]. It has been established that the downregulation of CB1 receptor between 20 to 60% in different brain regions is accountable for tolerance to some of the Δ^9-THC effects[149]. We demonstrated for the first time the decline in the response of CB receptor signaling in the continuous presence of SCs. The current study clearly demonstrates that there is rapid desensitization of CB receptors on stimulation with SCs for a prolonged period of time. Our findings might have an important implication for development of tolerance to SCs. The relationship between processes involved in CB receptor desensitization, internalization and development of tolerance remains to be established.

Although there is a considerable evidence for the desensitization of CB receptors, little progress has been made in elucidating the mechanisms that underlie it. Our data highlights the role of GRK2/3 in CB1 receptor desensitization to high concentration of agonist in AtT20 cells but suggests no role of GRK2/3 at lower concentration of SCs. It is tempting to propose that other mechanisms may be recruited by low concentration of SC induced desensitization of CB1 receptors. These findings may have a significant impact on application of cannabinoids therapeutics. These results also suggest the important areas for further investigation of the regulation of CB1 receptor signaling. It is worth noting that we were unable to obtain any evidence of the involvement of ERK1/2 in CB1 receptor desensitization. We feel that this might be a consequence of experimental approach used or cell line adopted for this experiments. In future studies we aim to look at other kinases that might have a role in CB1 receptor desensitization. We also intend to determine the effect of GRKs in CB1 internalization. This might give us a clear picture of CB receptor down-regulation caused by continuous exposure to SCs.

In this study, we used AtT20 cell line heterologously expressed CB1 or CB2 receptors to study in depth the mechanism involved in CB1 receptor downregulation. However, it is important to note that different cell lines have different GPCR signaling profile, which can influence receptor desensitization[144]. It is important to note that other factors are likely to affect the differences in the mechanism underlying the desensitization of same receptors. This may be, however, a result of substantial variation in the techniques to measure desensitization. For example, studies using electrophysiology involves the use of single cell or neuron to elucidate the mechanism underlie desensitization. We used real time, non-invasive assay to measure CB1 receptor desensitization. Thus we have measured the population response of the whole cells instead of using a single cell. The single cell

considered for electrophysiology may behave in a different manner than that of whole cell population, reflecting differences in cell's internal environment. But it is important to know that in real time assay, we cannot wash off the drugs before challenge. The experimental uncertainty thus has given rise to conflicting ideas about receptor regulation.

In conclusion, this work unravels the pharmacology of recently emerged SCs on human CB1 and CB2 receptors which may explain some of the adverse effects associated with their consumption. Although animal models have indicated that the SCs mediated effects are reversed by selective CB antagonist; it is yet to be shown in human models whether the toxicities are mediated by CB1/CB2 or something else afoot.

APPENDIX A

MPA assay data
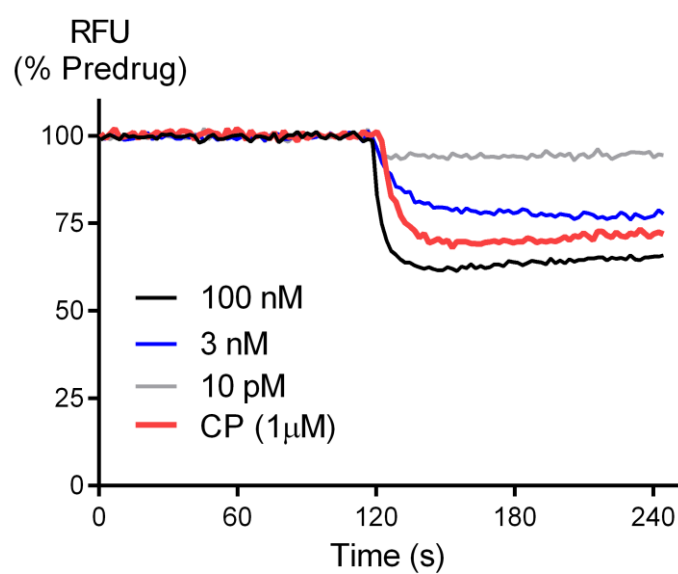
A) Representative trace of 5F-MDMDB-PICA on AtT20FlpIn-CB1 cells. Figure represents concentration dependent decrease in cellular hyperpolarization mediated by 5F-MDMB-PICA.
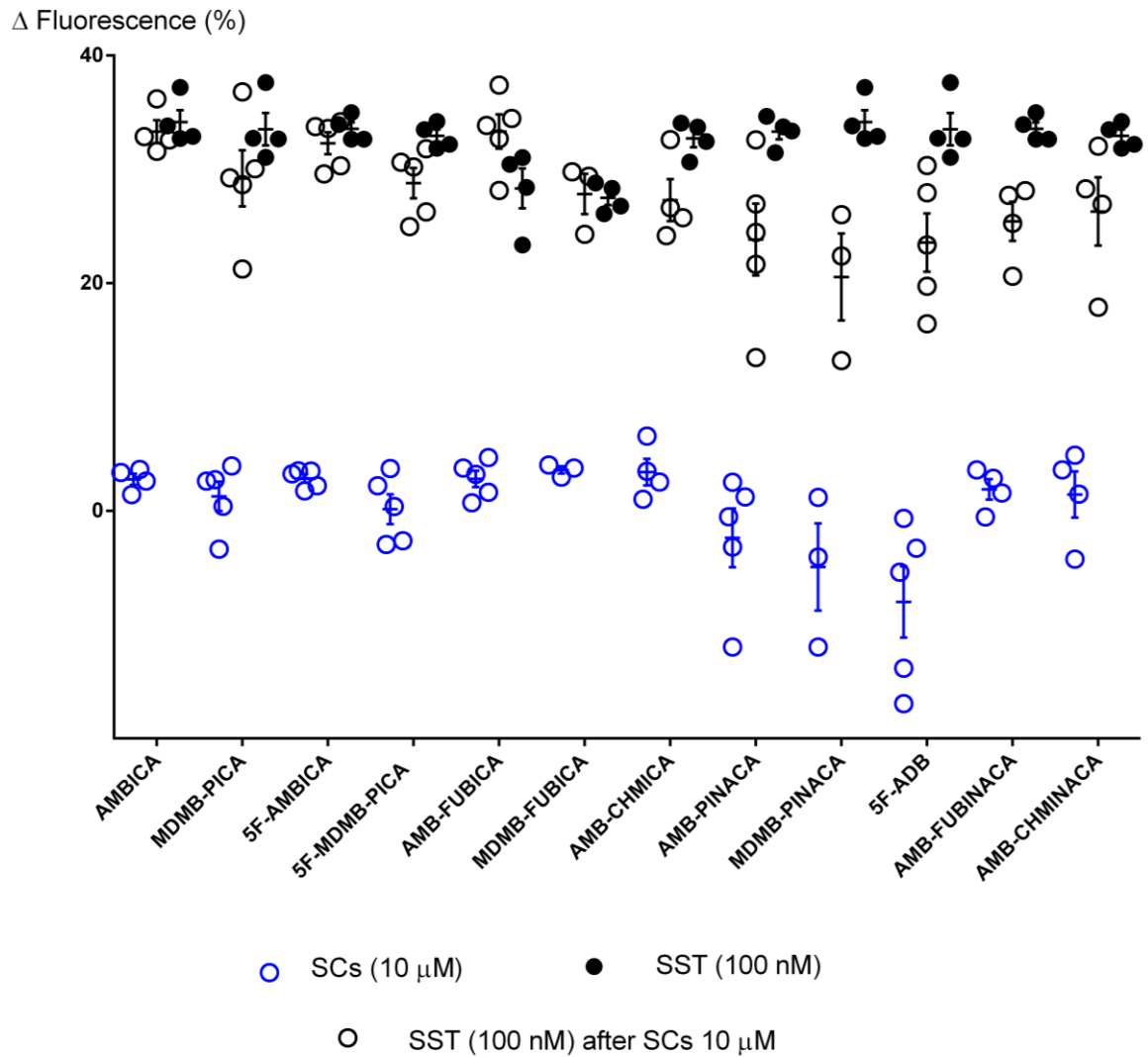
B) Scatter dot plot (following page) of all the other 12 SCs on ATt20FlpIn-WT cells. This figure represents the percentage change in fluorescence for SC's (10 µM), SST (100 nM) alone and SST in the continued presence of SCs in AtT20FlpIn-WT cells. None of these SCs produced a significant change in the membrane potential of AtT20FlpIn-WT cells, which do not express CB1 or CB2 receptors (Figure 8). No significant difference between SST alone and SST after SCs was found. Data represents mean ± SEM, n=3 to 5.

Δ Fluorescence (%)
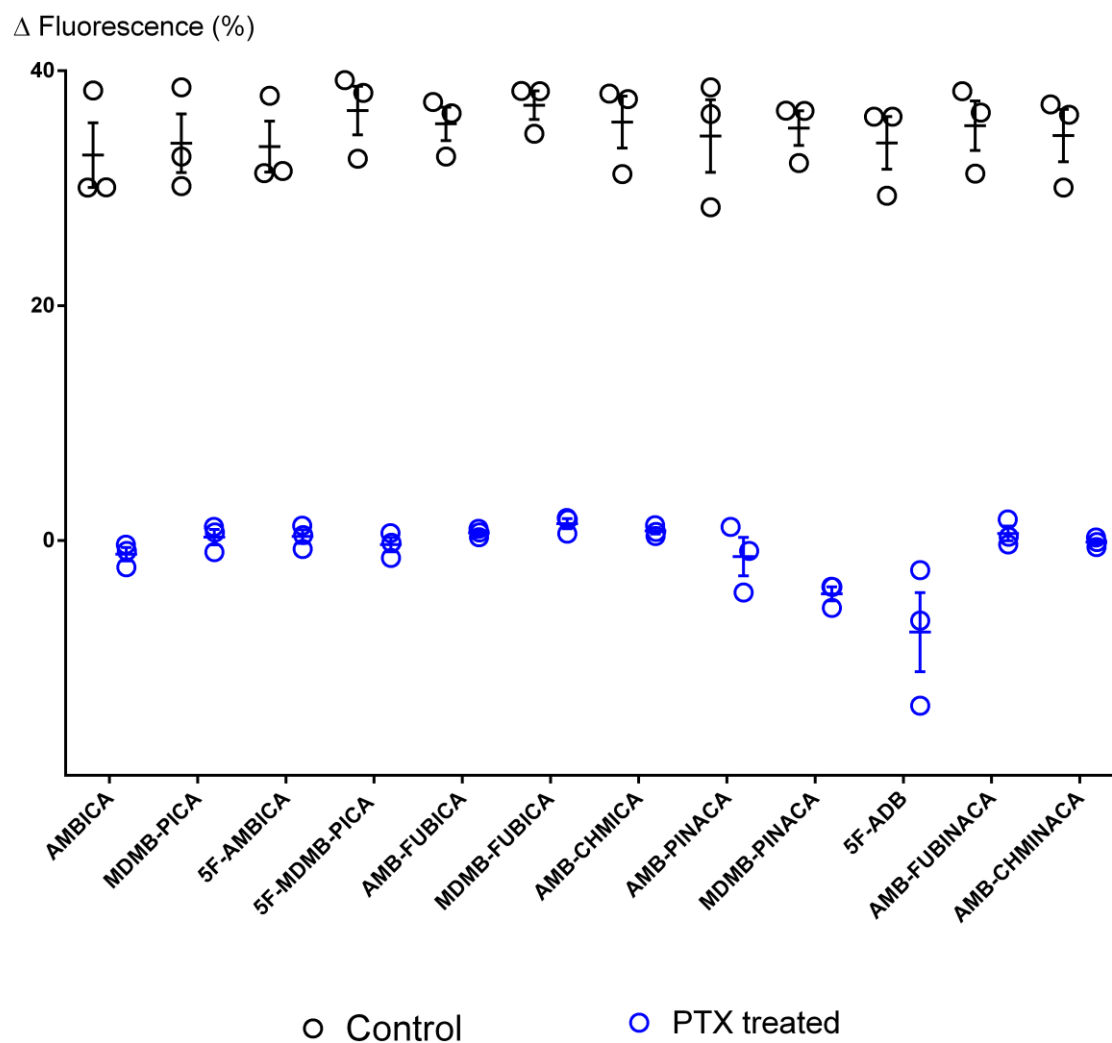
C) Scatter dot plot (following page) of all the other 12 SCs on ATt20FlpIn-CB1 treated with PTX. The PTX treated cells abolished the response of SCs completely as compared to control, signifying PTX sensitive $G\alpha_i$ mediated signaling. Data represents mean ± SEM, n=3, each in duplicate.
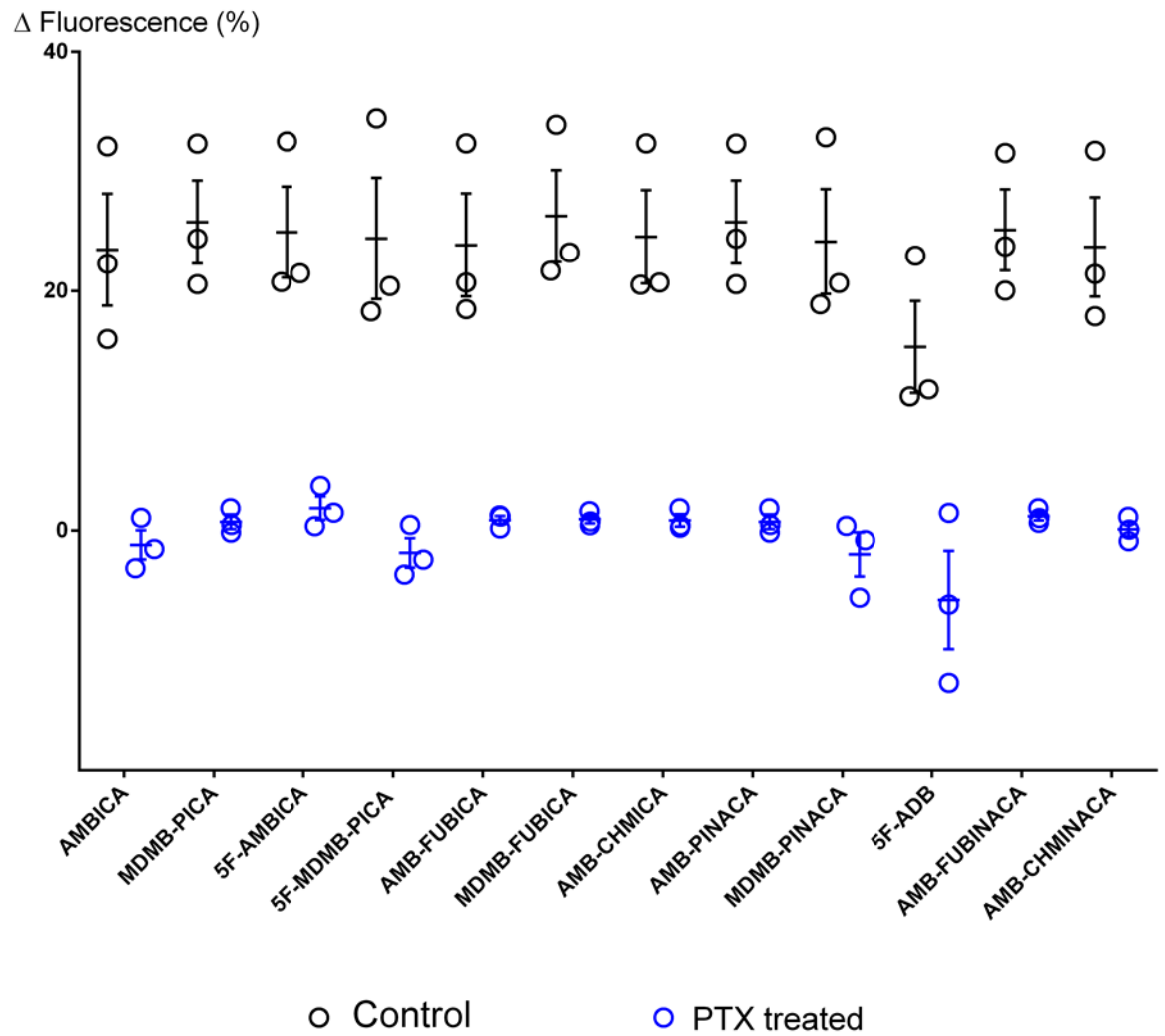
D) Scatter dot plot of all the other 12 SCs on ATt20FlpIn-CB2 treated with PTX. The PTX treated cells abolished the response of SCs completely as compared to control, signifying PTX sensitive $G\alpha_i$ mediated signaling. Data represents mean ± SEM, n=3, each in duplicate.
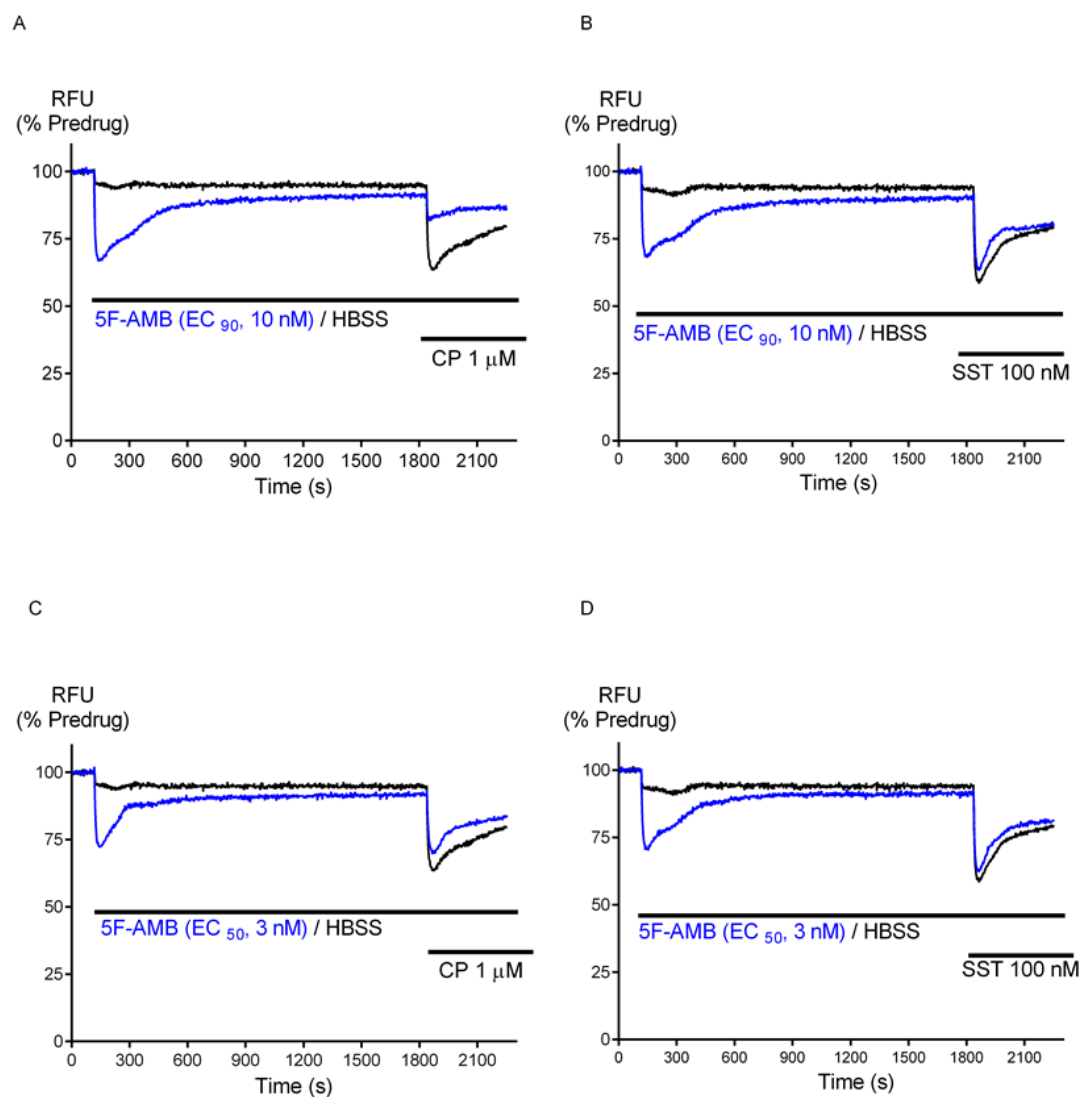
E) Homologous and Heterologous desensitization of CB1 receptor mediated by EC_{90} and EC_{50} of 5F-AMB. Trace A and C represents the homologous desensitization. challenged with CP-55,940 (1 μM) in the continuous presence of 5F-AMB to that of CP-55,940 alone, trace B and D shows heterologous desensitization, challenged with SST (100 nM) after 30 minutes of 5F-AMB.
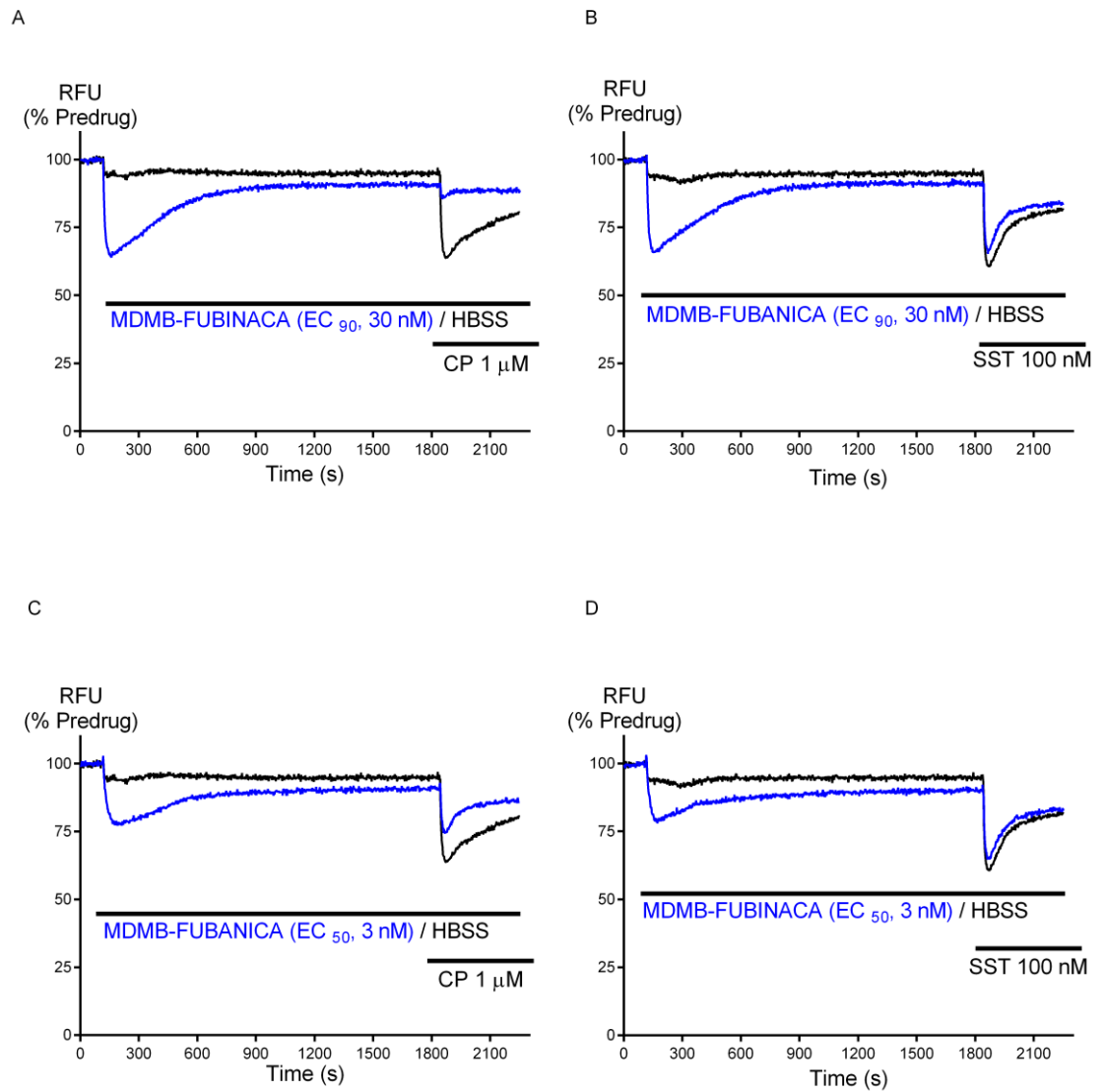
F) Homologous and Heterologous desensitization of CB1 receptor mediated by EC90 and EC50 of MDMB-FUBINACA. Trace A and C represents the homologous desensitization. challenged with CP-55,940 (1 µM) in the continuous presence of MDMB-FUBINACA to that of CP-55,940 alone, trace B and D shows heterologous desensitization, challenged with SST (100 nM) after 30 minutes of MDMB-FUBINACA.
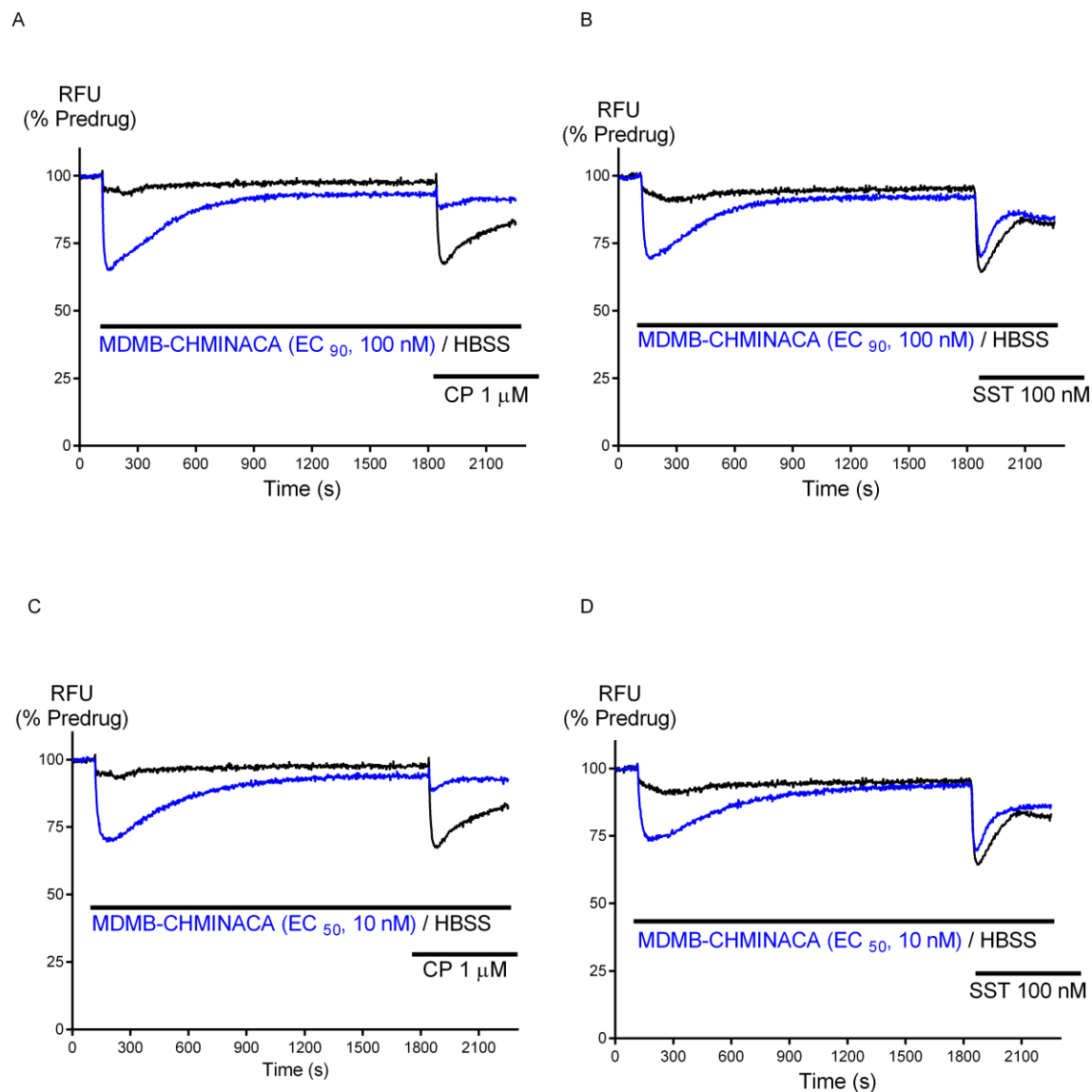
G) Homologous and Heterologous desensitization of CB1 receptor mediated by EC90 and EC50 of MDMB-CHMINACA. Trace A and C represents the homologous desensitization. challenged with CP-55,940 (1 µM) in the continuous presence of MDMB-CHMINACA to that of CP-55,940 alone, trace B and D shows heterologous desensitization, challenged with SST (100 nM) after 30 minutes of MDMB-CHMINACA.

Recipes, Materials and Equipment

1. Hank's Balanced Salt Solution with HEPES (HBSS)

Low Potassium HBSS

S.No.	Chemicals	Molecular Weight	Final concentration (mM)	Amount
1	NaCl	58.44	145	4.2g
2	HEPES	238.31	22	2.6g
3	Na_2HPO_4	141.96	0.338	24mg
4	$NaHCO_3$	84.01	4.17	175mg
5	KH_2PO_4	136.09	0.441	30mg
6	$MgSO_4$	120.37	0.407	24.5mg
7	$MgCl_2$	95.21	0.493	123µL of 2M solution
8	Glucose	180.2	5.55	500mg
9	$CaCl_2$	110.98	1.26	630µL of 1M solution
10	Milli-Q water			Quantity sufficient to 500mL

The pH is adjusted to 7.4 and osmolarity to 300-330 osm/L.

The solution is filtered through a 0.22 µm filter under the laminar flow hood for sterilisation and stored at 4ºC.

2. Materials

2.1 Tissue Culture

Name	Product Code	Supplier
Hygromycin B 100mg/ml	Ant-hm-5	InvivoGen
Leibovitz's L-15 Medium	11415-064	Gibco®
Penicillin(10,000U/mL)-Streptomycin (10,000µg/mL	15140-122	Gibco®
Poly-D-Lysine	P6407/P0899	Sigma-Aldrich®
Phosphate Buffered Saline (PBS)	20012-027	Gibco®
Trypsin-EDTA Solution 0.25%	T4049	Sigma-Aldrich®
Zeocin ™ 100mg/mL	Ant-zn-1	InvivoGen
D- (+)-Glucose	G7021	Sigma-Aldrich®
DMEM	D6429	Sigma-Aldrich®
Fetal Bovine Serum (FBS)	12003C	Sigma-Aldrich®

2.2 Chemicals

Name	Product Code	Supplier
$CaCl_2$	190464K	AUS Tritium (VWR)
Dimethyl Sulfoxide	D45040	Sigma-Aldrich®
Na_2HPO_4	SA026	Chem-Supply
D- (+)-Glucose	G7021	Sigma-Aldrich®
HEPES	H4034	Sigma-Aldrich®
$MgCl_2$	M8266	Sigma-Aldrich®
$MgSO_4$	M7506	Sigma-Aldrich®
PBS Tablet	09-8912	Medicago
KCl	PA054	Chem-Supply
KH_2PO_4	26936.260	AnalaR Normapur

NaHCO3	S6297	Sigma-Aldrich®
NaCl	SA046	Sigma-Aldrich®
NaOH	221465	Sigma-Aldrich®
FLIPR®Membrane Potential Blue Assay Kit	R8034	Molecular Devices
Triton-X	30632	BDH Chem. (VWR)
Tween-20	0777	Amaresco

2.3 Immunocytochemistry

Anti-phospho-Ser377	3451	Cell Signaling
Anti-phosho-ERK	4696	Cell Signaling

3 Equipments

Name	Supplier
Benchtop 314 Incubator (Ambient CO2)	Lab-Line
Centrifuge 5430	Eppendorf
Flex Station® 3 Multi-Mode Microplate Reader	Molecular Devices
HeraCell™ 150i CO2 Incubators	Thermo Scientific™
Magnetic Stirrer with Heating MR Hei-Standard	Heidolph
Microcentrifuge 5415R	Eppendorf
Microscope Olympus CKX41	Olympus
Mr Frosty™ freezing container	Thermo Scientific™
Pipettes (including automated multi-channel)	Gilson® and Eppendorf
Water Bath- Constant temperature (NBCT2)	Labec

REFRENCES

1   Lee, M. A. *Smoke signals: A social history of Marijuana-Medical, Recreational and Scientific*. (2012).

2   ElSohly, M., Gul, W. & Pertwee, R. Handbook of Cannabis, Oxford University Press Oxford, UK, (2014).

3   Russo, E. B. History of cannabis and its preparations in saga, science, and sobriquet. *Chemistry & Biodiversity* **4**, 1614-1648 (2007).

4   Amar, M. B. Cannabinoids in medicine: A review of their therapeutic potential. *Journal of Ethnopharmacology* **105**, 1-25 (2006).

5   Bonnie, R. J. & Whitebread, C. H. The forbidden fruit and the tree of knowledge: an inquiry into the legal history of American marijuana prohibition. *Virginia Law Review*, 971-1203 (1970).

6   Bewley-Taylor, D. & Jelsma, M. Fifty years of the 1961 Single Convention on Narcotic Drugs: A reinterpretation. *Series on Legislative Reform of Drug Policies*, 1-20 (2011).

7   Gaoni, Y. & Mechoulam, R. Isolation, structure, and partial synthesis of an active constituent of hashish. *Journal of the American Chemical Society* 86, 1646-1647 (1964).

8   Reggio, P. H. Endocannabinoid binding to the cannabinoid receptors: what is known and what remains unknown. *Current Medicinal Chemistry* 17, 1468-1486 (2010).

9   Wilson, R. S., May, E. L., Martin, B. R. & Dewey, W. L. 9-Nor-9-hydroxyhexahydrocannabinols. Synthesis, some behavioral and analgesic properties, and comparison with the tetrahydrocannabinols. *Journal of Medicinal Chemistry* 19, 1165-1167 (1976).

10   Matsuda, L. A., Lolait, S. J., Brownstein, M. J., Young, A. C. & Bonner, T. I. Structure of a cannabinoid receptor and functional expression of the cloned cDNA. *Nature* 346, 561-564 (1990).

11   Mackie, K. Cannabinoid receptors as therapeutic targets. *Annu. Rev. Pharmacol. Toxicol.* 46, 101-122 (2006).

12   Glass, M., Faull, R. & Dragunow, M. Cannabinoid receptors in the human brain: a detailed anatomical and quantitative autoradiographic study in the fetal, neonatal and adult human brain. *Neuroscience* 77, 299-318 (1997).

13   Svíženská, I., Dubový, P. & Šulcová, A. Cannabinoid receptors 1 and 2 (CB1 and CB2), their distribution, ligands and functional involvement in nervous system structures—a short review. *Pharmacology Biochemistry and Behavior* 90, 501-511 (2008).

14   Fride, E. & Mechoulam, R. Pharmacological activity of the cannabinoid receptor agonist, anandamide, a brain constituent. *European Journal ofPpharmacology* 231, 313-314 (1993).

15   Mechoulam, R., Hanuš, L. O., Pertwee, R. & Howlett, A. C. Early phytocannabinoid chemistry to endocannabinoids and beyond. *Nature Reviews Neuroscience* 15, 757-764 (2014).

16   Brandt, S. D., King, L. A. & Evans-Brown, M. The new drug phenomenon. *Drug Testing and Analysis* **6**, 587-597 (2014).

17   Elliott, S. & Evans, J. A 3-year review of new psychoactive substances in casework. *Forensic Science International* 243, 55-60 (2014).

18   Fattore, L. Synthetic cannabinoids—further evidence supporting the relationship between cannabinoids and psychosis. *Biological Psychiatry* 79, 539-548 (2016).

19   Vardakou, I., Pistos, C. & Spiliopoulou, C. Spice drugs as a new trend: mode of action, identification and legislation. *Toxicology letters* **197**, 157-162 (2010).

20   Auwärter, V. *et al.* 'Spice'and other herbal blends: harmless incense or cannabinoid designer drugs? *Journal of Mass Spectrometry* 44, 832-837 (2009).

21   Wiley, J., Barrett, R., Lowe, J., Balster, R. & Martin, B. Discriminative stimulus effects of CP 55,940 and structurally dissimilar cannabinoids in rats. *Neuropharmacology* 34, 669-676 (1995).

22   Gurney, S., Scott, K., Kacinko, S., Presley, B. & Logan, B. Pharmacology, toxicology, and adverse effects of synthetic cannabinoid drugs. *Forensic Science Review* 26, 53-78 (2014).

23   Spaderna, M., Addy, P. H. & D'Souza, D. C. Spicing things up: synthetic cannabinoids. *Psychopharmacology* 228, 525-540 (2013).

24   Fattore, L. & Fratta, W. Beyond THC: the new generation of cannabinoid designer drugs. *Frontiers in Behavioral Neuroscience* **5** (2011).

25   Stuart, J. M. *The Pharmacology of Novel Illicit Synthetic Cannabinoids*, Macquarie University, PhD Thesis (2015).

26   Lindigkeit, R. *et al.* Spice: a never ending story? *Forensic Science International* 191, 58-63 (2009).

27   Paronis, C. A., Thakur, G. A., Vemuri, K., Makriyannis, A. & Bergman, J. Partial Agonist and Antagonist Effects of Δ9-tetrahydrocannabinol (Δ9THC) in rats. *The FASEB Journal* 21, A409-A409 (2007).

28   Fredriksson, R., Lagerström, M. C., Lundin, L.-G. & Schiöth, H. B. The G-protein-coupled receptors in the human genome form five main families. Phylogenetic analysis, paralogon groups, and fingerprints. *Molecular Pharmacology* 63, 1256-1272 (2003).

29   Horn, F. *et al.* GPCRDB information system for G protein-coupled receptors. *Nucleic Acids Research* 31, 294-297 (2003).

30   Pertwee, R. G. Pharmacology of cannabinoid CB 1 and CB 2 receptors. *Pharmacology & Therapeutics* 74, 129-180 (1997).

31   Mackie, K., Lai, Y., Westenbroek, R. & Mitchell, R. Cannabinoids activate an inwardly rectifying potassium conductance and inhibit Q-type calcium currents in AtT20 cells

transfected with rat brain cannabinoid receptor. *The Journal of Neuroscience* 15, 6552-6561 (1995).

32   Henry, D. J. & Chavkin, C. Activation of inwardly rectifying potassium channels (GIRK1) by co-expressed rat brain cannabinoid receptors in Xenopus oocytes. *Neuroscience Letters* 186, 91-94 (1995).

33   Howlett, A. & Fleming, R. Cannabinoid inhibition of adenylate cyclase. Pharmacology of the response in neuroblastoma cell membranes. *Molecular Pharmacology* 26, 532-538 (1984).

34   Glass, M. & Felder, C. C. Concurrent stimulation of cannabinoid CB1 and dopamine D2 receptors augments cAMP accumulation in striatal neurons: evidence for a Gs linkage to the CB1 receptor. *The Journal of Neuroscience* 17, 5327-5333 (1997).

35   Turu, G. & Hunyady, L. Signal transduction of the CB1 cannabinoid receptor. *Journal of Molecular Endocrinology* 44, 75-85 (2010).

36   Sugiura, T. *et al.* 2-Arachidonoylglycerol, a putative endogenous cannabinoid receptor ligand, induces rapid, transient elevation of intracellular free Ca 2+ in neuroblastoma× glioma hybrid NG108-15 cells. *Biochemical and Biophysical Research Communications* 229, 58-64 (1996).

37   Howlett,A.CannabinoidReceptorSignaling,53-79,Springer, (2005).

38   Cheng, Y. & Hitchcock, S. A. Targeting cannabinoid agonists for inflammatory and neuropathic pain. *Expert Opinion on Investigational Drugs* 16, 951-965 (2007).

39   Basu, S., Ray, A. & Dittel, B. N. Cannabinoid receptor 2 is critical for the homing and retention of marginal zone B lineage cells and for efficient T-independent immune responses. *The Journal of Immunology* 187, 5720-5732 (2011).

40   Di Marzo, V., Bifulco, M. & De Petrocellis, L. The endocannabinoid system and its therapeutic exploitation. *Nature reviews Drug Discovery* **3**, 771-784 (2004).

41   Increase in synthetic cannabinoid (K2)-related adverse events and emergency department visits, New York City, NYC Health (2016).

42   Winstock, A., Lynskey, M., Borschmann, R. & Waldron, J. Risk of emergency medical treatment following consumption of cannabis or synthetic cannabinoids in a large global sample. *Journal of Psychopharmacology* 29, 698-703 (2015).

43   Palamar, J. J. & Barratt, M. J. Synthetic cannabinoids: undesirable alternatives to natural marijuana. *The American Journal of Drug and Alcohol Abuse*, 1-3 (2016).

44   Seely, K. A., Prather, P. L., James, L. P. & Moran, J. H. Marijuana-based drugs: innovative therapeutics or designer drugs of abuse? *Molecular Interventions* 11, 36 (2011).

45   Malan Jr, T. P, IBRAHIM M. M*., Deng, H., Liu, Q., Mata, H.P., Vanderah, T., Porreca, F., Markiyaanis, A.,* CB 2 cannabinoid receptor-mediated peripheral antinociception. *Pain* 93, 239-245 (2001).

46   Wikipedia, S. Cannabinoids: 11-hydroxy-thc, 11-nor-9-carboxy-thc, 2-arachidonoylglycerol, 2-arachidonyl. (2009).

47   Wikipedia,2-[(1R,2R,5R)-5-hydroxy-2-(3-hydroxypropyl)cyclohexyl]-5-(2-methyloctan-2-yl)phenol,CP-55,940; Naphthalen-1-yl-(1-pentylindol-3-yl)methanone JWH-018 (2010).

48   Aung, M. M. *et al.* Influence of the N-1 alkyl chain length of cannabimimetic indoles upon CB 1 and CB 2 receptor binding. *Drug and Alcohol Dependence* 60, 133-140 (2000).

49   Terranova, J.-P. *et al.* Improvement of memory in rodents by the selective CB1 cannabinoid receptor antagonist, SR 141716. *Psychopharmacology* 126, 165-172 (1996).

50   Huffman, J. W., Dai, D., Martin, B. R. & Compton, D. R. Design, synthesis and pharmacology of cannabimimetic indoles. *Bioorganic & Medicinal Chemistry Letters* 4, 563-566 (1994).

51   Huffman, J. W. *et al.* Synthesis and pharmacology of a very potent cannabinoid lacking a phenolic hydroxyl with high affinity for the CB2 receptor. *Journal of Medicinal Chemistry* 39, 3875-3877 (1996).

52   Wiley, J. L. *et al.* Structure-activity relationships of indole-and pyrrole-derived cannabinoids. *Journal of Pharmacology and Experimental Therapeutics* 285, 995-1004 (1998).

53   Wiley, J. L., Marusich, J. A. & Huffman, J. W. Moving around the molecule: relationship between chemical structure and in vivo activity of synthetic cannabinoids. *Life sciences* 97, 55-63 (2014).

54   Wiley, J. L., Marusich, J. A., Martin, B. R. & Huffman, J. W. 1-Pentyl-3-phenylacetylindoles and JWH-018 share in vivo cannabinoid profiles in mice. *Drug and Alcohol Dependence* 123, 148-153 (2012).

55   Banister, S. D. *et al.* Effects of bioisosteric fluorine in synthetic cannabinoid designer drugs JWH-018, AM-2201, UR-144, XLR-11, PB-22, 5F-PB-22, APICA, and STS-135. *ACS Chemical Neuroscience* **6**, 1445-1458 (2015).

56   Banister, S. D. *et al.* Structure–activity relationships of synthetic cannabinoid designer drug RCS-4 and its regioisomers and C4 homologues. *Forensic Toxicology* 33, 355-366 (2015).

57   Banister, S. D. *et al.* The synthesis and pharmacological evaluation of adamantane-derived indoles: cannabimimetic drugs of abuse. *ACS Chemical Neuroscience* 4, 1081-1092 (2013).

58   Banister, S. D. *et al.* Pharmacology of Valinate and tert-Leucinate Synthetic Cannabinoids 5F-AMBICA, 5F-AMB, 5F-ADB, AMB-FUBINACA, MDMB-FUBINACA, MDMB-CHMICA, and Their Analogues. *ACS Chemical Neuroscience* (2016).

59   Howlett, A. *et al.* International Union of Pharmacology. XXVII. Classification of cannabinoid receptors. *Pharmacological Reviews* 54, 161-202 (2002).

60   Perez-Reyes, M., Timmons, M. C., Davis, K. & Wall, E. A comparison of the pharmacological activity in man of intravenously administered 1368-11368-11368-1, cannabinol, and cannabidiol. *Experientia* 29, 1368-1369 (1973).

61   Bylund, D. B. & Toews, M. L. Radioligand binding methods: practical guide and tips. *American Journal of Physiology-Lung Cellular and Molecular Physiology* 265, L421-L429 (1993).

62   Hill, S. J., Williams, C. & May, L. T. Insights into GPCR pharmacology from the measurement of changes in intracellular cyclic AMP; advantages and pitfalls of differing methodologies. *British Journal of Pharmacology* 161, 1266-1275 (2010).

63   Connor, M. & Traynor, J. Constitutively active μ-opioid receptors. *Methods in Enzymology* 484, 445-469 (2009).

64   Delom, F. & Fessart, D. Role of phosphorylation in the control of clathrin-mediated internalization of GPCR. *International Journal of Cell Biology* (2011).

65   Lefkowitz, R. J. G protein-coupled receptors III. New roles for receptor kinases and β-arrestins in receptor signaling and desensitization. *Journal of Biological Chemistry* 273, 18677-18680 (1998).

66   Von Zastrow, M. Regulation of g protein-coupled receptors by phosphorylation and endocytosis. (2002).

67   Marie, N., Aguila, B. & Allouche, S. Tracking the opioid receptors on the way of desensitization. *Cellular Signaling* 18, 1815-1833 (2006).

68   Connor, M., Osborne, P. B. & Christie, M. J. μ-Opioid receptor desensitization: Is morphine different? *British Journal of Pharmacology* 143, 685-696 (2004).

69   Lefkowitz, R. J. & Shenoy, S. K. Transduction of receptor signals by ß-arrestins. *Science* 308, 512-517 (2005).

70   Marie, N., Lecoq, I., Jauzac, P. & Allouche, S. Differential sorting of human δ-opioid receptors after internalization by peptide and alkaloid agonists. *Journal of Biological Chemistry* 278, 22795-22804 (2003).

71   Liu, J.-G. & Anand, K. Protein kinases modulate the cellular adaptations associated with opioid tolerance and dependence. *Brain Research Reviews* 38, 1-19 (2001).

72   Koch, T. & Höllt, V. Role of receptor internalization in opioid tolerance and dependence. *Pharmacology & Therapeutics* 117, 199-206 (2008).

73   Williams, J. T. *et al.* Regulation of μ-opioid receptors: Desensitization, phosphorylation, internalization, and tolerance. *Pharmacological Reviews* 65, 223-254 (2013).

74   Hausdorff, W. P., Caron, M. G. & Lefkowitz, R. Turning off the signal: desensitization of beta-adrenergic receptor function. *The FASEB Journal* 4, 2881-2889 (1990).

75   Grimsey, N. L., Graham, E. S., Dragunow, M. & Glass, M. Cannabinoid Receptor 1 trafficking and the role of the intracellular pool: implications for therapeutics. *Biochemical Pharmacology* 80, 1050-1062 (2010).

76   Freedman, N.J. and Lefkowitz, R.J. Desensitization of G protein-coupled receptors. *Recent progress in hormone research*, *51*,319-51 (1995).

77   Swanson, J., Gupta, S., Guinta, D., Flynn, D., Agler, D., Lerner, M., Williams, L., Shoulson, I. and Wigal, S.,. Acute tolerance to methylphenidate in the treatment of attention deficit hyperactivity disorder in children. *Clinical Pharmacology & Therapeutics*, *66*(3), 295-305 (1999)

92

78   McMillan, D., Dewey, W. & Harris, L. Characteristics of tetrahydrocannabinol tolerance. *Annals of the New York Academy of Sciences* 191, 83-99 (1971).

79   Pertwee, R., Stevenson, L. & Griffin, G. Cross-tolerance between delta-9-tetrahydrocannabinol and the cannabimimetic agents, CP 55,940, WIN 55,212-2 and anandamide. *British Journal of Pharmacology* 110, 1483-1490 (1993).

80   Abood, M. E., Sauss, C., Fan, F., Tilton, C. L. & Martin, B. R. Development of behavioral tolerance to Δ9-THC without alteration of cannabinoid receptor binding or mRNA levels in whole brain. *Pharmacology Biochemistry and Behavior* 46, 575-579 (1993).

81   De Fonseca, F. R., Gorriti, M., Fernandez-Ruiz, J., Palomo, T. & Ramos, J. Downregulation of rat brain cannabinoid binding sites after chronic Δ9-tetrahydrocannabinol treatment. *Pharmacology Biochemistry and Behavior* 47, 33-40 (1994).

82   Oviedo, A., Glowa, J. & Herkenham, M. Chronic cannabinoid administration alters cannabinoid receptor binding in rat brain: a quantitative autoradiographic study. *Brain Research* 616, 293-302 (1993).

83   Zhuang, S.-y. *et al.* Effects of long-term exposure to Δ 9-THC on expression of cannabinoid receptor (CB1) mRNA in different rat brain regions. *Molecular Brain Research* 62, 141-149 (1998).

84   Burston, J. J., Wiley, J. L., Craig, A. A., Selley, D. E. & Sim-Selley, L. J. Regional enhancement of cannabinoid CB1 receptor desensitization in female adolescent rats following repeated Δ9-tetrahydrocannabinol exposure. *British Journal of Pharmacology* 161, 103-112 (2010).

85   Jin, W. *et al.* Distinct domains of the CB1 cannabinoid receptor mediate desensitization and internalization. *The Journal of Neuroscience* 19, 3773-3780 (1999).

86   Breivogel, C. S., Lambert, J. M., Gerfin, S., Huffman, J. W. & Razdan, R. K. Sensitivity to Δ9-tetrahydrocannabinol is selectively enhanced in beta-arrestin2-/-mice. *Behavioural Pharmacology* 19, 298 (2008).

87   Katona, I. *et al.* Presynaptically located CB1 cannabinoid receptors regulate GABA release from axon terminals of specific hippocampal interneurons. *The Journal of Neuroscience* 19, 4544-4558 (1999).

88   Rinaldi-Carmona, M. *et al.* Modulation of CB1 cannabinoid receptor functions after a long-term exposure to agonist or inverse agonist in the Chinese hamster ovary cell expression system. *Journal of Pharmacology and Experimental Therapeutics* 287, 1038-1047 (1998).

89   Leterrier, C., Bonnard, D., Carrel, D., Rossier, J. & Lenkei, Z. Constitutive endocytic cycle of the CB1 cannabinoid receptor. *Journal of Biological Chemistry* 279, 36013-36021 (2004).

90   Hsieh, C., Brown, S., Derleth, C. & Mackie, K. Internalization and recycling of the CB1 cannabinoid receptor. *Journal of Neurochemistry* 73, 493-501 (1999).

91   Walsh, K. B. Targeting GIRK channels for the development of new therapeutic agents. *Ion channel screening: Advances in Technologies and Analysis*, 66 (2011).

92   Siderovski, D. *Regulators of G Protein Signaling*. Vol. 390 Academic Press, (2004).

93   Steiner, H. & Tseng, K. Y. *Handbook of basal ganglia structure and function*. Vol. 24 , Academic Press, (2010).

94   Knapman, A., Abogadie, F., McIntrye, P. & Connor, M. A real-time, fluorescence-based assay for measuring μ-opioid receptor modulation of adenylyl cyclase activity in chinese hamster ovary cells. *Journal of Biomolecular Screening*, 1087057113501391 (2013).

95   Junqueira Santiago, M. Regulation of the μ-opioid receptor signaling in naturally occurring variants and phosphorylation site mutants, Phd Thesis, (2015).

96   Knapman, A. & Connor, M. Fluorescence-based, high-throughput assays for μ-opioid receptor activation using a membrane potential-sensitive dye. *Opioid Receptors: Methods and Protocols*, 177-185 (2015).

97   Molecular Devices, FLIPR membrane potential Assay kits.

98   Carlino, M. S. *et al.* Differential activity of MEK and ERK inhibitors in BRAF inhibitor resistant melanoma. *Molecular Oncology* 8, 544-554 (2014).

99   Chaikuad, A. *et al.* A unique inhibitor binding site in ERK1/2 is associated with slow binding kinetics. *Nature Chemical Biology* 10, 853-860 (2014).

100   Blakey, K. *et al.* Identification of the novel synthetic cannabimimetic 8-quinolinyl 4-methyl-3-(1-piperidinylsulfonyl) benzoate (QMPSB) and other designer drugs in herbal incense. *Forensic Science International* 260, 40-53 (2016).

101   Uchiyama, N., Asakawa, K., Kikura-Hanajiri, R., Tsutsumi, T. & Hakamatsuka, T. A new pyrazole-carboxamide type synthetic cannabinoid AB-CHFUPYCA [N-(1-amino-3-methyl-1-oxobutan-2-yl)-1-(cyclohexylmethyl)-3-(4-fluorophenyl)-1H-pyrazole-5-carboxamide] identified in illegal products. *Forensic Toxicology* 33, 367-373 (2015).

102   Qian, Z., Hua, Z., Liu, C. & Jia, W. Four types of cannabimimetic indazole and indole derivatives, ADB-BINACA, AB-FUBICA, ADB-FUBICA, and AB-BICA, identified as new psychoactive substances. *Forensic Toxicology* 34, 133-143 (2016).

103   "EMCDDA–Europol Joint Report on MDMB-CHMICA". European Monitoring Centre for Drugs and Drug Addiction (EMCDDA), (2016).

104   Westin, A. A. *et al.* Sudden cardiac death following use of the synthetic cannabinoid MDMB-CHMICA. *Journal of Analytical Toxicology* 40, 86-87 (2016).

105   Drug Enforcement Administration, D. o. J. Schedules of controlled substances: temporary placement of four synthetic cannabinoids into Schedule I. Final order. *Federal Register* 79, 7577 (2014).

106   Drug Enforcement Administration, D. o. J. Schedules of controlled substances: temporary placement of three synthetic cannabinoids into schedule I. Final order. *Federal Register* 80, 5042 (2015).

107   Shevyrin, V. *et al.* Identification and analytical characteristics of synthetic cannabinoids with an indazole-3-carboxamide structure bearing a N-1-methoxycarbonylalkyl group. *Analytical and Bioanalytical Chemistry* 407, 6301-6315 (2015).

108   25 killed, over 700 hospitalized: Cheap 'Spice' designer drug causes severe poisoning across Russia", (2014).

109   National Forensic Laboratory Information System NFLIS, Mid-Year Report (2015).

110   Europen Monitoring Centre for Drugs and Drug Addiction, Europol 2014 Annual Report on Implementation of Council Decision 2005/387/JHA, Implementation reports, Luxemborg (2015)

111   Hill, S. L. *et al.* Clinical toxicity following analytically confirmed use of the synthetic cannabinoid receptor agonist MDMB-CHMICA. A report from the Identification Of Novel psychoActive substances (IONA) study. *Clinical Toxicology*, 1-6 (2016).

112   Шестаков, Д. А., Дикаев, С. У. & Данилов, А. П. ЛЕТОПИСЬ САНКТ-ПЕТЕРБУРГСКОГО МЕЖДУНАРОДНОГО КРИМИНОЛОГИЧЕСКОГО КЛУБА. ГОД 2014. *Криминология: вчера, сегодня, завтра* (2015).

113   Risk assessment report on a new psychoactive substance: methyl 2-[[1- (cyclohexylmethyl)-1H-indole-3-carbonyl]amino]-3,3-dimethylbutanoate(MDMB-CHMICA),EMCDDA (2016).

114   Luk, T. *et al.* Identification of a potent and highly efficacious, yet slowly desensitizing CB1 cannabinoid receptor agonist. *British Journal of Jharmacology* 142, 495-500 (2004).

115   Iversen, L. Cannabis and the brain. *Brain* 126, 1252-1270 (2003).

116   Caspersen, S. G. & Tau, G. Clinical Handbook of Adolescent Addiction (2014).

117   Frost, J. M. *et al.* Indol-3-ylcycloalkyl ketones: Effects of N1 substituted indole side chain variations on CB2 cannabinoid receptor activity. *Journal of Medicinal Chemistry* **53**, 295-315 (2009).

118   Wiley, J. L. *et al.* Cannabinoids in disguise: Δ 9-tetrahydrocannabinol-like effects of tetramethylcyclopropyl ketone indoles. *Neuropharmacology* 75, 145-154 (2013).

119   Banister, S. D. *et al.* Pharmacology of Indole and Indazole Synthetic Cannabinoid Designer Drugs AB-FUBINACA, ADB-FUBINACA, AB-PINACA, ADB-PINACA, 5F-AB-PINACA, 5F-ADB-PINACA, ADBICA, and 5F-ADBICA. *ACS Chemical Neuroscience* 6, 1546-1559 (2015).

120   Huffman, J.W. and Padgett, L.W. Recent developments in the medicinal chemistry of cannabimimetic indoles, pyrroles and indenes. *Current medicinal chemistry*, *12*,1395-1411, (2005).

121.   Song, Z.H., Slowey, C.A., Hurst, D.P. and Reggio, P.H.. The Difference between the CB1 and CB2 Cannabinoid Receptors at Position 5.46 Is Crucial for the Selectivity of WIN55212-2 for CB2. *Molecular pharmacology*, *56*,834-840, (1999).

122   Howlett, A., Qualy, J. M. & Khachatrian, L. L. Involvement of Gi in the inhibition of adenylate cyclase by cannabimimetic drugs. *Molecular Pharmacology* 29, 307-313 (1986).

123   Kouznetsova, V., Geers, M. G. & Brekelmans, W. M. Multi-scale constitutive modelling of heterogeneous materials with a gradient-enhanced computational homogenization scheme. *International Journal for Numerical Methods in Engineering* 54, 1235-1260 (2002).

124   Daigle, T. L., Kearn, C. S. & Mackie, K. Rapid CB 1 cannabinoid receptor desensitization defines the time course of ERK1/2 MAP kinase signaling. *Neuropharmacology* 54, 36-44 (2008).

125   Daigle, T. L., Kwok, M. L. & Mackie, K. Regulation of CB1 cannabinoid receptor internalization by a promiscuous phosphorylation-dependent mechanism. *Journal of Neurochemistry* 106, 70-82 (2008).

126   Macey, T. A., Lowe, J. D. & Chavkin, C. Mu opioid receptor activation of ERK1/2 is GRK3 and arrestin dependent in striatal neurons. *Journal of Biological Chemistry* 281, 34515-34524 (2006).

127   Schmidt, H. *et al.* Involvement of Mitogen-Activated Protein Kinase in Agonist-Induced Phosphorylation of the μ-Opioid Receptor in HEK 293 Cells. *Journal of Neurochemistry* 74, 414-422 (2000).

128   Jie, L. *et al.* Functional CB1 cannabinoid receptors in human vascular endothelial cells. *Biochemical Journal* 346, 835-840 (2000).

129   Rueda, D., Galve-Roperh, I., Haro, A. & Guzmán, M. The CB1 cannabinoid receptor is coupled to the activation of c-Jun N-terminal kinase. *Molecular Pharmacology* 58, 814-820 (2000).

130   Downer, E. J., Fogarty, M. P. & Campbell, V. A. Tetrahydrocannabinol-induced neurotoxicity depends on CB1 receptor-mediated c-Jun N-terminal kinase activation in cultured cortical neurons. *British Journal of Pharmacology* 140, 547-557 (2003).

131   Molina-Holgado, F. *et al.* Neuroprotective effects of the synthetic cannabinoid HU-210 in primary cortical neurons are mediated by phosphatidylinositol 3-kinase/AKT signaling. *Molecular and Cellular Neuroscience* 28, 189-194 (2005).

132   Graham, E. S. *et al.* Induction of Krox-24 by endogenous cannabinoid type 1 receptors in Neuro2A cells is mediated by the MEK-ERK MAPK pathway and is suppressed by the phosphatidylinositol 3-kinase pathway. *Journal of Biological Chemistry* 281, 29085-29095 (2006).

133   He, J. C. *et al.* The Gαo/i-coupled cannabinoid receptor-mediated neurite outgrowth involves Rap regulation of Src and Stat3. *Journal of Biological Chemistry* 280, 33426-33434 (2005).

134   Lowe, J. D. *et al.* Role of G Protein–Coupled Receptor Kinases 2 and 3 in μ-Opioid Receptor Desensitization and Internalization. *Molecular Pharmacology* 88, 347-356 (2015).

135   Chen, Y. J. *et al.* Identification of phosphorylation sites in the COOH-terminal tail of the μ-opioid receptor. *Journal of Neurochemistry* **1**24, 189-199 (2013).

136   Tulipano, G. & Schulz, S. Novel insights in somatostatin receptor physiology. *European Journal of Endocrinology* 156, S3-S11 (2007).

137   Shenoy, S. K. *et al.* β-Arrestin-dependent, G protein-independent ERK1/2 activation by the β2 adrenergic receptor. *Journal of Biological Chemistry* 281, 1261-1273 (2006).

138   Fan, F., Compton, D. R., Ward, S., Melvin, L. & Martin, B. R. Development of cross-tolerance between delta 9-tetrahydrocannabinol, CP 55,940 and WIN 55,212. *Journal of Pharmacology and Experimental Therapeutics* 271, 1383-1390 (1994).

139   Romero, J., Berrendero, F., García-Gil, L., Ramos, J. A. & Fernández-Ruiz, J. J. Cannabinoid receptor and WIN-55,212-2-stimulated [35S] GTPγS binding and cannabinoid receptor mRNA levels in the basal ganglia and the cerebellum of adult male rats chronically exposed to Δ9-tetrahydrocannabinol. *Journal of Molecular Neuroscience* 11, 109-119 (1998).

140   Kaufmann, K. *et al.* ML297 (VU0456810), the first potent and selective activator of the GIRK potassium channel, displays antiepileptic properties in mice. *ACS Chemical Neuroscience* 4, 1278-1286 (2013).

141   Allouche, S., Noble, F. & Marie, N. Opioid receptor desensitization: mechanisms and its link to tolerance. *Monitoring endogenous GPCRs: Lessons for Drug Design*, 115 (2015).

142   Ikeda, S., Keneko, M. & Fujiwara, S. inventors; Takeda Pharmaceutical Company Ltd. *Ikeda S, Keneko M, and Fujiwara S, assignees. Cardiotonic agent comprising GRK inhibitor. World patent WO2007034846* (2007).

143   Thal, D. M., Yeow, R. Y., Schoenau, C., Huber, J. & Tesmer, J. J. Molecular mechanism of selectivity among G protein-coupled receptor kinase 2 inhibitors. *Molecular Pharmacology* 80, 294-303 (2011).

144   Hauger, R. L., Risbrough, V., Brauns, O. & Dautzenberg, F. M. Corticotropin releasing factor (CRF) receptor signaling in the central nervous system: new molecular targets. *CNS & Neurological Disorders-Drug Targets, Formerly Current Drug Targets-CNS & Neurological Disorders,* 5, 453-479 (2006).

143   Dang, V. C., Napier, I. A. & Christie, M. J. Two distinct mechanisms mediate acute μ-opioid receptor desensitization in native neurons. *The Journal of Neuroscience* 29, 3322-3327 (2009).

144   Atwood, B. K., Lopez, J., Wager-Miller, J., Mackie, K. & Straiker, A. Expression of G protein-coupled receptors and related proteins in HEK293, AtT20, BV2, and N18 cell lines as revealed by microarray analysis. *BMC Genomics* 12, 14 (2011).

145   Kohout, T. A. *et al.* Differential desensitization, receptor phosphorylation, β-arrestin recruitment, and ERK1/2 activation by the two endogenous ligands for the CC chemokine receptor 7. *Journal of Biological Chemistry* 279, 23214-23222 (2004).

146   Pertwee, R. The pharmacology of cannabinoid receptors and their ligands: an overview. *International Journal of Obesity* **30**, S13-S18 (2006).

147   Henstridge, C. M. Off-target cannabinoid effects mediated by GPR55. *Pharmacology* 89, 179-187 (2012).

148   Tapert, S. F., Schweinsburg, A. D. & Brown, S. A. The influence of marijuana use on neurocognitive functioning in adolescents. *Current Drug Abuse Reviews* 1, 99-111 (2008).

149   Romero, J. *et al.* Effects of chronic exposure to Δ 9-tetrahydrocannabinol on cannabinoid receptor binding and mRNA levels in several rat brain regions. *Molecular Brain Research* 46, 100-108 (1997).